Western University
Scholarship@Western

Digitized Theses | Digitized Special Collections

1971

A Calorimeter Apparatus For Studying The Thermodynamic Properties Of Heavy Water And Measurements On The Enthalpy Of Saturated Liquid Heavy Water

James Shih-chu Chan

Follow this and additional works at: https://ir.lib.uwo.ca/digitizedtheses

Recommended Citation
Chan, James Shih-chu, "A Calorimeter Apparatus For Studying The Thermodynamic Properties Of Heavy Water And Measurements On The Enthalpy Of Saturated Liquid Heavy Water" (1971). *Digitized Theses*. 453.
https://ir.lib.uwo.ca/digitizedtheses/453

This Dissertation is brought to you for free and open access by the Digitized Special Collections at Scholarship@Western. It has been accepted for inclusion in Digitized Theses by an authorized administrator of Scholarship@Western. For more information, please contact tadam@uwo.ca, wlswadmin@uwo.ca.

The author of this thesis has granted The University of Western Ontario a non-exclusive license to reproduce and distribute copies of this thesis to users of Western Libraries. Copyright remains with the author.

Electronic theses and dissertations available in The University of Western Ontario's institutional repository (Scholarship@Western) are solely for the purpose of private study and research. They may not be copied or reproduced, except as permitted by copyright laws, without written authority of the copyright owner. Any commercial use or publication is strictly prohibited.

The original copyright license attesting to these terms and signed by the author of this thesis may be found in the original print version of the thesis, held by Western Libraries.

The thesis approval page signed by the examining committee may also be found in the original print version of the thesis held in Western Libraries.

Please contact Western Libraries for further information:
E-mail: libadmin@uwo.ca
Telephone: (519) 661-2111 Ext. 84796
Web site: http://www.lib.uwo.ca/

A CALORIMETER APPARATUS FOR STUDYING THE THERMODYNAMIC PROPERTIES OF HEAVY WATER AND MEASUREMENTS ON THE ENTHALPY OF SATURATED LIQUID HEAVY WATER

by

James Shih-Chu Chan

Faculty of Engineering Science

Submitted in partial fulfillment
of the requirements for the degree of
Doctor of Philosophy

Faculty of Graduate Studies
The University of Western Ontario
London, Canada.

September 1970

© James Shih-Chu Chan 1971

ABSTRACT

A non-flow calorimeter apparatus has been designed, constructed and developed for studying the thermodynamic properties of heavy water and other important engineering fluids from room temperature to their respective critical point. Detailed descriptions of the apparatus along with the theory of experimental method and the calibration of the instrumentation are herein given.

The performance of the apparatus was superior to that of Osborne's apparatus which was employed to investigate the thermophysical properties of light water and yielded the various saturation data utilized by the compilers of the various national steam tables. For example, the constant mass experiments of this thesis conducted on saturated liquid heavy water are reproducible to ± 0.1 percent whereas the scatter of Osborne's data of the constant mass experiments is 0.5 percent.

The enthalpy change of saturated heavy water has been investigated from 50 to 300°C with this apparatus. It is estimated that the heavy water enthalpy measurements obtained in this work is accurate to ± 0.2 percent. The measurements on the enthalpy of heavy water at temperatures of around 300°C confirmed that the corresponding extrapolated values proposed by Baker are in error by approximately +4%.

ACKNOWLEDGEMENTS

The gratitude and appreciation of the author are expressed for Dr. E. S. Nowak's guidance and encouragement and making available various manuscripts.

The author is highly indebted to Mr. W. Haessler for the use of the isothermal enclosure for this work. He also wishes to thank Messrs. W. G. Trick, L. S. Thomas and C. M. Ivey for their invaluable suggestions.

This research was supported by funds and equipment from the Atomic Energy of Canada Limited, the National Research Council of Canada and The University of Western Ontario through Grants-in-aid awarded to Dr. E. S. Nowak.

TABLE OF CONTENTS

Page No.

Page No.

LIST OF TABLES

LIST OF FIGURES

NOMENCLATURE

A	Area
A	Numerical constant
a	Radius of the inner cylinder, see Eq. 21
B	Numerical constant
b	Radius of the outer cylinder, see Eq. 21
c_p	Specific heat at constant pressure
c_{p_c}	Specific heat of the empty calorimeter
c_{p_g}	Specific heat of saturated vapour
c_{p_f}	Specific heat of saturated liquid
F	Safety factor
h	Specific enthalpy
h_f	Specific enthalpy of saturated liquid
h_{fg}	Specific enthalpy of vaporization
h_g	Specific enthalpy of saturated vapour
M	Mass of the fluid sample
M_H	Mass of the fluid sample in the high filling experiment
M_L	Mass of the fluid sample in the low filling experiment
m_f	Mass of the saturated liquid
m_g	Mass of the saturated vapour
P	Saturation pressure

Q	Energy added to the calorimeter
Q_g	Energy added during vapour withdrawal test
Q_f	Energy added during liquid withdrawal test
Q_H	Energy added during the high filling mass experiment
Q_L	Energy added during the low filling mass experiment
q_E	Heat leak
R, r	Radius of the sample
S_f	Enthropy of saturated liquid
S_g	Enthropy of saturated vapour
T	Absolute temperature (^oK), T = t + 273.16
T_f	Final Temperature
T_i	Initial Temperature
t	Temperature (^oC)
t	Wall thickness of the calorimeter, See Eq. 1B
u	Specific internal energy
u_f	Specific internal energy of saturated liquid
u_g	Specific internal energy of saturated vapour
V	Internal volume of the calorimeter
v_f	Specific volume of saturated liquid
v_g	Specific volume of saturated vapour
Z	Calorimeter constant, see Eq. 25
θ	$\theta = T - T_i$, the excess temperature, see Eq. 17
α	Thermal diffusivity ($\alpha = \frac{k}{\rho c_p}$), see Eq. 17 & 20
α	Measured quantity ($\alpha = h_f - T\, v_f \frac{dp}{dT}$), see Eq. 21A
α	Temperature coefficient, see Eq. 23
β	Heating rate, see Eq. 17 & 20

β	Measured quantity ($\beta = T\, v_f \frac{dp}{dT}$), see Eq. 23A
β	Temperature coefficient, see Eq. 23
γ	Measured quantity ($\gamma = T\, v_g \frac{dp}{dT}$), see Eq. 22A
τ	Time
σ	Stefan-Boltzmann's constant, see Eq. 24
σ	Stress, see Eq. 1B
ε	Emissivity
ρ	Density
q_s	Heat equivalent of mechanical work by the fluid sample straining the calorimeter shell
Int.J./G.	International joule per gram

CHAPTER 1

INTRODUCTION

1-1. Objective of Present Work

The dramatic growth of electric energy consumption throughout the world has stimulated the development of nuclear power stations. In this regard Canada has been engaged in the design and development of heavy water moderated and heavy water cooled nuclear reactors (Candu) for the past twenty years. Several large scale commercial Candu power plants are currently under construction in this country as well as abroad. By 1976, more than 5000 megawatts will be generated by such reactors presently under construction in Ontario at a cost of approximately 3×10^9 dollars. The Vice-President of Atomic Energy of Canada Limited, Dr. W. B. Lewis (1)*, has predicted that Candu reactor will hold a strong competition with any other type reactor even looking forward one hundred years. Table 1 gives a summary of all heavy water power stations in the world (2).

Accurate and detailed information for the thermodynamic properties of heavy water is of considerable relevance in the design and operation of Candu type heavy water power plants. For example, accurate informa-

*Numbers in parentheses refer to reference in the Bibliography.

TABLE 1

HEAVY WATER POWER REACTORS (2)

Power Station	Capacity (MW)	Date of Full Power Operation	Moderator		Coolant			
			Material	Average Temp.(°C)	Coolant	Pressure (kg/cm^2)	Inlet Temp.(°C)	Outlet Temp.(°C)
Rolphton (Canada)	20	1962	D_2O	40	D_2O	60	249	275
Agesta (Sweden)	10	1964	D_2O	215	D_2O	35.7	207	220
Carolinas (United States)	17	1964	D_2O	68	D_2O	105	263	291
Karlsruhe (West Germany)	57	1966	D_2O	120	D_2O	90	251	280
Winfrith (United Kingdom	100	1968	D_2O	60	H_2O	67	275	281
Douglas Pt. I (Canada)	208	1968	D_2O	54	D_2O	87	249	293
Lucerns (Switzerland)	85	1968	D_2O	50	CO_2	60	217	382
Brenilis (France)	70	1970	D_2O	60	CO_2	60	260	500
Marviken (Sweden)	140	1972	D_2O	170	D_2O	50.5	110	263

TABLE 1 (Continued)

Power Station	Capacity (MW)	Date of Full Power Operation	Moderator		Coolant			
			Material	Average Temp.(^{o}C)	Coolant	Pressure (kg/cm^2)	Inlet Temp.(^{o}C)	Outlet Temp.(^{o}C)
Kanupp (Pakistan)	125	1970	D_2O	60	D_2O	109	246	293
Muhleberg (Switzerland)	306	1971	D_2O	-	-	-	-	-
Pickering 1 & 2 (Canada)	1016	1971	D_2O	54	D_2O	88.5	249	293
Rajasthan RAPP 1 (India)	200	1969	D_2O	-	D_2O	104	250	293
Niederaichbach (West Germany)	100	1971	D_2O	85	CO_2	60	253	550
Gentilly (Canada)	250	1971	D_2O	60	H_2O	60	269	270
Atucha CNA (Argentina)	319	1972	D_2O	170	D_2O	115	272	306
Bohunice A1 (Czechoslovakia)	140	1972	D_2O	-	CO_2	-	105	425
Cirene (Italy)	40	1972	D_2O	-	H_2O	40	-	-

TABLE 1 (Continued)

Power Station	Capacity (MW)	Date of Full Power Operation	Moderator		Coolant			
			Material	Average Temp.(^{o}C)	Coolant	Pressure (kg/cm^{2})	Inlet Temp.(^{o}C)	Outlet Temp.(^{o}C)
Pickering 3 (Canada)	508	1972	D_2O	54	D_2O	88.5	249	293
Rajasthan RAPP 2 (India)	200	1973	D_2O	-	D_2O	104	249	293
Kalpakkam 1 (India)	400	1973	D_2O	-	-	-	-	-
Pickering 4 (Canada)	508	1973	D_2O	54	D_2O	88.5	249	293
Bruce 1,2,3 & 4 (Canada)	3000	1976	D_2O	65	D_2O	112	249	299

tion on the enthalpy difference is one of the most important design factors required to estimate the size and capacity of heavy water circulation pumping equipment and heat exchangers. Furthermore a knowledge of the latent heat of heavy water is essential for the safe operation of boiling heavy water power reactors.

There is little precise information for the thermodynamic properties of heavy water, especially at high pressures and temperatures. In all probability, the next generation of Candu nuclear power plants (3) will be designed to operate at higher pressures and temperatures or to use D_2O coolant in the boiling mode to improve thermal efficiency. Dr. E. S. Nowak of Faculty of Engineering Science, The University of Western Ontario at the request of Atomic Energy of Canada Limited initiated a comprehensive experimental program to study the thermal behaviour of heavy water over a wide range of temperatures and pressures. The main purpose of the research of this thesis was to design and develop a non-flow calorimeter apparatus to accurately investigate the thermodynamic properties of heavy water liquid and vapour from room temperature to the critical point. A by-product of the above research has been the determination of the enthalpy of saturated heavy water liquid from 50 to 300°C.

1-2. Literature Review

Table 2 summarizes the individual investigations conducted on the enthalpy and specific heat (c_p) of heavy water.

Brown et al (4) conducted the first investigation on the specific heat of heavy water at atmospheric pressure from 4 to 65°C. Cockett et al (5) conducted measurements from 10 to 50°C. Euken et al (6) conducted measurements from 20 to 130°C and claimed their measurements

TABLE 2

MEASUREMENTS ON ENTHALPY AND SPECIFIC HEAT (c_p) OF HEAVY WATER

Investigator(s) & Date	Type of Measurement	Temperature Range (^oC)	Pressure Range (kg/cm^2)	Method of Investigation	Stated Accuracy %
Brown, Barnes & Maass 1935	c_p	4 to 65	1	Calorimetric Method	±0.5
Cockett & Ferguson 1939	c_p	10 to 50	1	Calorimetric Method	-
Euken & Eigen 1951	c_p	20 to 130	0.02 to 2.8	Flow Method	±0.15
Baker 1959	c_p	30 to 200	0.04 to 16.8	Comparitive Method	±0.7
Rivkin & Egorov 1959	c_p	20 to 300	50 to 100	Flow Method	-
	c_p	20 to 450	50 to 300	Flow Method	±3
Sheindlin & Gorbunova 1964	Enthalpy	350 to 460	250 to 500	Flow Method	-
Nowak 1966	Enthalpy	248.89 to 293.33	39.8 to 80.4	Calorimetric Method	±1
Nowak & Chan 1969	Enthalpy	32.2 to 176.6	0.04 to 9.3	Calorimetric Method	±0.5

accurate to ± 0.15 percent.

Baker (7) conducted extensive investigations on the specific heat of saturated liquid heavy water from 30 to 200°C. He estimated that the enthalpy values derived for saturated liquid heavy water in the above mentioned temperature range from his specific heat data were accurate to ± 1.5 percent. Above 200°C Baker estimated the enthalpy values for saturated liquid heavy water by subtracting the enthalpy values for saturated vapour proposed by Friedman (8) from the latent heat of vaporization proposed by Kirshenbaum (9). It should be pointed out that the enthalpy values for saturated liquid heavy water in the tables of Elliott (10) and Bishop (11) are essentially identical to the values proposed by Baker.

Rivkin et al (12,13) conducted the measurements on the specific heat of compressed heavy water from 20 to 450°C and pressure up to 300 kg/cm^2 with an accuracy of the order of ± 3 percent. The Sheindlin et al (14) measurements on enthalpy of heavy water in supercritical region extended to 460°C and 500 kg/cm^2.

Dr. Nowak (15,16) conducted the measurements on saturated liquid heavy water from 248.89 to 293.33°C. Information from his studies was required by the Atomic Energy of Canada Limited for the design of heat exchangers and heavy water pumping equipment in the nuclear power plants being constructed at Pickering, Ontario. He found that the enthalpy change for the above mentioned temperature interval was approximately five percent lower than the value obtained by Baker.

In order to verify the previous measurements conducted on saturated heavy water liquid up to 200°C, Dr. Nowak and the writer

(17,18) of this thesis conducted more measurements from 32.2 to 176.6°C on a thin walled calorimeter. Their measurements are accurate to ± 0.5 percent and in reasonable accord with the earlier measurements of Brown, Cockett, Euken, Baker and Rivkin. These measurements indicated that percentage deviation between the specific heat of saturated heavy water liquid and saturated light water liquid is a strong function of temperature varying from 0.25% at 40°C to approximately 3.6% at 175°C.

The foregoing literature review indicates that only fragmentary experimental data on the enthalpy of saturated heavy water liquid. There appears to be a complete lack of data for the enthalpy of vaporization of heavy water even at moderate values of pressure and temperature.

CHAPTER 2

THEORY OF METHOD

2-1. General Description of Method

The method employed in this work is well known non-flow calorimetric method. This method has been used successfully for studying the thermodynamic properties of saturated light water liquid and vapour by Osborne (19,20,21,22) and his co-workers at the National Bureau of Standards in the United States.

The principle of this method is quite simple. A sample, part liquid and part vapour, of heavy water or any fluid is enclosed in a container or calorimeter. Heat energy is introduced electrically to the sample for performing measurements on three different types of thermodynamic processes. The first type of experiment is a constant mass experiment in which a fixed amount of sample contained in the calorimeter receives energy such as to change it from an initial saturation state to a final saturation state. The second type of experiment is a vapour withdrawal process in which a known amount of vapour is withdrawn when energy is added to the contents of the calorimeter under isothermal conditions. The third type of experiment is a liquid withdrawal test in which a measured amount of saturated liquid is removed when heat is added to the contents in the calorimeter

under isothermal conditions. The experiment of the first type evaluates the enthalpy of saturated liquid while the experiment of the second type evaluates the enthalpy of evaporation. The third experiment yields a measured quantity which is complementary to the measured quantities obtained in the first two experiments.

For purposes of conserving the input energy, the calorimeter is completely enveloped by a thin metal shield or adiabatic shield whose temperature can be varied quickly and matched to the temperature of the calorimeter shell. Under ideal test conditions there should be no difference in the temperature between the calorimeter shell and the adiabatic shield, consequently the sample in the calorimeter would neither gain nor lose heat from or to the surroundings. But in practice, the ideal condition is seldom achieved and a small net heat exchange invariably occurs between the calorimeter and the adiabatic shield. This small amount of heat leak may be minimized by a proper design and operation of the apparatus which will be described in Chapter 3 of this thesis.

2-2. Theory of Experimental Method

A) Constant mass experiment

This type of experiment may be described as a non-flow continuous heating process in which a fixed amount of sample contained in the calorimeter is taken from one chosen saturation state to another chosen saturation state. Two experiments of this kind are performed in the same temperature interval with different amounts of mass in the calorimeter. The first experiment is carried out on the calorimeter charged with a large amount (high filling) of sample whereas the second experi-

ment is carried out on the calorimeter charged with a small amount (low filling) of sample. It is possible to obtain the enthalpy change or specific heat, c_p, of the fluid without making any tare measurement of the heat capacity of the empty calorimeter. This procedure is extremely useful in the elimination of the errors due,to the heat leak, the small volume change of the calorimeter and the mechanical work involving the straining of the calorimeter shell by the fluid sample.

There are basically two different processes by which the proportion of saturated liquid to saturated vapour changes as energy is added to a calorimeter. This may be explained by reference to the constant mass and constant volume processes shown in Figure 1 and Figure 2. If the heat addition process follows the path a_1a_2, the saturated vapour condenses into liquid until finally a point a_2 is reached at which saturated liquid occupies almost the entire inner volume of the calorimeter. On the other hand if the process follows path b_1b_2 saturated liquid evaporates into saturated vapour until finally a point b_2 is reached at which saturated vapour occupies almost the entire inner volume of the calorimeter.

According to the First Law of Thermodynamics, the energy balance for the constant volume heat addition processes shown diagrammatically in Figure 2 can be written as

$$Q + m_{f_1} u_{f_1} + m_{g_1} u_{g_1} = m_{f_2} u_{f_2} + m_{g_2} u_{g_2} + c_{p_c} \Delta T + q_E + q_s \quad \ldots\ldots\ldots\ldots\ldots\ldots (1)$$

By utilizing the definition of enthalpy and expressing the internal volume of the calorimeter in terms of the masses of saturated liquid and vapour and the specific volumes of saturated liquid and vapour and

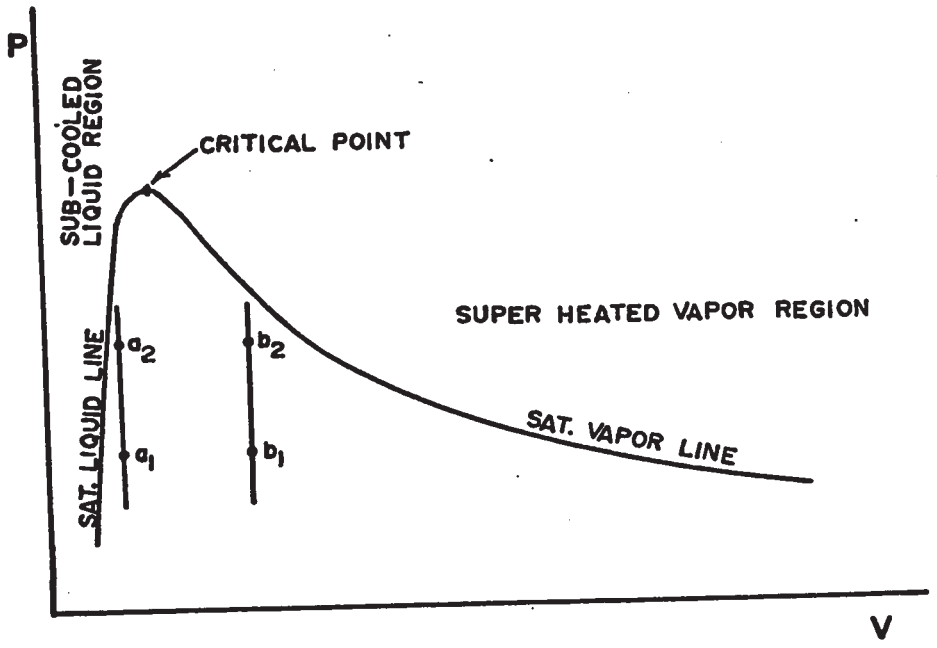

FIGURE 1 PRESSURE — VOLUME DIAGRAM

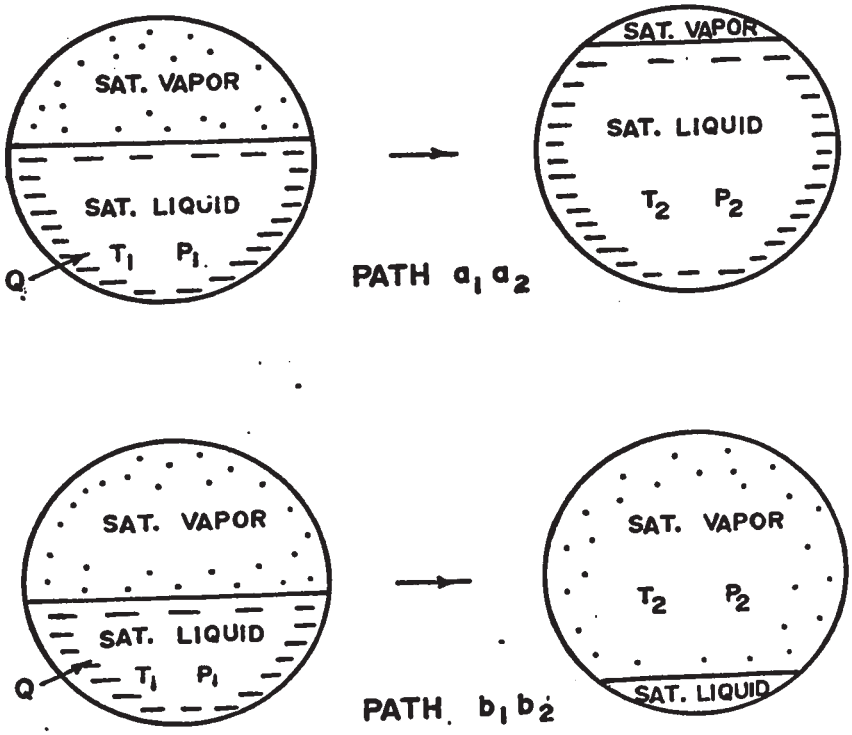

FIGURE 2 CHANGES IN THE PROPORTIONS OF SATURATED LIQUID & VAPOR DURING A CONSTANT MASS & A CONSTANT VOLUME HEAT ADDITION PROCESS

by employing the Clausius Clapeyron equation, the following equation may be derived from equation (1),

$$Q = M\,(h_f - T\,v_f \frac{dp}{dT})_1^2 + V\,(T\frac{dp}{dT} - p)_1^2 + c_{p_c}\,\Delta T + q_E + q_s \qquad \ldots\ldots\ldots\ldots\ldots\ldots (2)$$

Details of the derivation of equation (2) may be found in Appendix A. If Q_H and Q_L denote the measured quantities of total energy added in the high and low filling experiments having a fluid mass of M_H and M_L respectively, then the equation (2) may be written in the following two forms:

$$Q_H = M_H\,(h_f - T\,v_f \frac{dp}{dT})_1^2 + V\,(T\frac{dp}{dT} - p)_1^2 + c_{p_c}\,\Delta T + q_{E_H} + q_s \qquad \ldots\ldots\ldots\ldots\ldots\ldots (3)$$

$$Q_L = M_L\,(h_f - T\,v_f \frac{dp}{dT})_1^2 + V\,(T\frac{dp}{dT} - p)_1^2 + c_{p_c}\,\Delta T + q_{E_L} + q_s \qquad \ldots\ldots\ldots\ldots\ldots\ldots (4)$$

Subtracting equation (4) from equation (3) and rearranging the terms yields the following expression*

$$\frac{Q_H - Q_L}{M_H - M_L} = \Delta(h_f - T\,v_f \frac{dp}{dT}) \qquad \ldots\ldots\ldots\ldots\ldots\ldots (5)$$

Equation (5) infers that a constant mass experiment is substantially a determination of the enthalpy change of a saturated liquid from an initial saturation state at temperature T_1 to a final saturation state at temperature T_2. The term $T\,v_f \frac{dp}{dT}$ which may be determined

---

*It is traditional to assume that the net heat exchange between the calorimeter and the adiabatic shield remains the same during both types of experiments, i.e. $q_{E_H} = q_{E_L}$. Chapter 3 gives details of how the apparatus was designed and utilized to ensure equality between $q_{E_H} = q_{E_L}$.

by a liquid withdrawal test is an extremely small quantity at the lower temperature and only becomes significant at the higher temperatures and pressures. More specifically the correction term is approximately 1%, 6%, 20% of the enthalpy change of saturated liquid of heavy water at temperatures of 100, 200 and 300°C respectively. Figure 3 shows the variation of $\Delta\ (h_f - T\ v_f \frac{dp}{dT})$, $T\ v_f \frac{dp}{dT}$ and $T\ v_g \frac{dp}{dT}$ for saturated light water.

B) Vapour withdrawal test

The vapour withdrawal test is virtually a determination of the latent heat of vaporization. In this type of experiment a small amount of liquid of the contents in the calorimeter is evaporated by adding energy and withdrawn as saturated vapour. During this test the temperature of the system is maintained at an initial saturation state at temperature T_1 so that the metal calorimeter itself would neither gain nor lose energy. The following heat balance may be written for the isothermal vapour withdrawal process as shown diagrammatically in Figure 4,

$$Q_g + m_{f_1} u_{f_1} + m_{g_1} u_{g_1} = \Delta M\ h_g + m_{f_2} u_{f_2} + m_{g_2} u_{g_2} \quad \text{.....(6)}$$

By using the relationship between the internal energy and the enthalpy and employing the Clausius Clapeyron equation, equation (6) may be reduced to the following expression,

$$\frac{Q_g}{M_1 - M_2} = T\ v_g \frac{dp}{dT} \quad \text{.....(7)}$$

Details of the derivation of equation (7) is given in Appendix A.

---

*Since the temperature difference between the calorimeter and the adiabatic shield is extremely small, the heat leak q_E can be considered negligible in the vapor and liquid withdrawal tests.

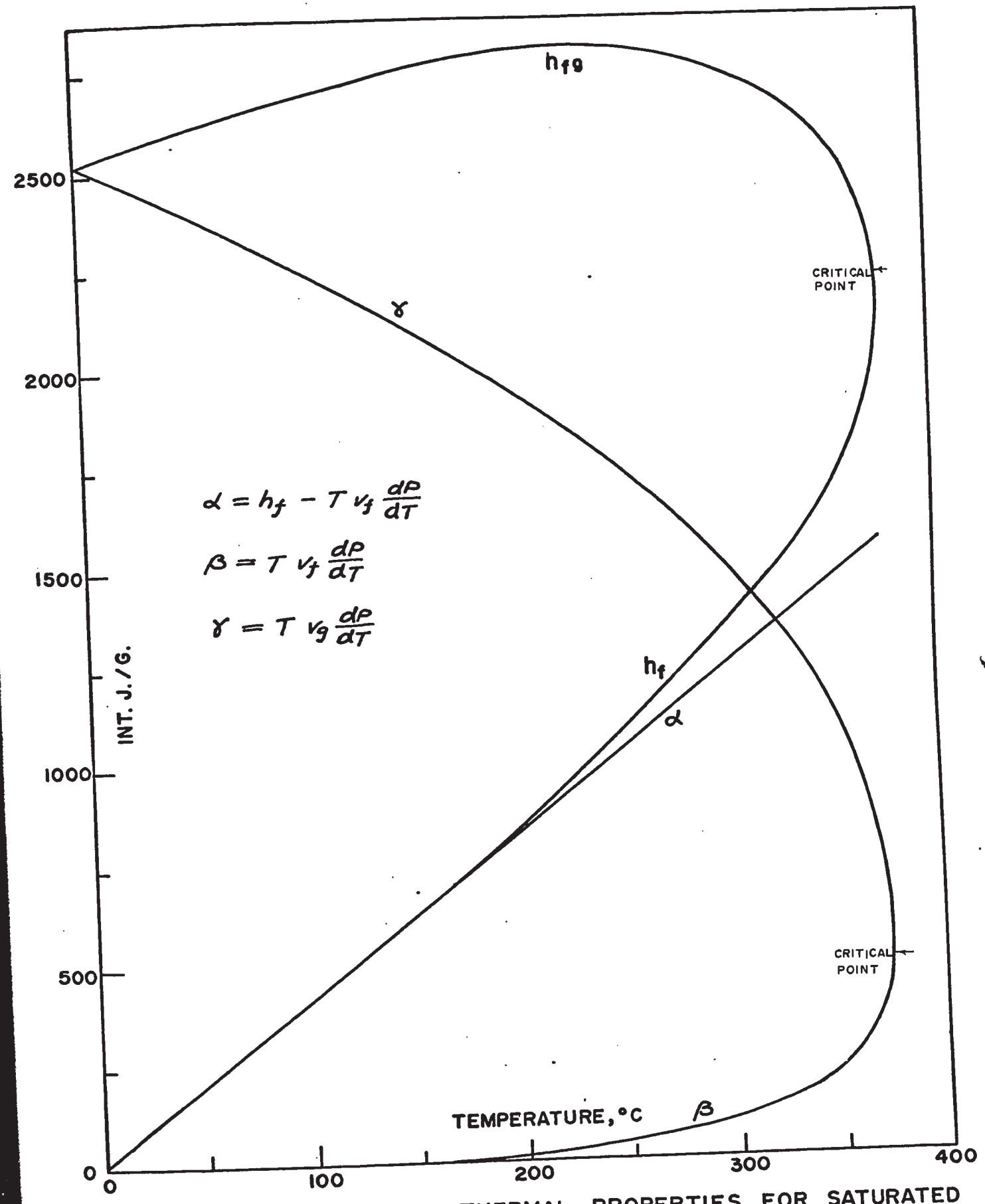

FIGURE 3 FUNDAMENTAL THERMAL PROPERTIES FOR SATURATED LIGHT WATER

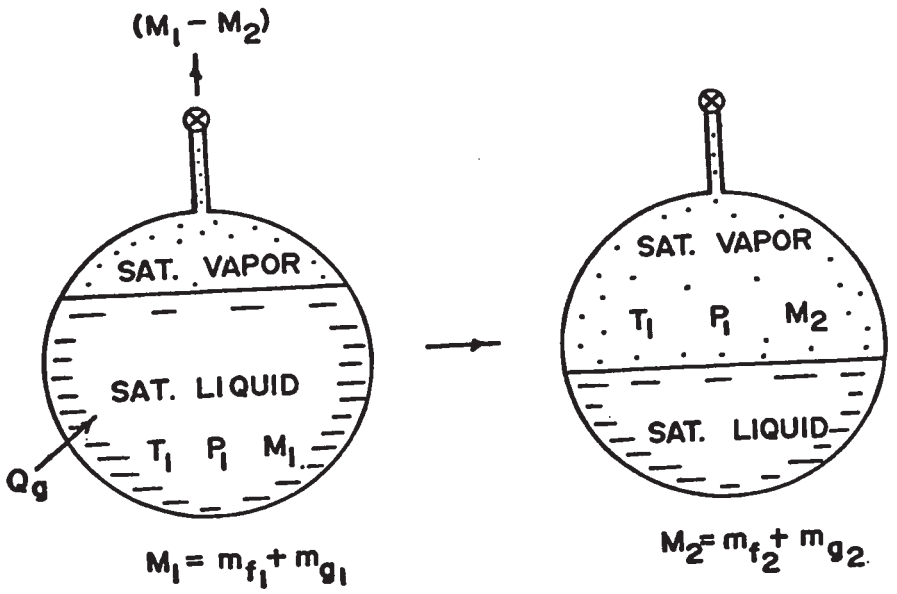

FIGURE 4 ISOTHERMAL HEAT ADDITION SATURATED VAPOR WITHDRAWAL PROCESS

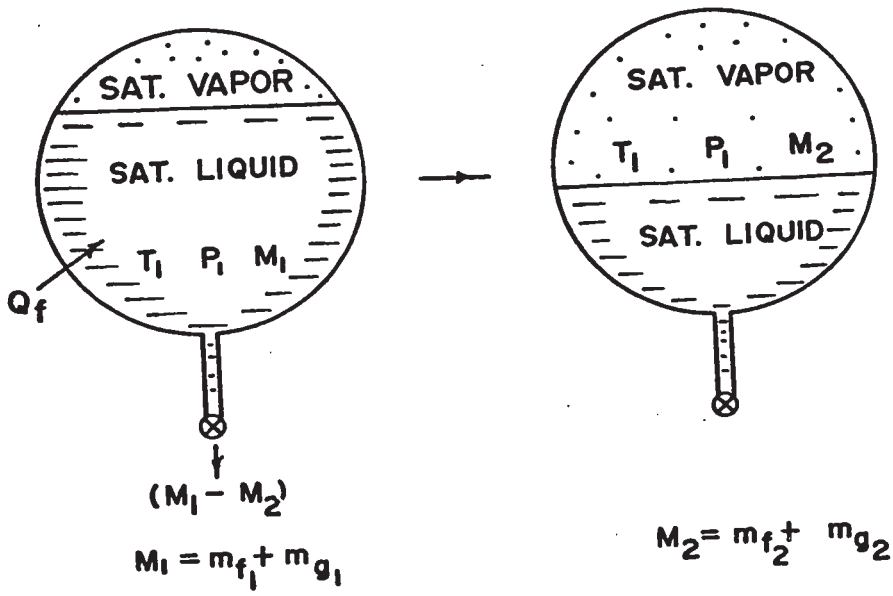

FIGURE 5 ISOTHERMAL HEAT ADDITION SATURATED LIQUID WITHDRAWAL PROCESS

In this type of experiment energy is required not only to evaporate the portion of mass withdrawn from the calorimeter but also to produce an additional amount of vapour to fill up the space previously occupied as liquid in the calorimeter. The energy added to a unit mass withdrawn from the calorimeter is different from the latent heat of vaporization by this extra amount, and this correction turns out to be the same as that required to evaluate the enthalpy of saturated liquid from the result of constant mass experiment. More specifically it can easily be shown that $v_g T \, dp/dT \equiv h_{fg} + v_f T \, dp/dT$.

C) Liquid withdrawal test

The liquid withdrawal test is a determination of the corrections complementary to the other two types of experiments to evaluate the enthalpy of saturated liquid and the latent heat of vaporization. This correction may be measured directly by adding energy to the calorimeter and withdrawing just that portion of saturated liquid from the calorimeter necessary to maintain an isothermal condition. The energy required in this type of experiment is to evaporate enough liquid to fill the space which previously occupies by the small amount of liquid withdrawn from the calorimeter.

The heat balance of this type process shown in Figure 5 may be written as follows:

$$Q_f + m_{f_1} u_{f_1} + m_{g_1} u_{g_1} = \Delta M h_f + m_{f_2} u_{f_2} + m_{g_2} u_{g_2} \quad \ldots\ldots\ldots\ldots\ldots\ldots (8)$$

By making the same assumptions as described previously in the vapour withdrawal test and using the same techniques to simplify equation (8), the following expression may be easily obtained,

$$\frac{Q_f}{M_1 - M_2} = T\, v_f \frac{dp}{dT} \qquad \ldots\ldots\ldots\ldots\ldots\ldots (9)$$

Details of derivation of equation (9) is also found in Appendix A.

It should be mentioned that equation (9) was derived by assuming the energy added to the calorimeter is conserved and the temperature of the calorimeter is invariant. However it is extremely difficult to obtain these ideal conditions, consequently a correction described more fully in Chapter 8 was applied to the input energy term.

Let the measured quantities of the experiments of constant mass, saturated vapour withdrawal and saturated liquid withdrawal be denoted by Alpha, Gamma and Beta (i.e. α, γ and β) respectively. By simple algebraic combination of equations (5), (7) and (9) and without using any thermodynamic relation, it may be reduced to the following group of equations

$$\Delta h_f = \Delta \alpha + \Delta \beta \qquad \ldots\ldots\ldots\ldots\ldots\ldots (10)$$

$$\Delta h_g = \Delta \alpha + \Delta \gamma \qquad \ldots\ldots\ldots\ldots\ldots\ldots (11)$$

$$h_{fg} = \gamma - \beta \qquad \ldots\ldots\ldots\ldots\ldots\ldots (12)$$

These three equations show how the enthalpy change of saturated liquid and saturated vapour along with the enthalpy of vaporization can be determined directly by making three types of experiments as described previously. Other thermodynamic properties of saturated liquid and vapour may also be derived from the group of experimental data. The specific volume of saturated liquid and vapour may be obtained from equations (13) and (14),

$$v_f = \frac{\beta}{T \frac{dp}{dT}} \qquad \ldots\ldots\ldots\ldots\ldots\ldots (13)$$

$$v_g = \frac{\gamma}{T \frac{dp}{dT}} \qquad \ldots\ldots\ldots\ldots\ldots\ldots (14)$$

provided knowledge of the variation of saturation pressure with temperature is known. The entropy of saturated liquid and vapour may be derived from equations (15) and (16),

$$s_f = \frac{h_f}{T} + \int \frac{\alpha}{T^2} dT + c \qquad \ldots\ldots\ldots\ldots\ldots\ldots (15)$$

$$s_g = \frac{h_g}{T} + \int \frac{\alpha}{T^2} dT + c \qquad \ldots\ldots\ldots\ldots\ldots\ldots (16)$$

where constant c dependents upon the arbitrary datum chosen for the various quantities in the equations. The specific heat of saturated vapour and liquid may be obtained from equations (17) and (18),

$$c_{p_f} = T \frac{d}{dT} \left(\frac{h_f}{T}\right) + \frac{\alpha}{T} \qquad \ldots\ldots\ldots\ldots\ldots\ldots (17)$$

$$c_{p_g} = T \frac{d}{dT} \left(\frac{h_g}{T}\right) + \frac{\alpha}{T} \qquad \ldots\ldots\ldots\ldots\ldots\ldots (18)$$

Derivations of equations (15) to (18) are given in Appendix A.

CHAPTER 3

APPARATUS DESIGN

The main features of the apparatus may be explained by reference to the small-scale reproduction of the assembly drawing shown in Figure 6. The apparatus essentially consisted of three parts:

(i) The high pressure metal calorimeter to contain the fluid sample,

(ii) The thin-walled adiabatic shield surrounding the calorimeter,

(iii) The outer guard surrounding the calorimeter and adiabatic shield.

Figure 7 shows the apparatus during the initial stages of assembly. Details of the apparatus design are given in the following sections of this Chapter.

3-1. Calorimeter

The term calorimeter in this thesis denotes that part of the apparatus containing the heavy water sample under investigation. It consists of a spherical thin walled metal shell, a silver heat diffusion system, and two electric heaters (upper and bottom zone heaters). They are described separately below.

A) Calorimeter Shell

In calorimetric measurement the temperature and the electric

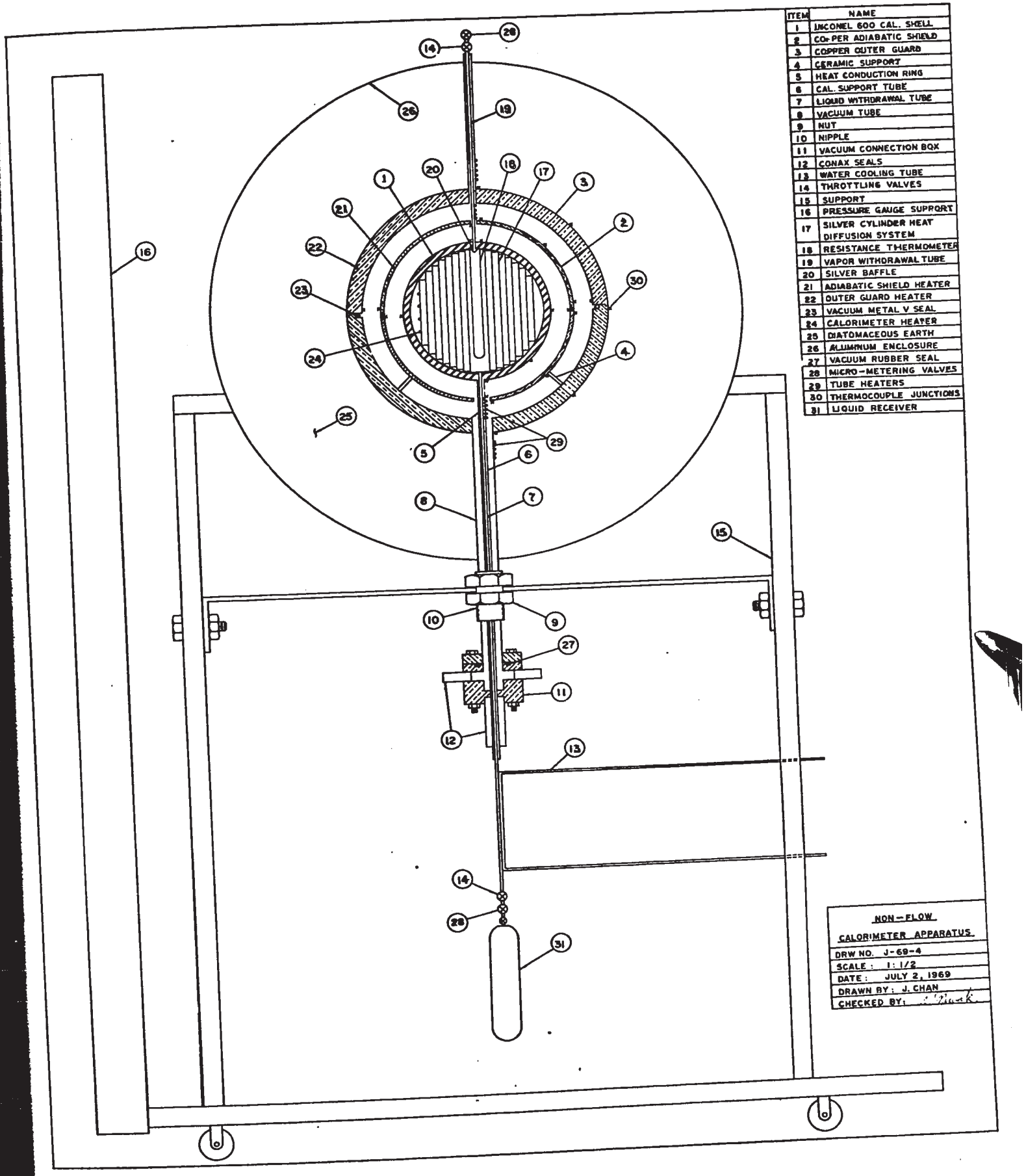

FIGURE 6. NON-FLOW CALORIMETER APPARATUS

FIGURE 7 APPARATUS DURING INITIAL STAGES OF ASSEMBLY

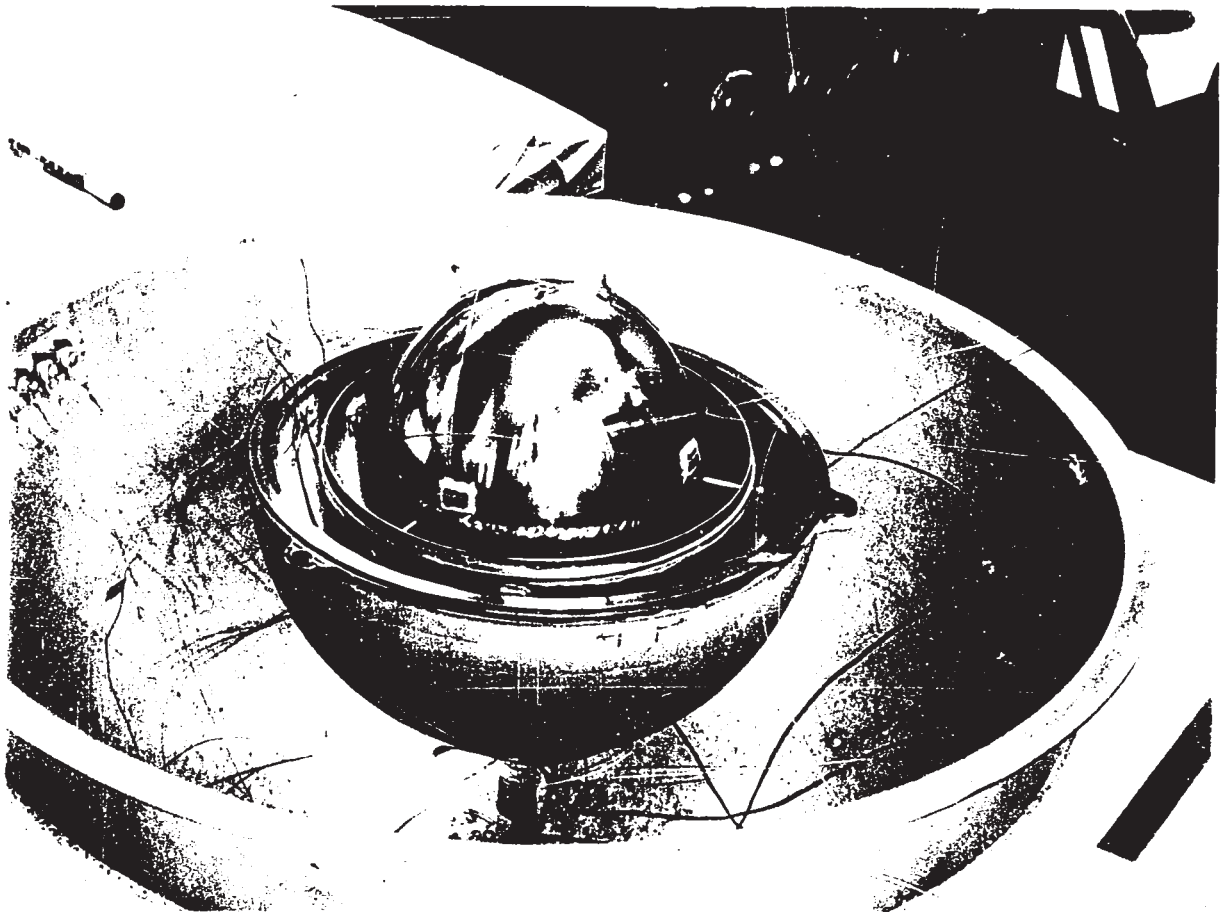

FIGURE 7 APPARATUS DURING INITIAL STAGES OF ASSEMBLY

input energy are relatively easy to measure accurately to within 0.03 percent with modern techniques and instrumentation. The largest uncertainty in performing constant mass experiment is the uncertainty in heat exchange between the calorimeter and its immediate surroundings which results from experimental departures from the ideal adiabatic condition. On the other hand the largest uncertainty in making liquid and vapour withdrawal test is the uncertainty in energy absorbed or released by the calorimeter which results from experimental departures from the ideal isothermal condition. In order to minimize these uncertainties in experiments, the following criteria proposed by Nowak (16) were carefully considered in design of the present calorimeter;

(i) The energy absorbed by the calorimeter shell should be small in comparison to that absorbed by the fluid contents,

(ii) The thermal diffusivity of the metal shell should be as large as possible,

(iii) The calorimeter shell material should be corrosion resistant, machinable and weldable,

(iv) The ratio of the inner volume of the calorimeter to its surface area should be large. More specifically, the surface heat loss should be small in comparison to the total energy added to the fluid contents.

The first three criteria governed the choice of the calorimeter shell material while the last criterion governed the size and geometry of the calorimeter.

Inconel 600 was chosen for the calorimeter shell because thorough study of the properties of all materials revealed that it

possessed the various desirable characteristics for the present application.

Two hemispheres, having a radius of 2.5 inches and a wall thickness of 0.25 inches, were machined from a 6 inches diameter Inconel 600 bar. Figure 8 is a photograph of the calorimeter shell taken during machining. The calorimeter was formed by welding the two hemispheres shown in Figure 9 together at the equator. It was designed for operation up to 225 kg/cm^2 (3200 psia) and 375^{o}C. The design calculations are given in Appendix B. Figure 10 is a photograph of the special welding jig holding the calorimeter shell prior to being welded together while Figure 11 is a photograph of the completed calorimeter.

The calorimeter was pressure tested before the apparatus was assembled. The following steps were used to detect any leakage in the calorimeter:

(i) Pressurize the calorimeter to 35 kg/cm^2 (500 psi) with gas and check leakage with SNOOP,*

(ii) Pressurize the calorimeter to 281 kg/cm^2 (4000 psi) with water at room temperature for 72 hours,

(iii) Pressurize the calorimeter with saturated steam at 350^{0}C for 48 hours.

No leakage was found during these proof tests.

B) Silver Heat Diffusion System

Since heavy water has a relatively low value of thermal

---

*Leak Detector, Nupro Company, 15635 Saranac Road, Cleveland, Ohio 44110, U.S.A.

FIGURE 8 MACHINING OF CALORIMETER SHELL

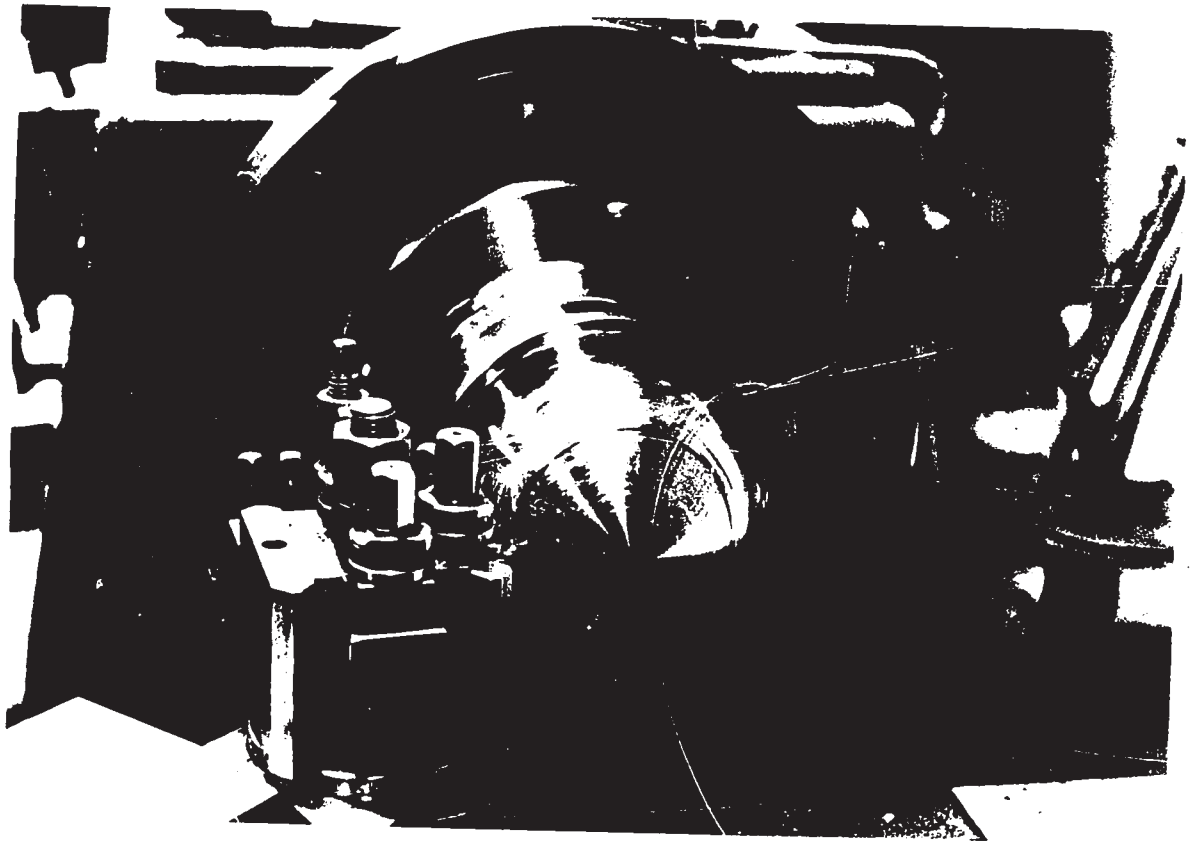

FIGURE 8 MACHINING OF CALORIMETER SHELL

FIGURE 9 VIEW OF CALORIMETER SHELL, THERMOWELL AND ELECTRICAL LEADOUTS

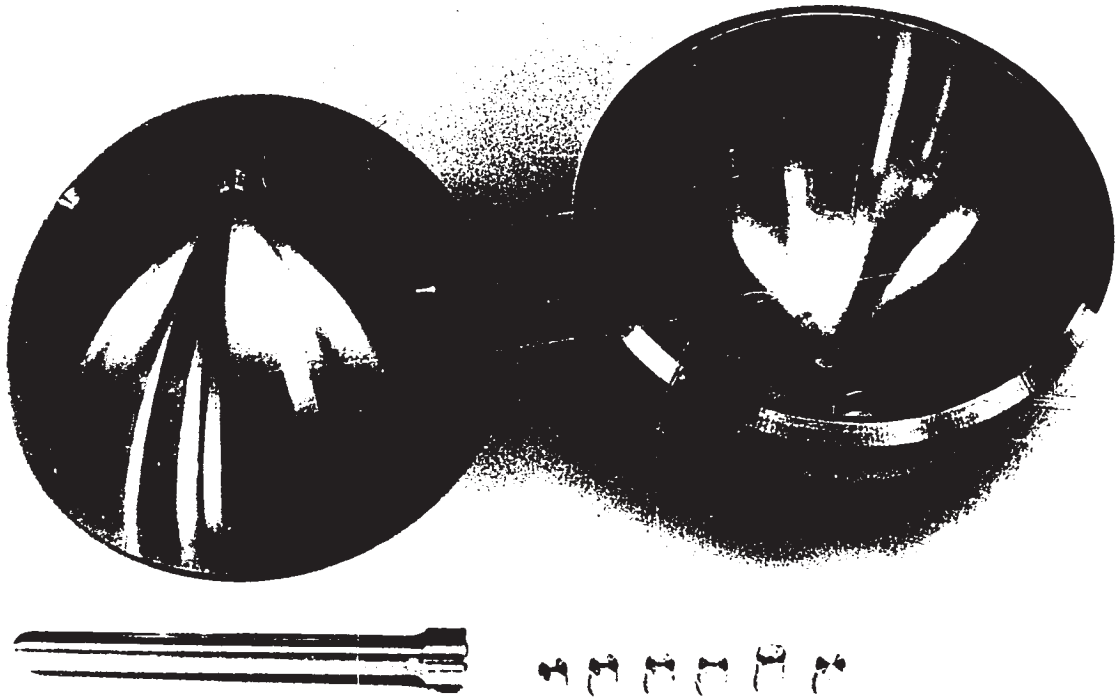

FIGURE 9 VIEW OF CALORIMETER SHELL, THERMOWELL AND ELECTRICAL LEADOUTS

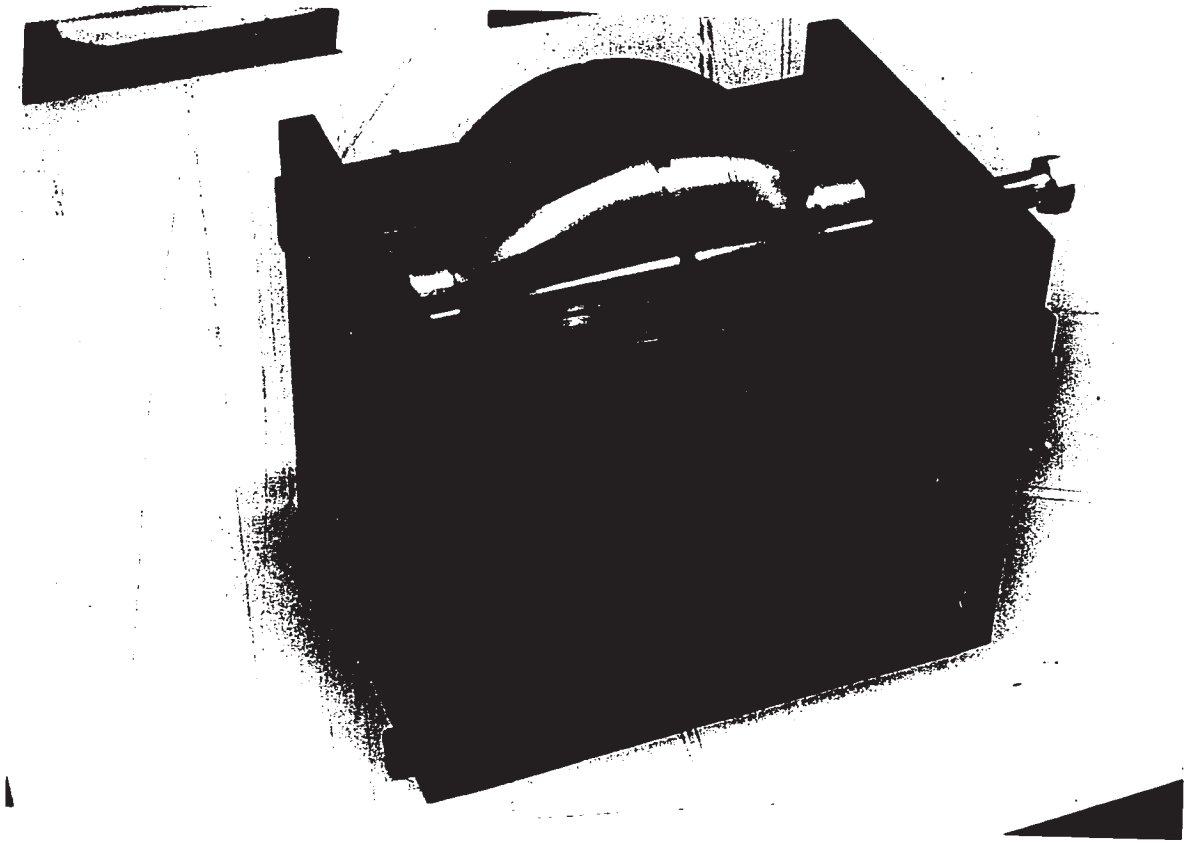

FIGURE 10 WELDING JIG HOLDING CALORIMETER SHELL PRIOR TO BEING WELDED TOGETHER

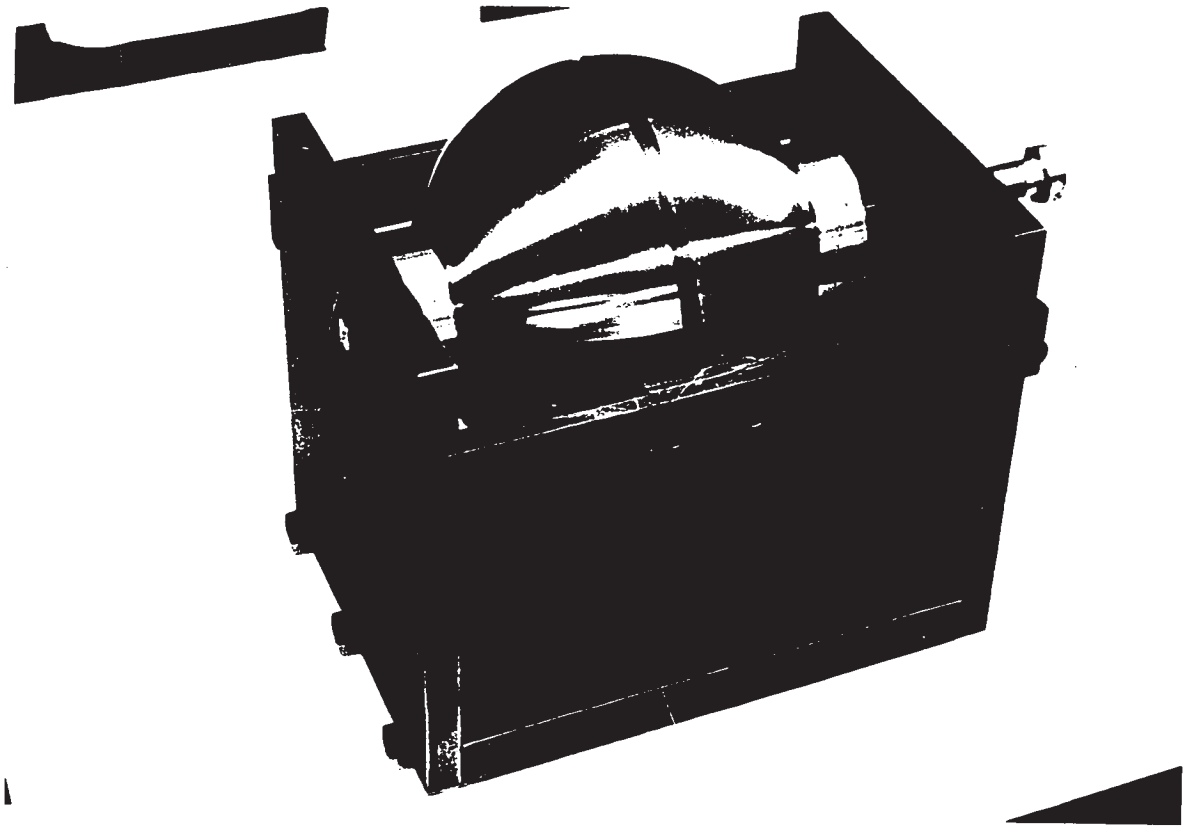

FIGURE 10 WELDING JIG HOLDING CALORIMETER SHELL PRIOR TO BEING WELDED TOGETHER

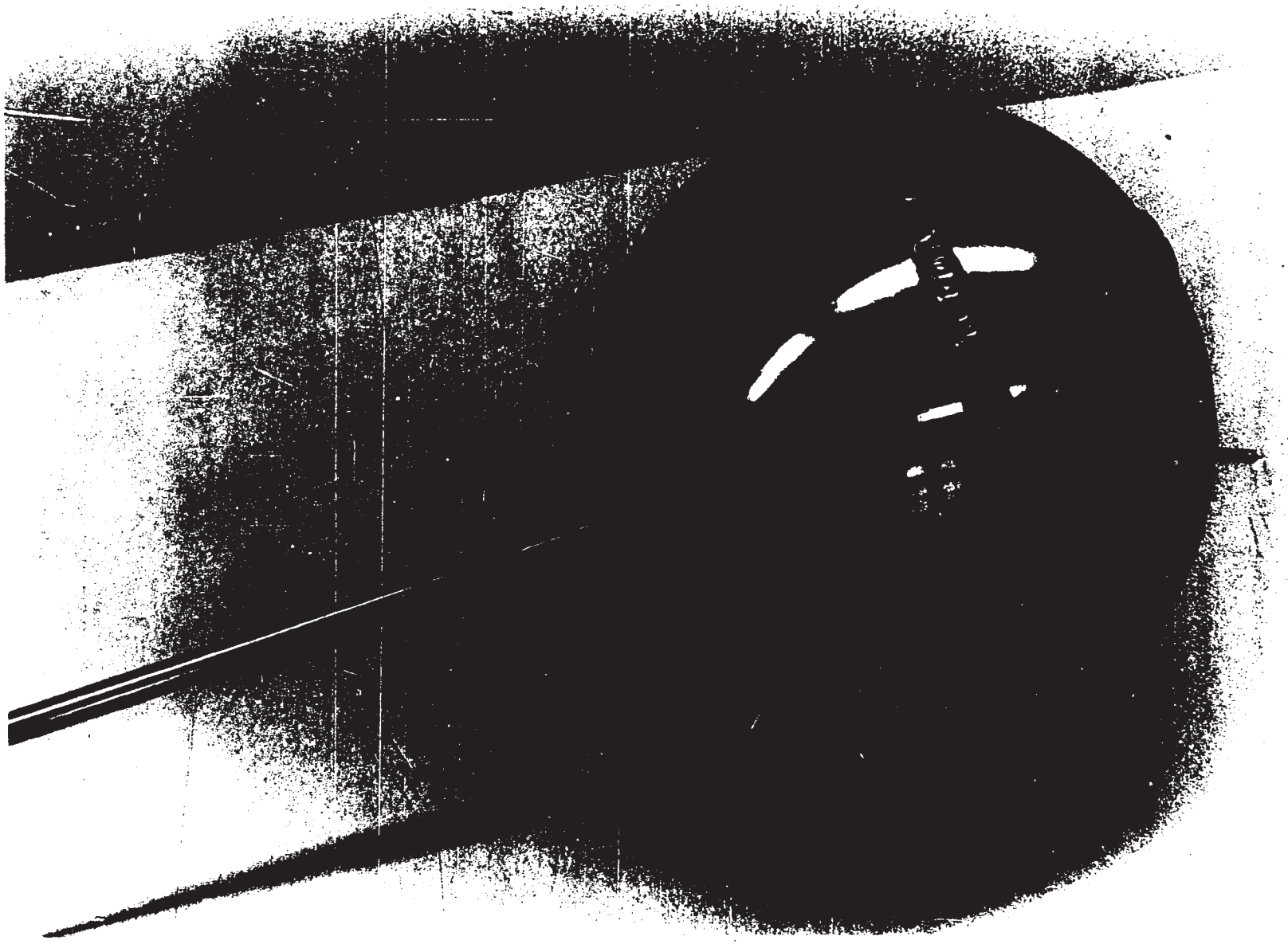

FIGURE 11 VIEW OF CALORIMETER

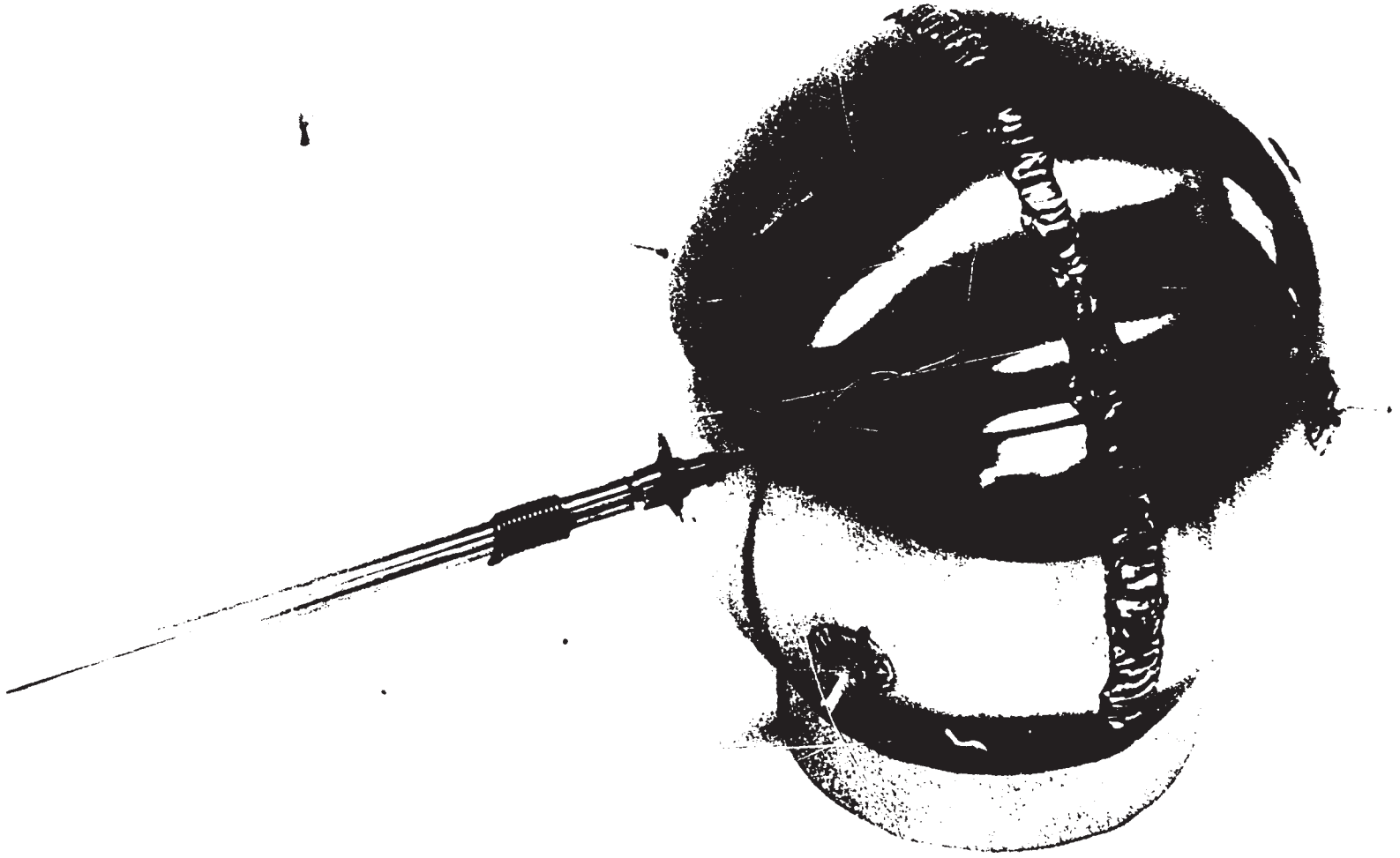

FIGURE 11 VIEW OF CALORIMETER

conductivity, large temperature variations of the order of tens of degrees would be produced in the heavy water sample if the heat were transferred from the surface of the calorimeter shell to the interior of the heavy water sample solely by heat conduction.

The equation for heat conduction in a spherical heavy water sample is

$$\frac{\partial (\theta r)}{\partial T} = \alpha \frac{\partial^2 (\theta r)}{\partial r^2} \qquad \ldots\ldots\ldots\ldots\ldots\ldots (17)$$

The solution to equation (17) must satisfy the initial requirement that the initial temperature in the sample is uniform and the boundary condition that surface temperature of the spherical sample increases uniformly with time, i.e.

$$\theta = 0 \quad \text{at} \quad T = 0$$

and

$$\theta = \beta T \quad \text{at} \quad r = R$$

Thus the general solution (23) to equation (17) is:

$$\theta = \beta T - \frac{\beta}{6\alpha}(R^2 - r^2) + \frac{2\beta R^2}{\alpha} \sum_{m=1}^{\infty} \frac{1}{m^3 \pi^3 (-1)^{m+1}} e^{-\frac{\alpha m^2 \pi^2 T}{R^2}} \frac{R}{\gamma} \operatorname{Sin} \frac{m\pi r}{R}$$

$$\ldots\ldots\ldots\ldots\ldots\ldots (18)$$

Hence the temperature difference between the center and the exterior surface of the heavy water sample is

$$\Delta\theta = \frac{\beta R^2}{6\alpha} - \frac{2\beta R^2}{\alpha} \sum_{m=1}^{\infty} \frac{1}{m^2 \pi^2 (-1)^{m+1}} e^{-\frac{\alpha m^2 \pi^2}{R^2} T}$$

or

$$\Delta\theta = \frac{\beta R^2}{6\alpha} - \frac{2\beta R^2}{\alpha\pi^2} e^{-\frac{\alpha\pi^2}{R^2} T} + \frac{2\beta R^2}{4\alpha\pi^2} e^{-\frac{4\alpha\pi^2}{R^2} T} - \frac{2\beta R}{9\alpha\pi^2} e^{-\frac{9\alpha\pi^2}{R^2} T}$$

$$\ldots\ldots\ldots\ldots\ldots\ldots (19)$$

The first term on the right hand side is a constant and hence it is called the steady state solution. The remaining exponential terms on the right hand side are transients in time and is called the transient solution. When the time T becomes sufficiently large, the exponential terms will approach zero and the temperature difference between the center and the surface of the sample approaches the steady state value of $\beta R^2/6\alpha$. A graph of the temperature difference versus time for various heating rates as parameters is given in Figure 12.

The foregoing analytical solutions for temperature variations in the heavy water sample are based entirely on the assumption that the heat transfer in the sample is by heat conduction. It can be seen that even for a small heating rate of approximately $10^{\circ}C$ per hour, the maximum temperature difference in the heavy water sample would approach $13^{\circ}C$. Since the thermodynamic properties are equilibrium properties, such temperature variations in the sample would vitiate the measurements.

In order to prevent the occurrence of large temperature variations in the heavy water sample, a heat diffusion system constructed from silver plates having a thickness of 0.01 inches was installed inside the calorimeter shell. The reason for choosing pure silver to fabricate the heat diffusion system is that it possesses an extremely high thermal conductivity and good oxidation characteristics. Figure 13 is a photograph of the completed silver heat diffusion system while Figure 14 is a photograph of the silver heat diffusion system during the initial phase of installation into the calorimeter shell.

Detailed drawings of the silver heat diffusion system are given in Figure 1C, 2C and 3C of Appendix C. The spacing between the

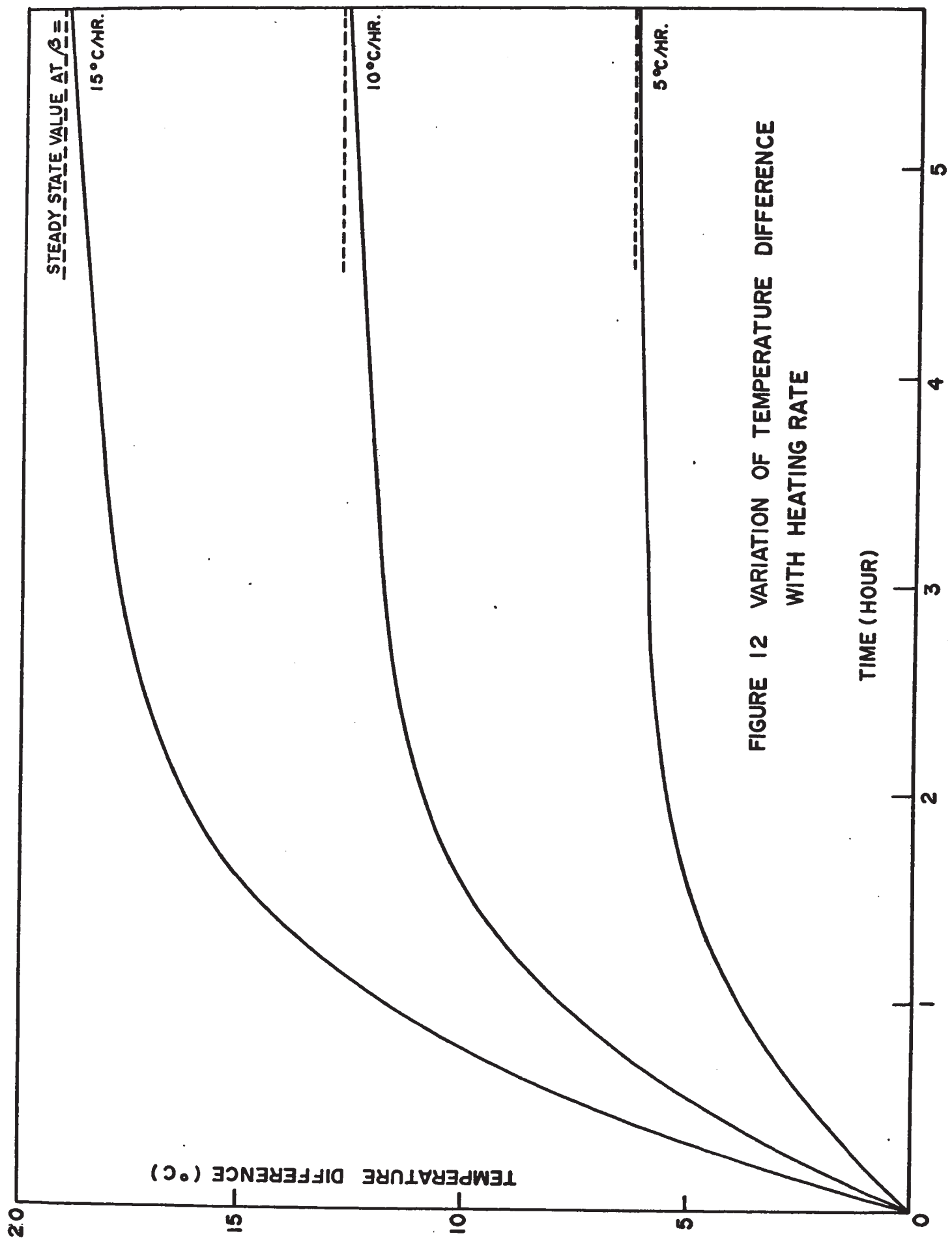

FIGURE 12 VARIATION OF TEMPERATURE DIFFERENCE WITH HEATING RATE

FIGURE 13 VIEW OF SILVER HEAT DIFFUSION SYSTEM

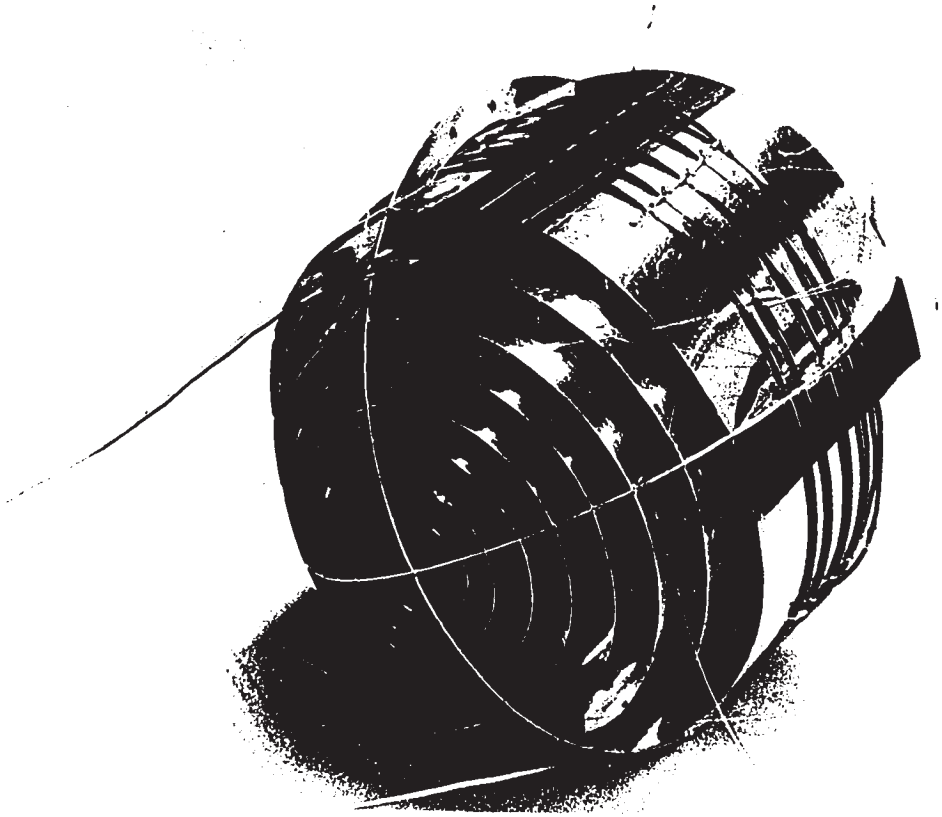

FIGURE 13 VIEW OF SILVER HEAT DIFFUSION SYSTEM

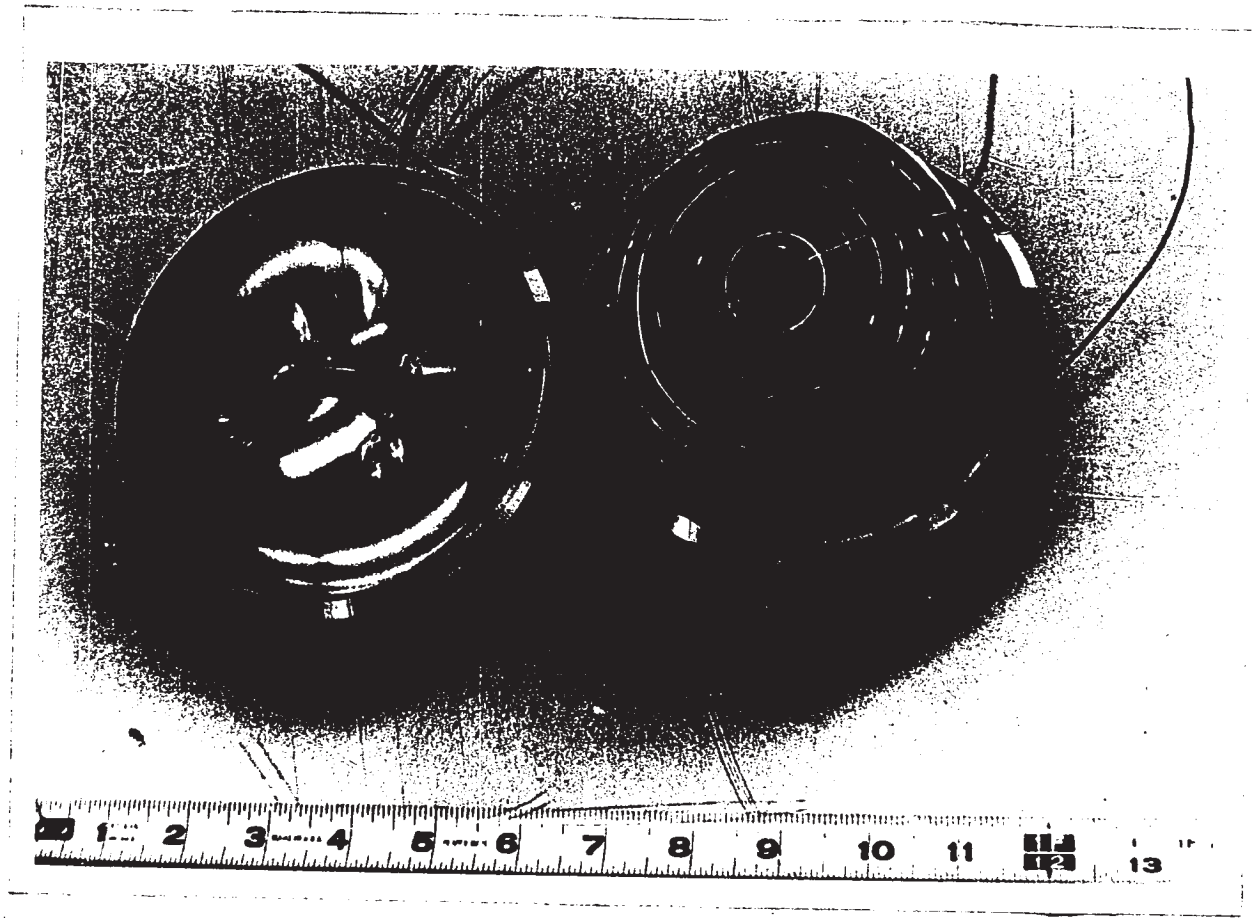

FIGURE 14 INSTALLATION OF HEAT DIFFUSION SYSTEM INTO CALORIMETER SHELL

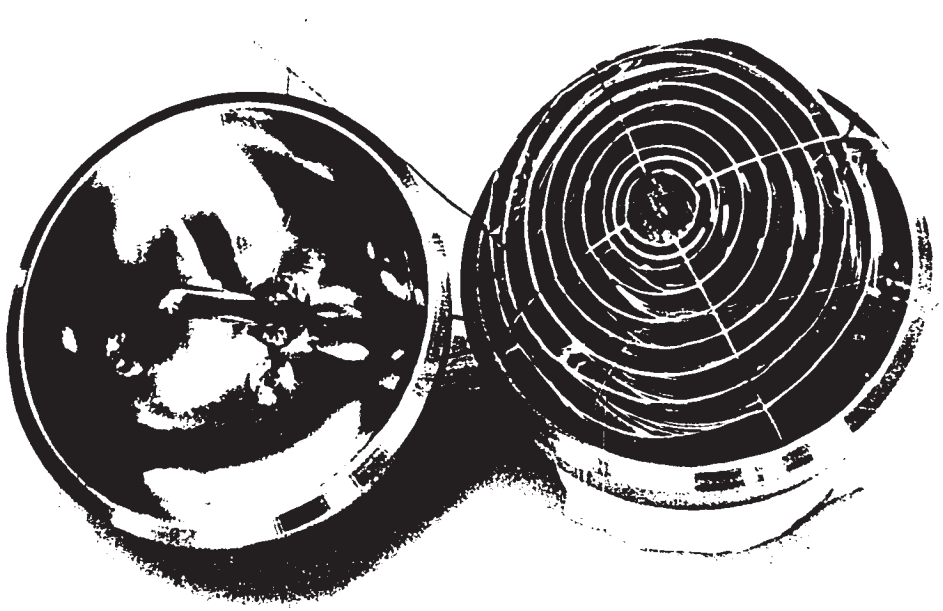

FIGURE 14 INSTALLATION OF HEAT DIFFUSION SYSTEM INTO CALORIMETER SHELL

concentric silver cylinders is one quarter of an inch while the total heat exchange surface of the heat diffusion system amounted to approximately 467 square inches.

The temperature distribution in the heavy water sample between the cylinders may be obtained from the following equation of heat flow

$$\frac{\partial^2 T}{\partial r^2} + \frac{1}{r}\frac{\partial T}{\partial r} = \frac{1}{\alpha}\frac{\partial T}{\partial} \qquad \ldots\ldots\ldots\ldots\ldots\ldots (20)$$

It was shown in reference 24 that the temperature difference between the surface of cylinders and the mid plane of the heavy water sample is

$$\Delta T = \frac{\beta}{4\alpha}(r^2 - a^2) + \frac{\beta(b^2-a^2)}{4\alpha \ln \frac{a}{b}}(\ln r - \ln a) \qquad \ldots\ldots\ldots\ldots\ldots\ldots (21)$$

where $r = \frac{a+b}{2}$

A graph of the temperature difference in the heavy water sample between the cylinder of 2.25 inches diameter and of 2.75 inches diameter for various heating rates is shown in Figure 15. It can be seen that at a heating rate of 10°C per hour the maximum temperature difference in the heavy water sample would not exceed 0.07°C. Based on test results the surface temperature variations along the calorimeter shell was found to be less than 0.2°C at a heating rate of 10°C per hour. In view of this it may be concluded that the silver heat diffusion system was effective in minimizing the temperature difference in the heavy water sample. The additional temperature variations on the calorimeter surface amounting to approximately 0.1°C may be attributed to, (i) heat conduction along the differential thermocouple

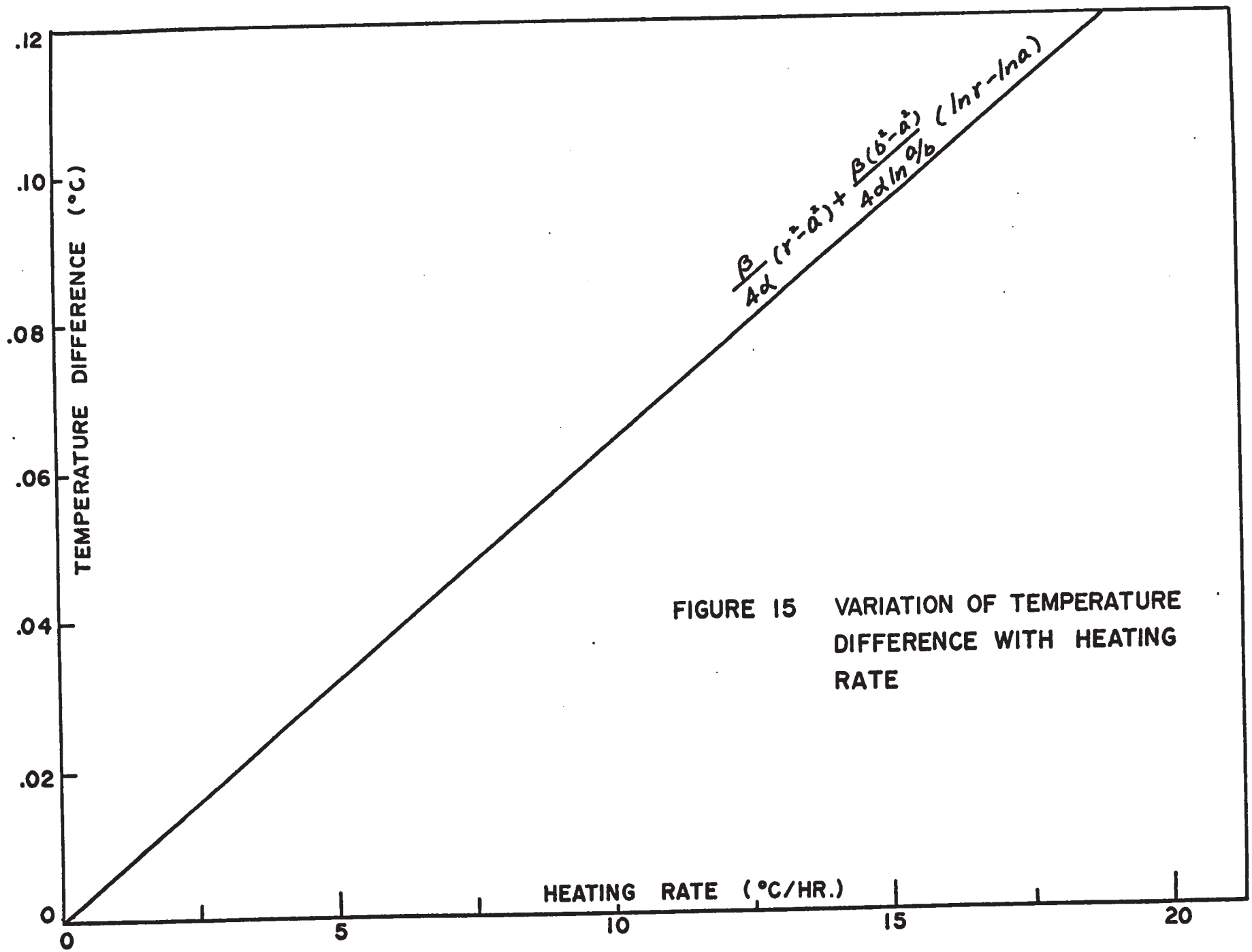

FIGURE 15 VARIATION OF TEMPERATURE DIFFERENCE WITH HEATING RATE

leads, power leads, resistance thermometer leads and support tubing, (ii) convection in the heavy water sample, (iii) uneven resistivity and heating of the calorimeter heater.

C) Calorimeter Heaters

The calorimeter heaters consisted of a single Inconel conductor approximately 0.01 inches in diameter insulated by magnesia oxide powder and sheathed in a 0.04 inches Inconel tube. A cross section of this special wire is shown in Figure 16. Two 30 feet lengths of this wire each having a total resistance of approximately 105 ohms were employed in the calorimeter as a bottom and upper zone heater. Both heaters were wrapped around the concentric cylinders of the heat diffusion system but at different locations. One heater was placed on the upper part of the silver heat diffusion system whereas the other was placed on the lower part of the heat diffusion system. Figure 1C of Appendix C gives an indication of how the heaters were wrapped around the concentric cylinders. During the low filling constant mass experiments, or the liquid withdrawal tests only the bottom zone heater of the calorimeter was employed. On the other hand during the high filling constant mass experiments both calorimeter heaters, bottom zone and upper zone heaters, were employed. With this arrangement, the temperature distributions over the metal surfaces of the calorimeter and adiabatic shield in the high filling and low filling experiments were essentially the same, consequently the heat leaks in these two types of experiments were almost identical. Figures 17 and 18 show the temperature variations on the surface of the calorimeter during a typical high filling and low filling constant mass experiment whereas the locations of the various differential thermocouples installed on

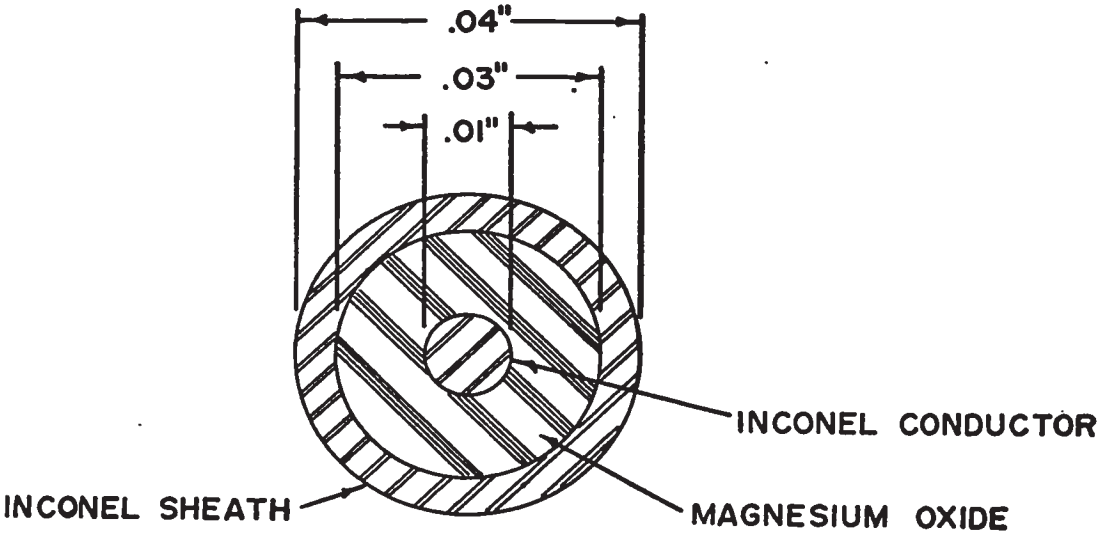

FIGURE 16 CROSS SECTION OF THERMOCOAX HEATING ELEMENT

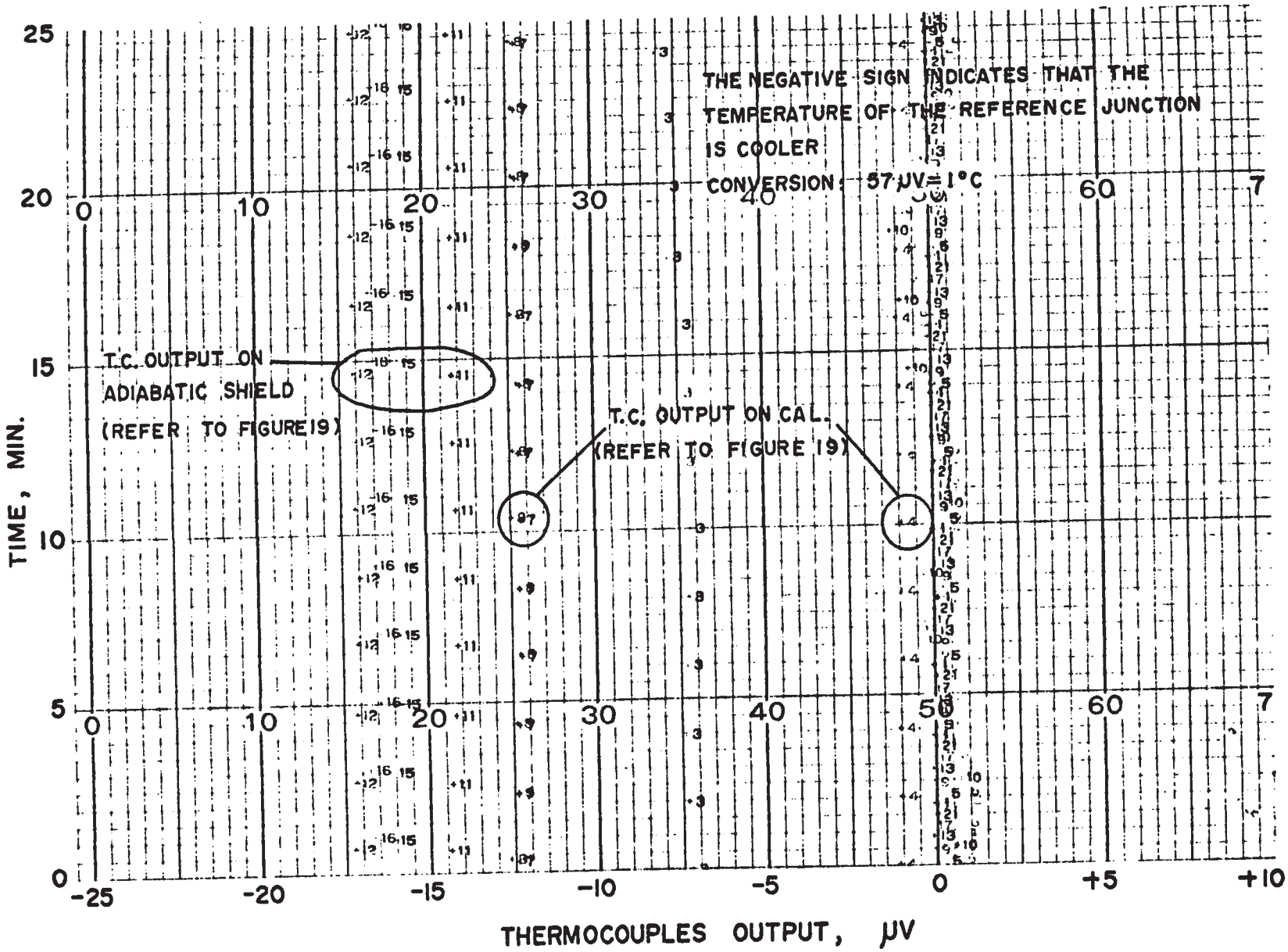

FIGURE 17 TEMPERATURE VARIATIONS ON THE CALORIMETER & ADIABATIC SHIELD DURING A TYPICAL HIGH FILLING CONSTANT MASS EXPERIMENT

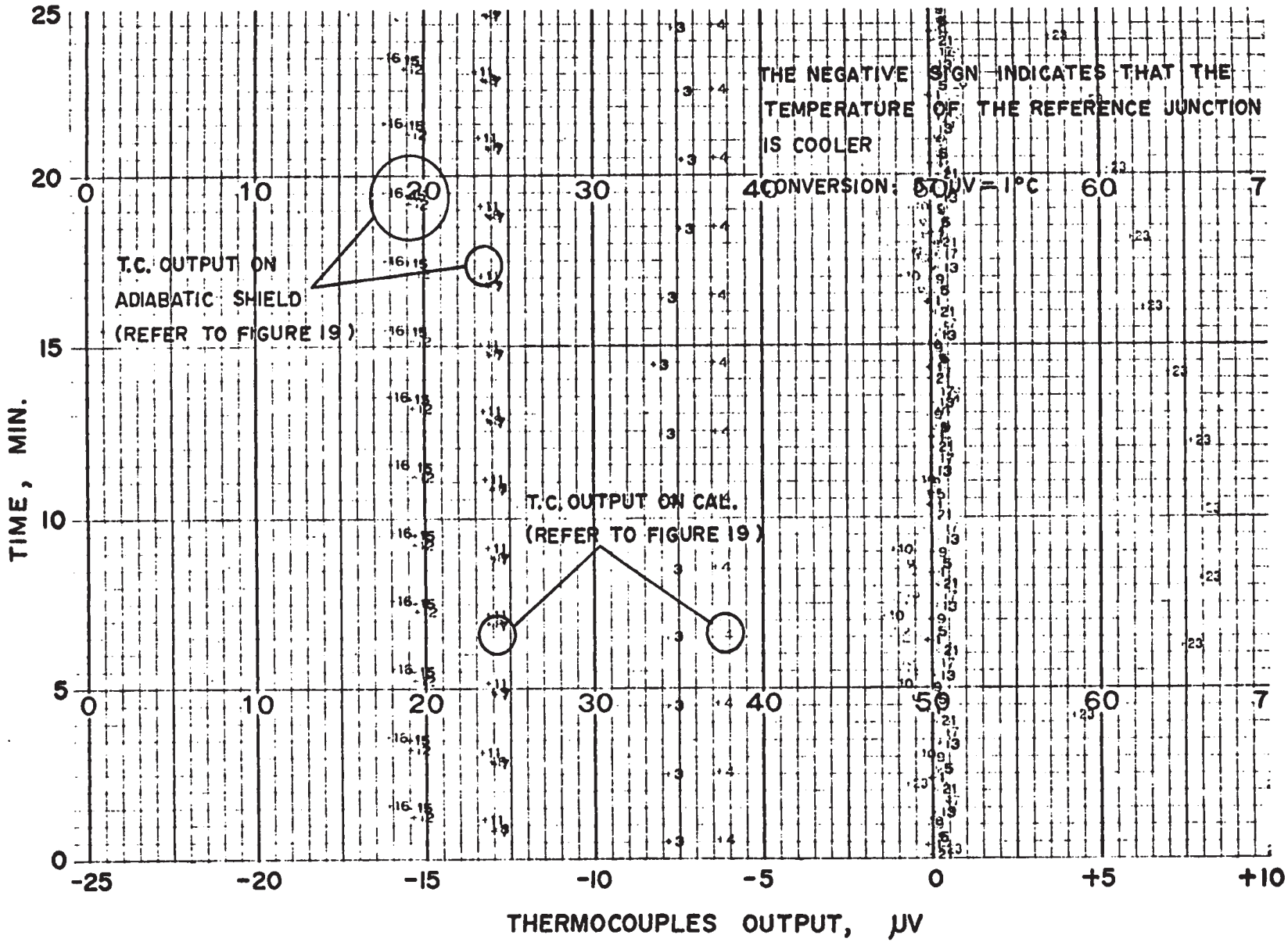

FIGURE 18 TEMPERATURE VARIATIONS ON THE CALORIMETER & ADIABATIC SHIELD DURING A TYPICAL LOW FILLING CONSTANT MASS EXPERIMENT

the calorimeter are given in Figure 19. It is evident that the difference in temperature variations on the calorimeter and adiabatic shield during high and low mass filling experiments were within approximately 0.03°C with the exception of the bottom part which seemed to differ by about 0.1°C.

Great care was taken that all parts of the calorimeter were clean before the calorimeter was assembled. They were washed with warm soapy water, acetone and then rinsed with distilled water and dried in a stream of nitrogen (25). The interior surface of the calorimeter shell was kept as clean as possible during welding process by purging argon into the vessel. Also the calorimeter was flushed several times by alternately injecting and evacuating hot distilled water after welding.

3-2. The Adiabatic Shield

The adiabatic shield as shown in Figure 20 was spun from sheets of oxygen free high thermal conductivity pure copper into hemispheres having a diameter of approximately 7 inches and a wall thickness of approximately 1/8 inches. The hemispheres were joined together by means of screws at the equator. Two Inconel sheathed heating coils were silver soldered in grooves which in turn were machined uniformly over the entire surface of the adiabatic shield. This method of fastening heating elements gave a very uniform surface temperature of the adiabatic shield. It was found for example that at a heating rate of 10°C per hour the temperature variations on the adiabatic shield were within 0.05°C with the exception of the bottom part which was about 0.25°C lower in temperature than the other

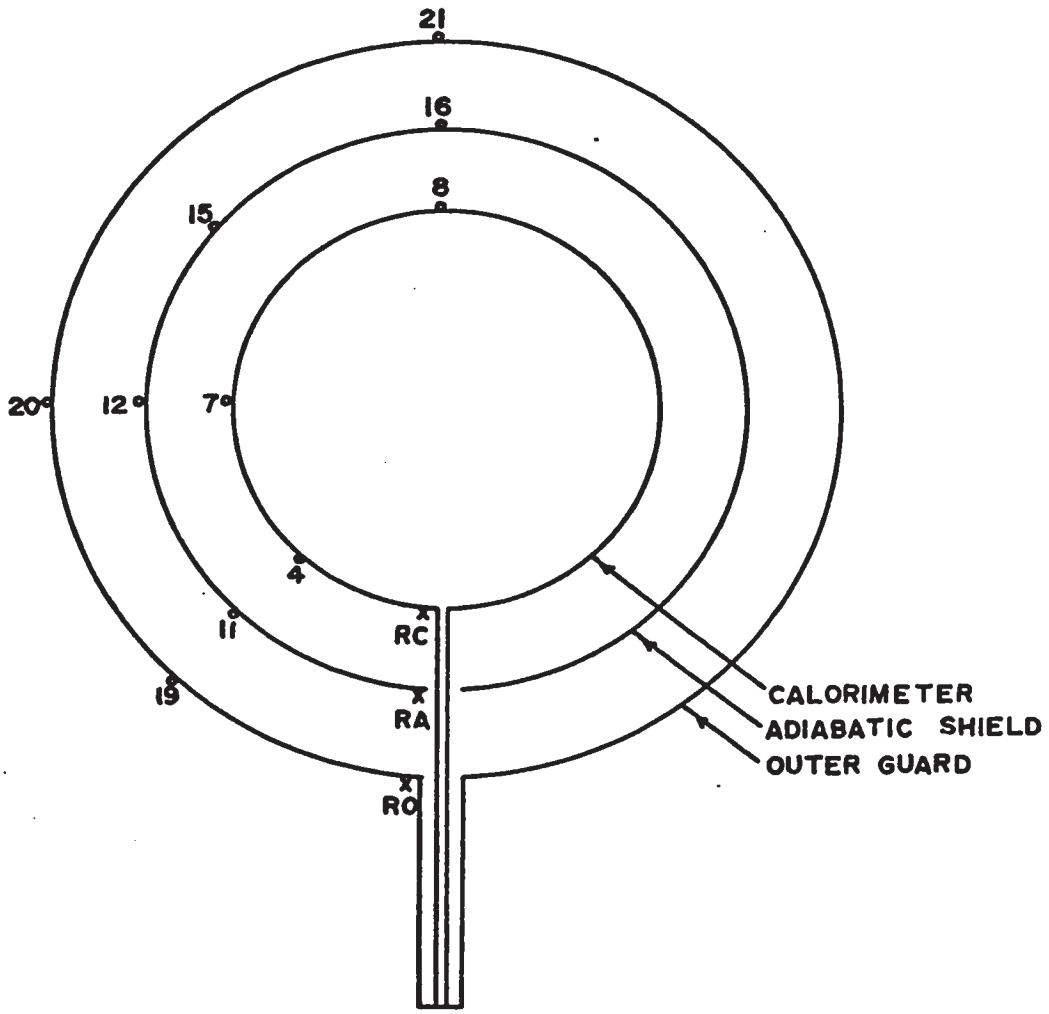

RC = REFERENCE JUNCTION OF T.C. NO. 4, 7, 8
RA = REFERENCE JUNCTION OF T.C. NO. 11, 12, 15 & 16
RO = REFERENCE JUNCTION OF T.C. NO. 19, 20 & 21

FIGURE 19 LOCATIONS OF DIFFERENTIAL THERMOCOUPLES INSTALLED ON APPARATUS

FIGURE 20 VIEW OF ADIABATIC SHIELD

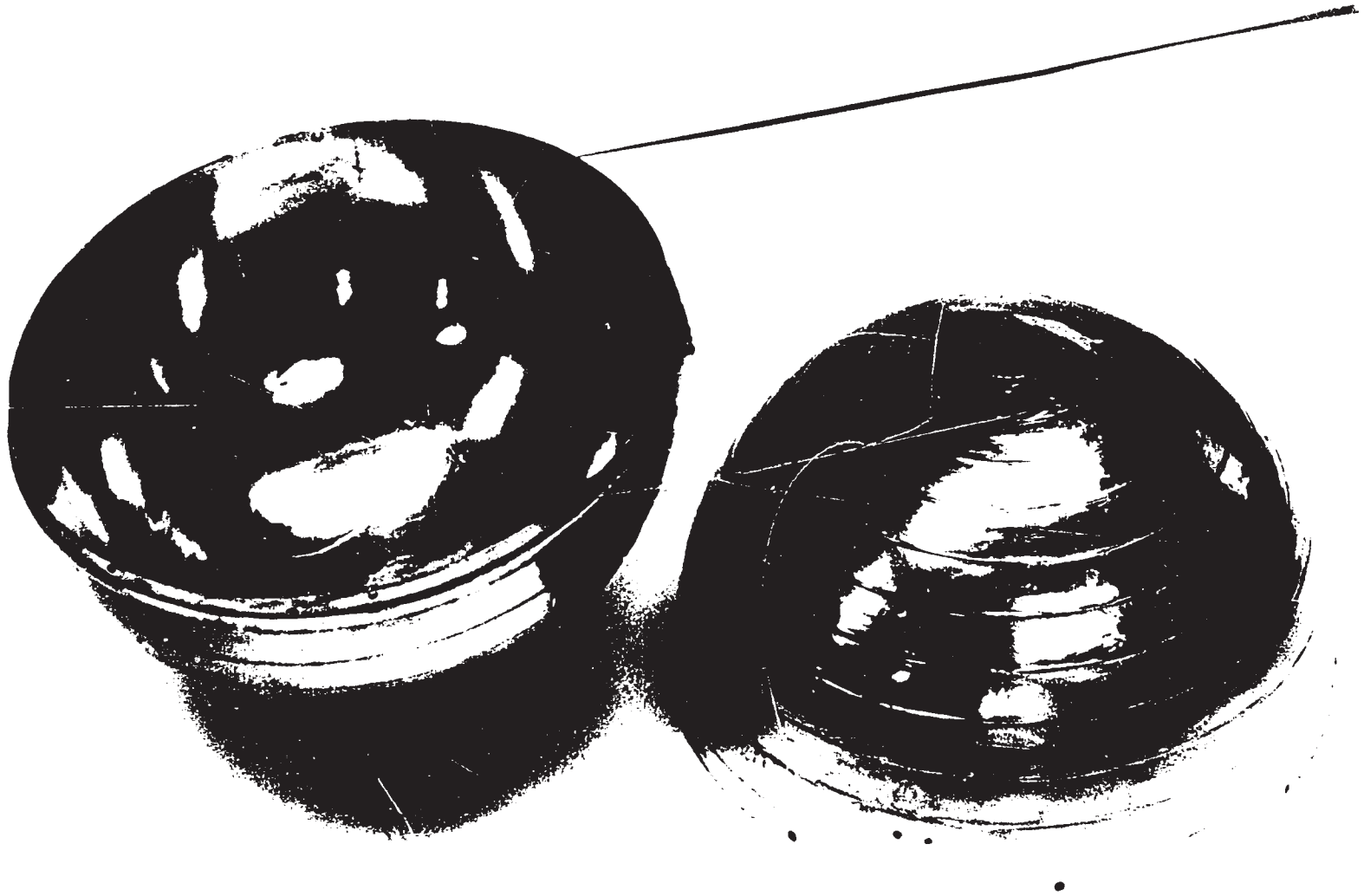

FIGURE 20 VIEW OF ADIABATIC SHIELD

parts* (Refer to Figure 17). This may be attributed to the extra thermal load on the bottom part produced by the leads of differential thermocouples, ceramic supports, and the power leads of adiabatic shield. It is noteworthy that the present adiabatic shield was an improvement regarding isothermality over the old adiabatic shield which was employed by the writer of this thesis in reference 24. For example, the temperature variations along the surface of the old adiabatic shield were as large as 0.5°C at a heating rate of 10°C per hour.

The main purpose of the adiabatic shield is to minimize heat exchange to or from the calorimeter. There are two ways to reduce the undesired heat exchange. Firstly, the heat transfer coefficient between the calorimeter and the adiabatic shield is made as small as possible. The heat transfer coefficient includes gaseous conduction, convection and radiation as well as thermal conduction through the solid connectors between the calorimeter and adiabatic shield. Secondly, the temperature of the calorimeter and the adiabatic shield are matched as closely as possible.

In the present apparatus the gaseous conduction and convection was minimized by evacuating the space between the calorimeter and the adiabatic shield to 0.02 mm Hg. Heat conduction along the various differential thermocouples were reduced by using a small size wire (#30 gauge or approximately 0.01" diameter). The thermal radiation was reduced by making the emissivity of the exterior surface of the calorimeter and the interior surface of the adiabatic shield as small as

---

*Supplementary tests with heating wires cemented to the surface of the adiabatic shield indicated that the temperature variations would most likely be in excess of 0.5°C.

possible. Hence the calorimeter was polished to a mirror finish, whereas the two surfaces of the adiabatic shield were gold plated and polished. Figure 21 is a photograph which serves to illustrate the surface finishes of the calorimeter, adiabatic shield and outer guard.

The temperature of the adiabatic shield was maintained at the same level to that of the calorimeter by means of a suitable automatic control system described in a later section.

3-3. The Outer Guard

The outer guard was somewhat different in construction to the adiabatic shield. It was made from 99.98 percent electrolytic tough pitch copper in the form of two thick-walled hemispheres approximately 8 3/4 inches and 9 3/4 inches in inside and outside diameters, respectively. The hemispheres were clamped together on a metal gasket installed at the equator. Four Inconel sheathed heating coils were embedded in the grooves which were machined uniformly over the entire surface of the heavy copper shell. These heating elements were connected in parallel. The outside surface of the guard was coated with Thermostix* cement. A stainless steel vacuum tube, 3/4 inch diameter, was connected to the bottom of the outer guard for evacuating the inside space. The whole assembly was mounted in a 20 inches diameter aluminium spherical container and insulated with diatomaceous earth. This outer guard was initially designed and built by Mr. W. Haessler (26), a graduate student of the Faculty of Engineering Science, The University of Western Ontario, and modified by the writer of this

---

*Thermostix, Adhesive Products Corporation, 1660 Boone Avenue, Bronx, N.Y., U.S.A.

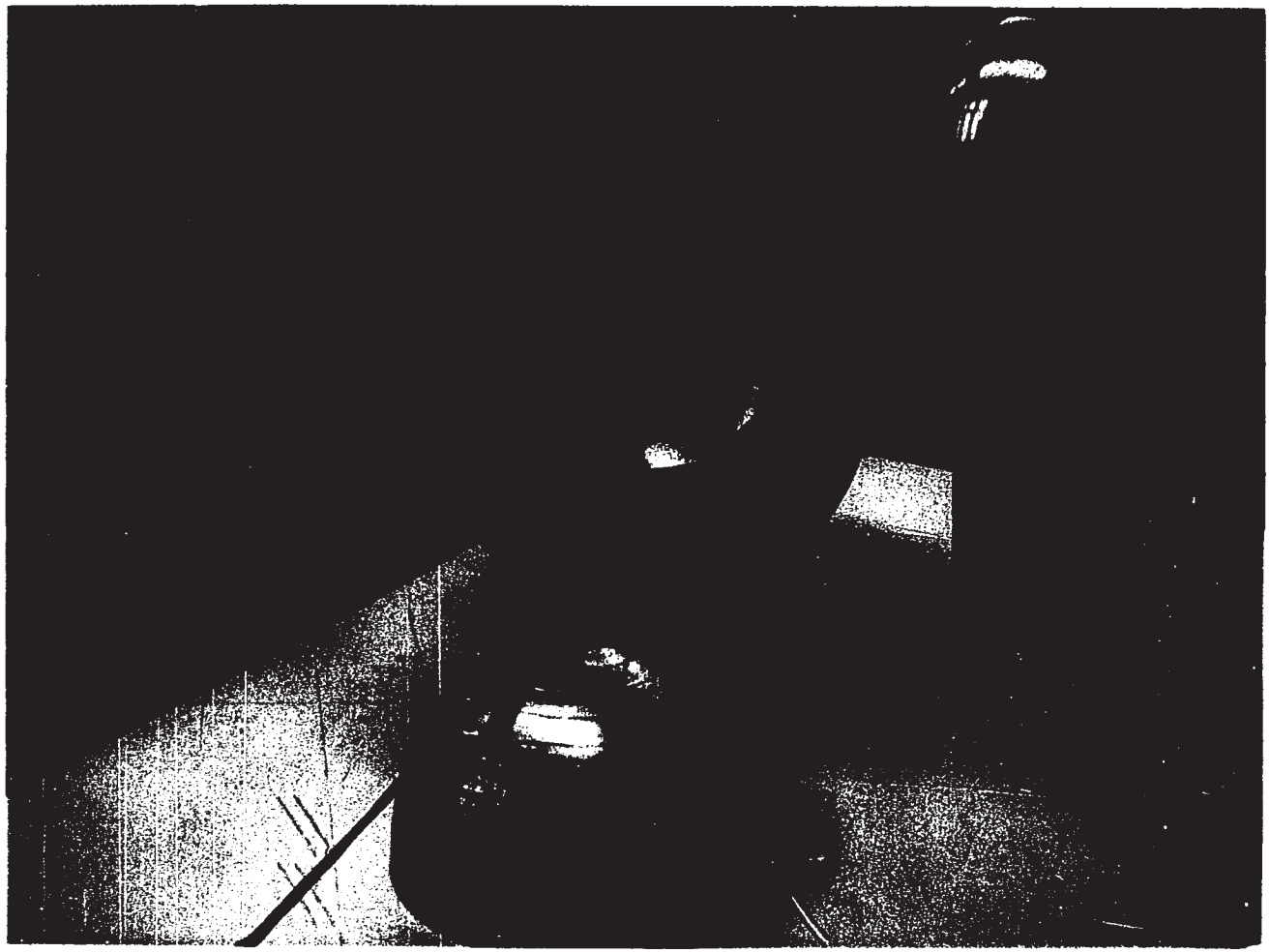

FIGURE 21 VIEW OF HIGHLY POLISHED CALORIMETER, GOLD PLATED ADIABATIC SHIELD AND OUTER GUARD

FIGURE 21 VIEW OF HIGHLY POLISHED CALORIMETER, GOLD PLATED ADIABATIC SHIELD AND OUTER GUARD

thesis. A view of the outer guard is given in Figure 22.

The outer guard is for the purpose of preventing the changes in the ambient in the laboratory from influencing the adiabatic shield and providing a high vacuum space to minimize heat transfer between the calorimeter and its surroundings. It also supplies most of the heat which is lost to the outside. This guard was successful in operating at a vacuum of 0.02 mm Hg and the temperature variation over the entire surface was less than 0.3°C at a heating rate of 10°C per hour and at a guard temperature of 300°C. Figure 23 shows the temperature variation on the outer guard during a typical constant mass experiment.

3-4. Connections to the Calorimeter

The calorimeter was supported by a 1/4 in. in diameter and 15 in. long Inconel tube. This tube was silver soldered to the bottom of the calorimeter and extended to the connection box without making any contact with the adiabatic shield and outer guard. An Inconel sheathed heater as shown in Figure 11 was silver soldered on this tube about 3/4 in. below the calorimeter. This heater was used to provide the heat which was lost along the tubes (calorimeter support and liquid withdrawal) to the outside ambient, consequently the heat loss from the calorimeter through these connections was prevented.*

The smaller liquid withdrawal tube which served for the introduction and removal of the liquid sample was installed inside of the calorimeter

---

*A short copper heat conduction ring was forced into the annulus between the withdrawal tube and the support tube to facilitate heat transfer from the support tube to the withdrawal tube.

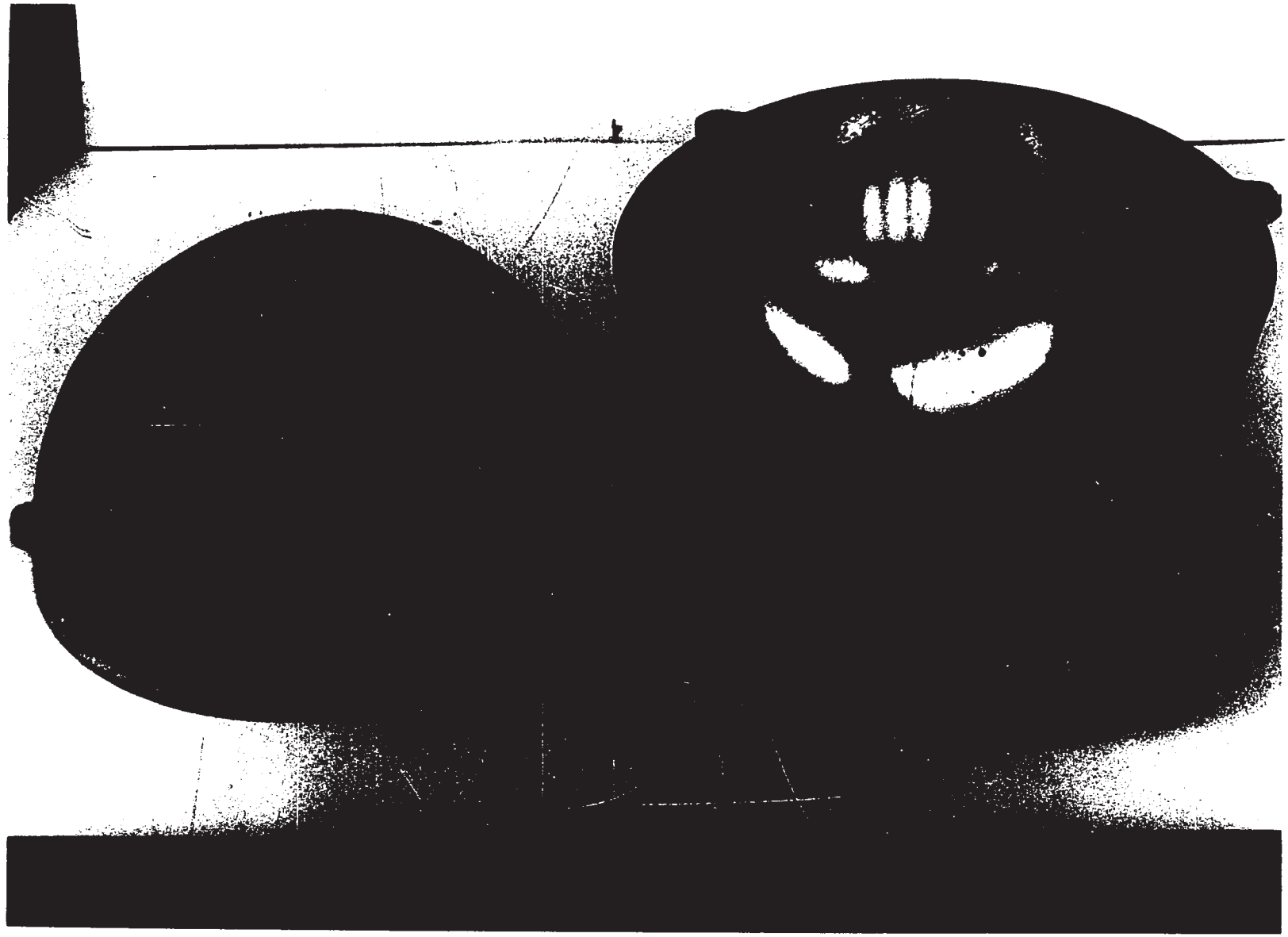

FIGURE 22 VIEW OF OUTER GUARD

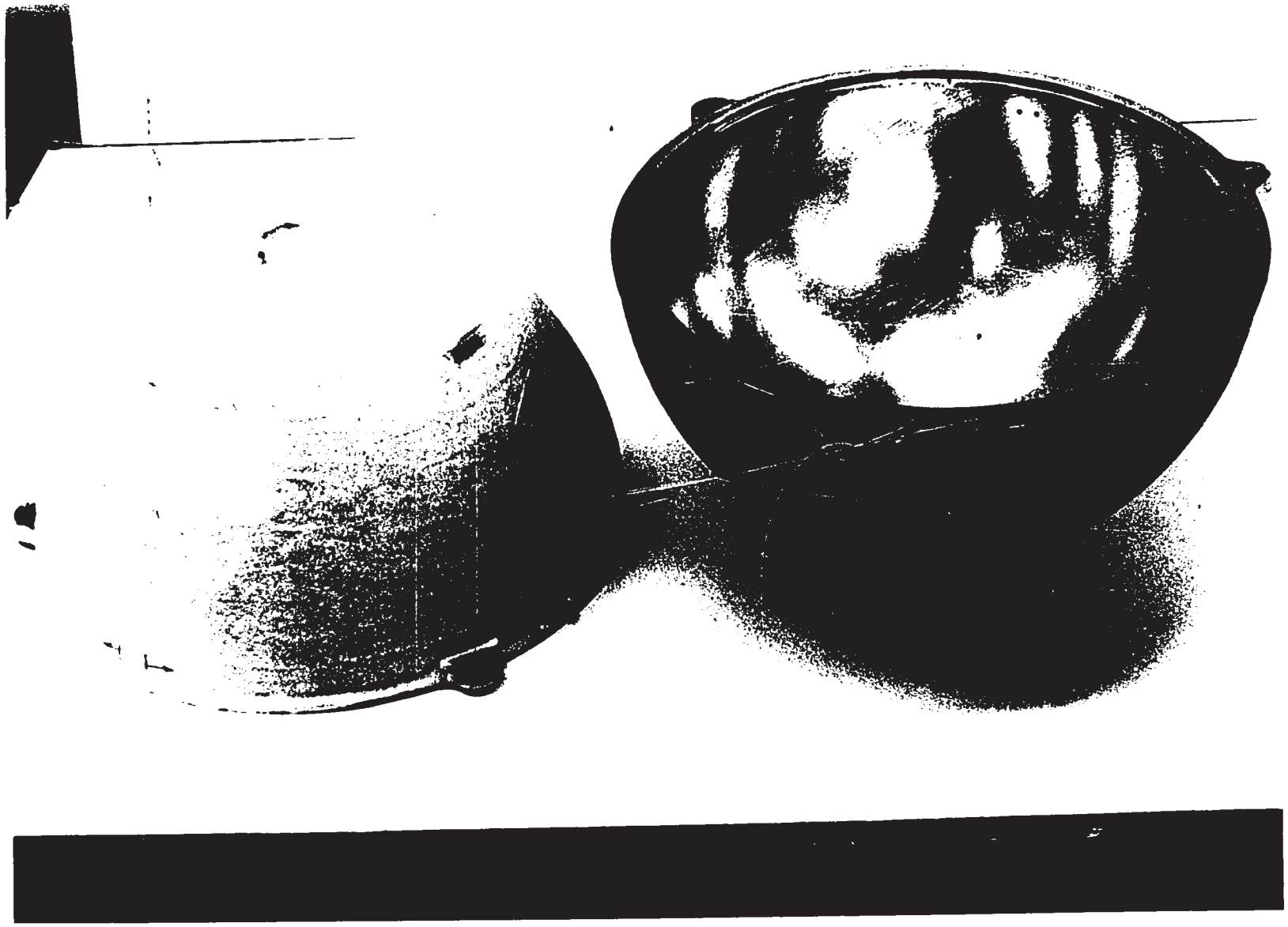

FIGURE 22 VIEW OF OUTER GUARD

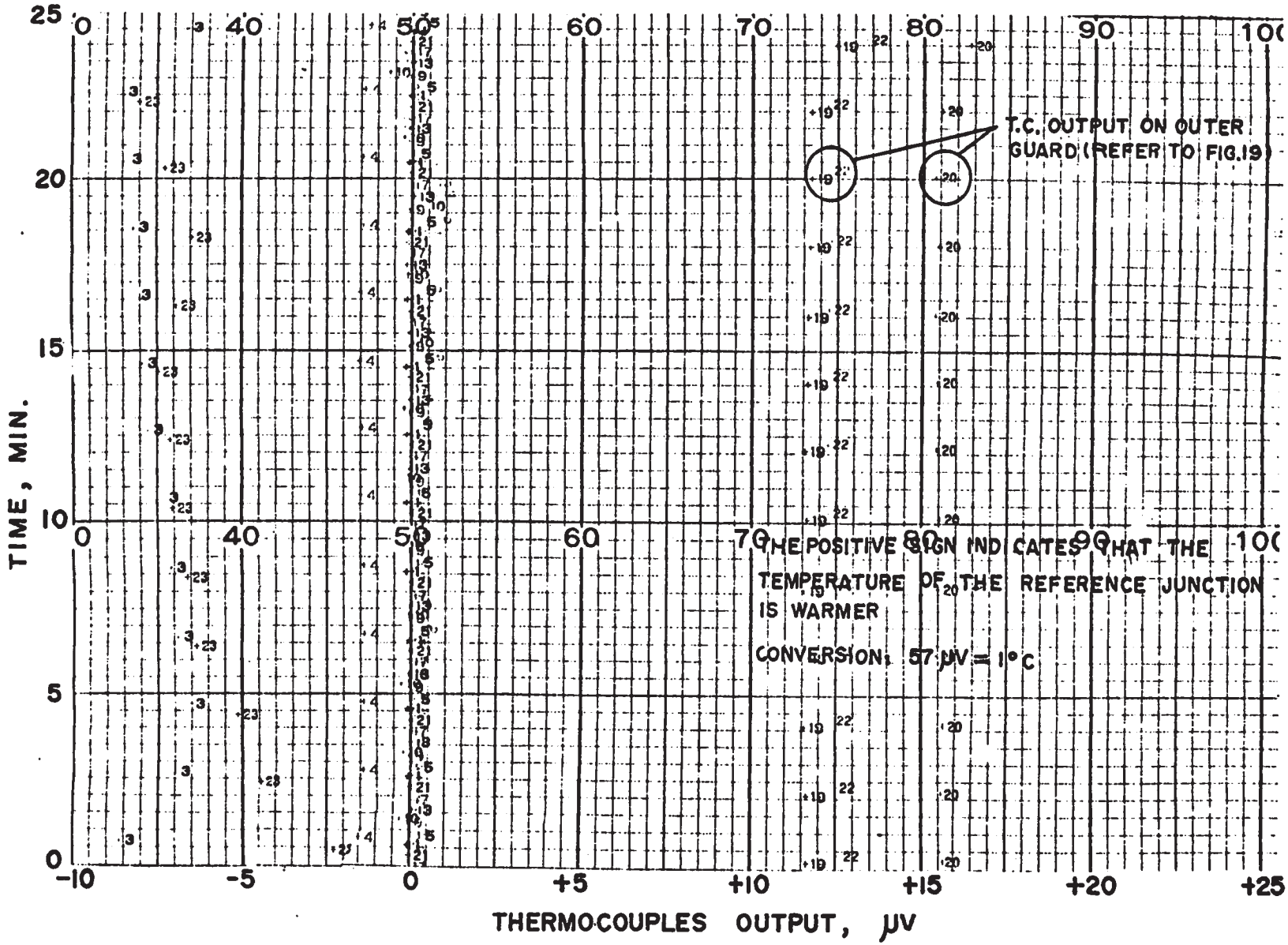

FIGURE 23 TEMPERATURE VARIATIONS ON THE OUTER GUARD

support tube. This tube was made from 1/16 in. diameter Inconel tubing 21 inches long. The volume of this liquid withdrawal tube amounted to only 0.06 percent of the internal volume of the calorimeter.

A vapour withdrawal tube will be fastened to the uppermost part of the calorimeter after completion of the constant mass experiments and liquid withdrawal tests. A baffle made from silver wire was installed under the vapour withdrawal tube to prevent any drops of liquid that might get into the vapour line during experiments.

3-5. Thermometric Installation

The thermometric installation of this apparatus included a platinum resistance thermometer capsule and fourteen differential thermocouples attached at various positions on the outer surface of the calorimeter, adiabatic shield and outer guard. The platinum resistance thermometer capsule used to measure the temperature of the heavy water sample was inserted into the thermowell located in the center of the calorimeter. Intimate thermal contact between the thermometer and the thermowell was obtained by packing the excess space around the thermpometer with magnesia oxide powder. The extension leads (pure platinum wire insulated with fiberglass) of the thermometer were fastened to the surface of the calorimeter for a distance of approximately 8 inches with Sauereisen* cement.

---

*Sauereisen No. 14, Sauereisen Cements Co., Pittsburgh 15, Penna., U.S.A.

Two four-junction differential thermocouples were employed to detect the temperature difference signals between the calorimeter and adiabatic shield, and between the adiabatic shield and outer guard. Two differential thermocouples were also used to control the power input to the tube heaters while ten differential thermocouples were used to measure the temperature variations on the surfaces of the calorimeter shell, adiabatic shield and outer guard. Figure 6 gives the indication of the location of these differential thermocouples. The common junctions for these thermocouples were located at the bottom of the calorimeter, adiabatic shield and outer guard.

The thermocouples used inside of this apparatus were fabricated with 30 gauge copper and constantan wires which were insulated with fiberglass. The thermocouple junctions were enclosed in silver tabs about 3/8 in. wide and 1/2 in. long. They were insulated from the silver tabs with mica strips. A cross section of this arrangement is shown in Figure 24. After inserting the junctions and the mica insulating strips into the silver tabs, the silver was crimped tightly on the mica by pressing in a vise. The sheathed junctions were held in place on the surface of the calorimeter by Thermostix* cement and on the surfaces of the adiabatic shield and outer guard by two screws (3/64 in. diameter). Qualitative test indicated that Thermostix gave a better bond than Sauereisen #1 and 33. Figure 25 and Figure 26 show how the thermojunctions and extension leads of the thermocouples were fastened or cemented to the surfaces of the calorimeter and the

---

*Thermostix, Adhesive Products Corporation, 1660 Boone Avenue, Bronx, N.Y., U.S.A.

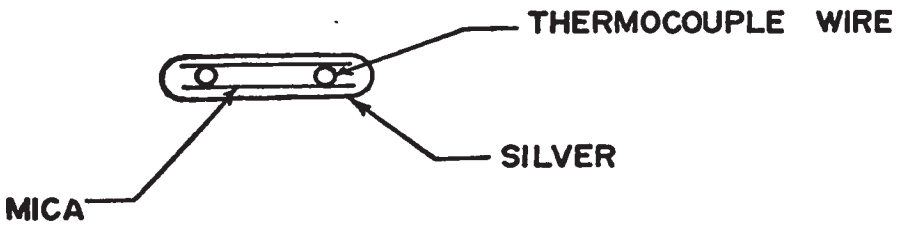

FIGURE 24 THERMOJUNCTIONS

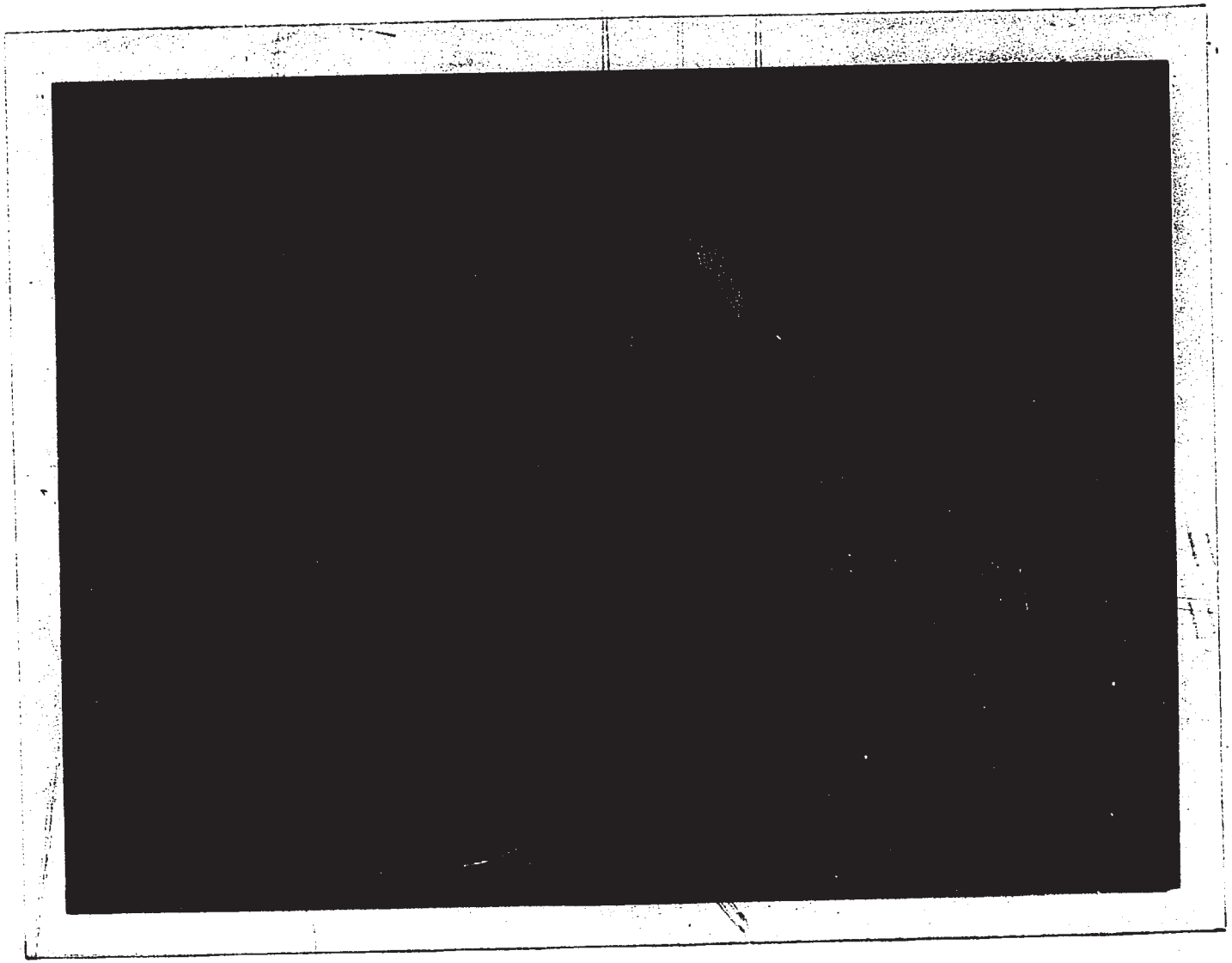

FIGURE 25 VIEW OF THERMOJUNCTIONS FASTENED ON CALORIMETER

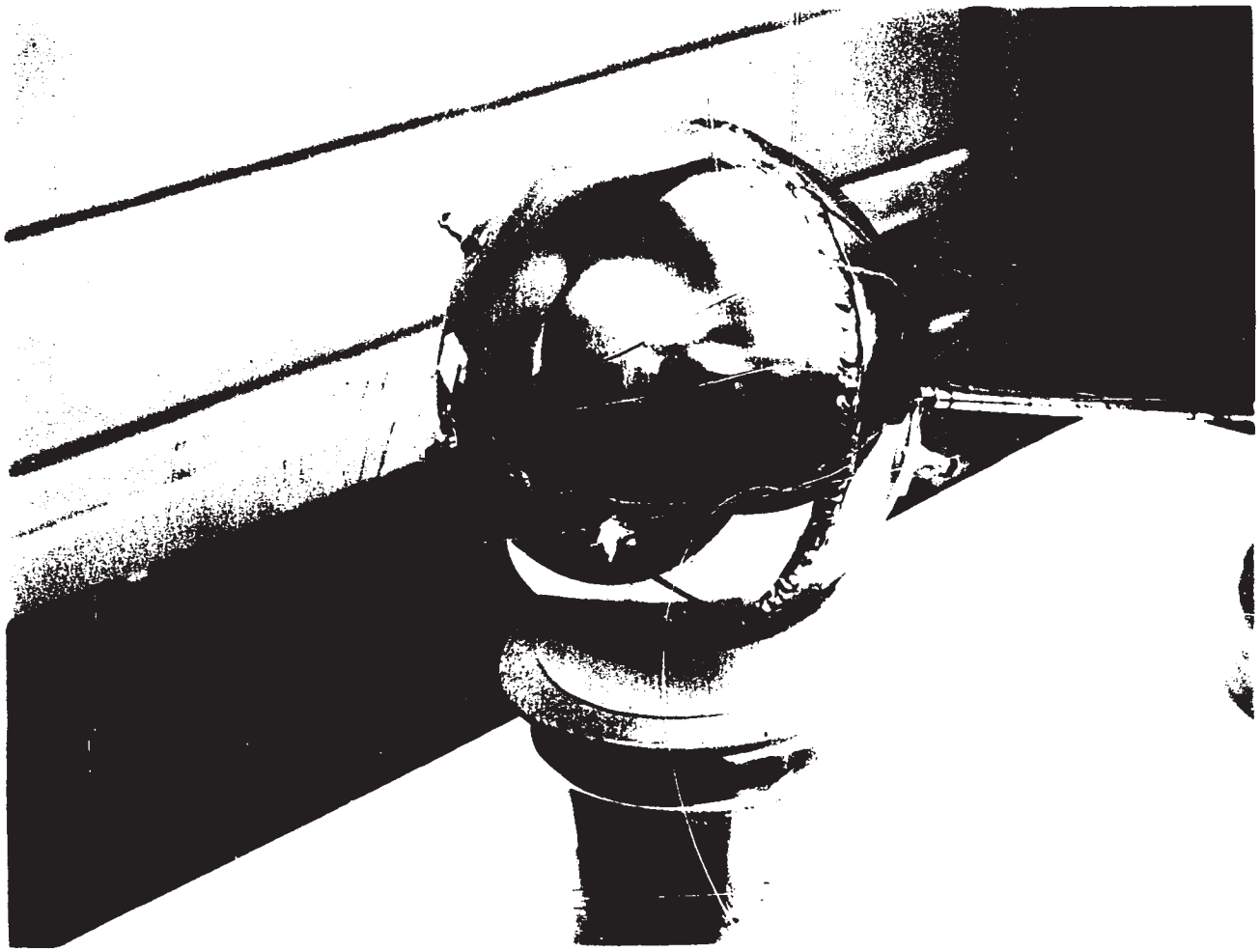

FIGURE 25 VIEW OF THERMOJUNCTIONS FASTENED ON CALORIMETER

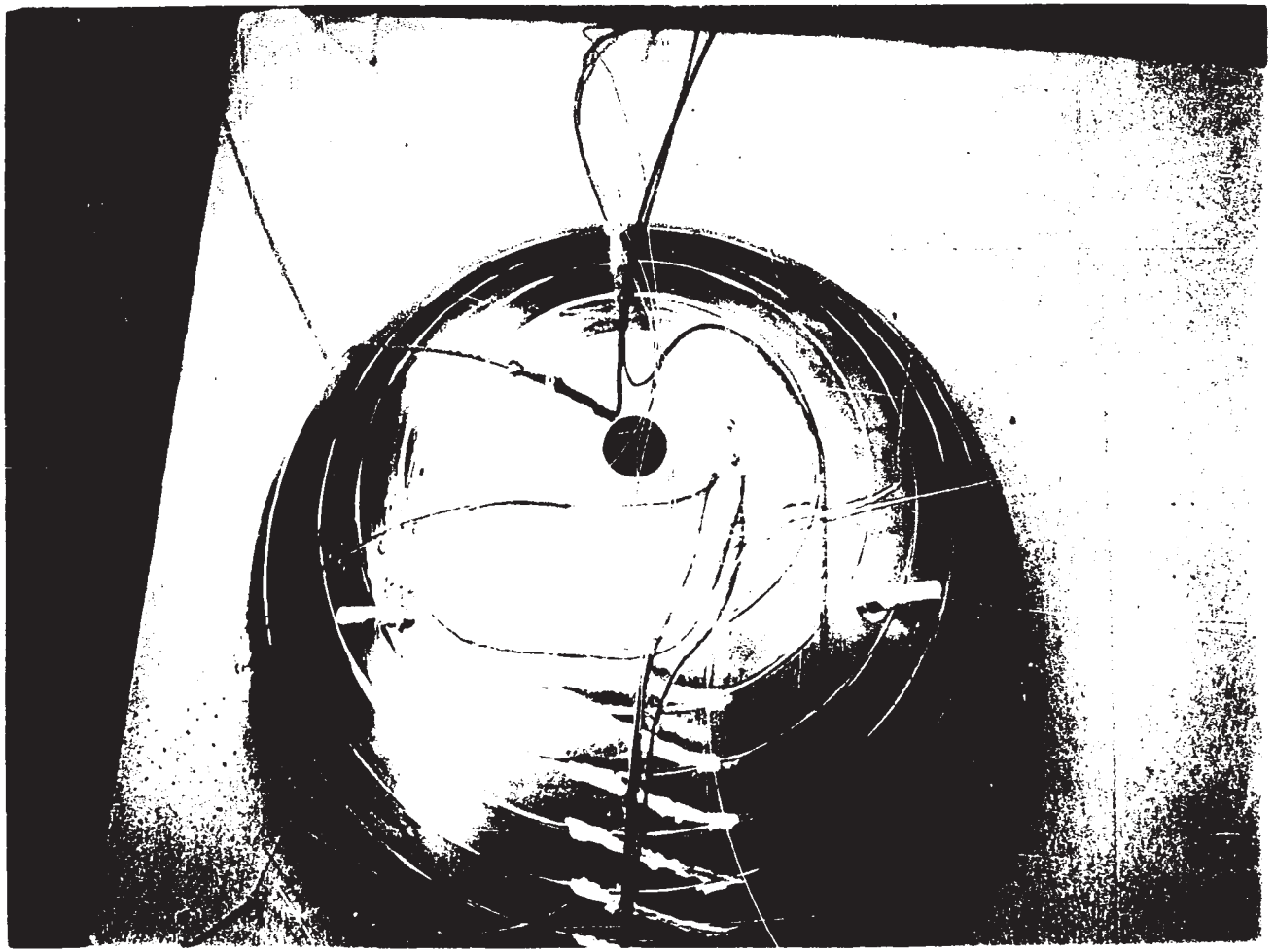

FIGURE 26 VIEW OF THERMOJUNCTIONS FASTENED ON ADIABATIC SHIELD

adiabatic shield.

The leads, which included eight power leads, fifteen thermocouple leads and four thermometer leads, entered the vacuum space through the Conax seals at the connection box as shown in Figure 6 and passed up to the calorimeter, adiabatic shield and outer guard through the vacuum tube.

3-6. The Control Valve

During the liquid or vapour withdrawal test, only a small amount of liquid or vapour of the sample is withdrawn from the calorimeter, thus the control valve must be able to make extremely small incremental adjustments to the flow rate. The success of these two types of experiments is largely dependent on the flow rate control. If the flow rate is too large the temperature of the fluid sample will drop whereas if the flow rate is too small the temperature of the fluid sample will increase.

Moyse (27), an undergraduate student at the Faculty of Engineering Science, The University of Western Ontario, conducted the liquid withdrawal tests on light water by employing a regular needle valve* having an orifice diameter of 0.08 inches. He found that with this type of valve the adjustments made to the flow rate were too coarse and the temperature of the fluid sample departed from isothermality during test as high as $0.1^{\circ}C$.

The control valve employed in this research for liquid withdrawal

---

*Needle Valve, #0 Series, Whitey Research Tool Co., 5525 Marshall Street, Oakland 8, California, U.S.A.

tests was a commercial micro-metering needle valve*. This valve utilized a 0.02 inches orifice diameter and a spring loaded stem to control the flow. The valve stem was tapered from 0.02 inches diameter to 0.01 inches diameter and was spring loaded to avoid damage to the valve when over closed. The fine flow control feature of this valve was combined with a forty turn micrometer handle to give precise control and repeatable flow control settings. Figure 27 shows the construction of the micro-metering needle valve. With this valve the liquid withdrawal flow rate at approximately 4 grams per minute was easily obtainable. The temperature of the fluid sample during a liquid withdrawal test could be maintained to with ± 0.02^{o}C by adjusting the valve properly. Table 3 gives the valve setting and the approximate flow rate at various saturation temperatures of heavy water whereas Figure 28 shows the temperature variations of the calorimeter with time during a typical run of liquid withdrawal test. It is evident that this micro-metering needle valve is suitable for the liquid withdrawal test.

*Micro-metering Needle Valve, #22 Series, Whitey Research Tool Co.

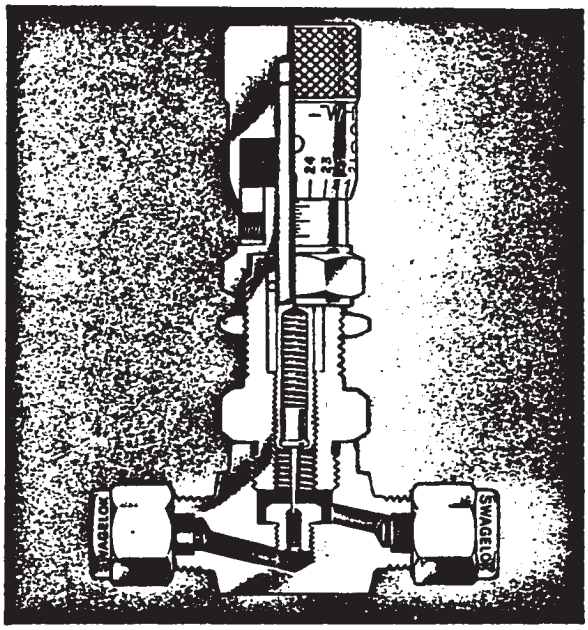

END CONNECTION	PART NUMBER	A	B	B_1	D	E	H	
							OPEN	CLOSED
$\frac{1}{8}$ SWAGELOK	22RS2	$2\frac{3}{16}$	$1\frac{3}{32}$	$1\frac{3}{32}$	$1\frac{7}{32}$	$\frac{1}{4}$	$3\frac{9}{16}$	$3\frac{5}{16}$

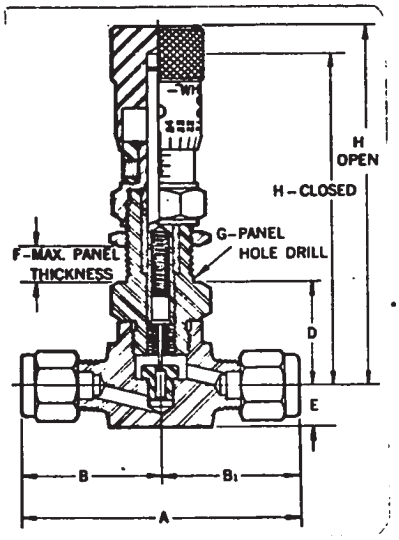

SPECIFICATIONS

MATERIALS:
Type 316 stainless steel for: Bonnet
Body — Glands
Stem — Stem spring
Micrometer handle — Packing nut
Panel nut — Fitting components

PACKING: Viton-A O-ring
HANDLE: Stainless steel micrometer handle with glare proof finish.
PRESSURE RATING: 3000 psi at room temperature.

TEMPERATURE RATING: 400-500° F. Maximum with Viton-A packing.

ORIFICE SIZE: .020"

FIGURE 27 THE MICRO-METERING NEEDLE VALVE

TABLE 3

CONTROL VALVE SETTING AND FLOW RATE AT VARIOUS SATURATION TEMPERATURES OF HEAVY WATER

Temperature (°C)	Valve Setting (Turns)	Approximate Flow Rate (g/Min.)
100	$3\frac{12}{25}$	3.7
125	$4\frac{18}{25}$	4.7
150	$3\frac{20}{25}$	3.9
175	$3\frac{7}{25}$	3.5
200	$4\frac{4}{25}$	4.2
225	$4\frac{7}{25}$	4.3
250	$4\frac{15}{25}$	4.6
275	$4\frac{13}{25}$	4.5
300	$4\frac{12}{25}$	4.5

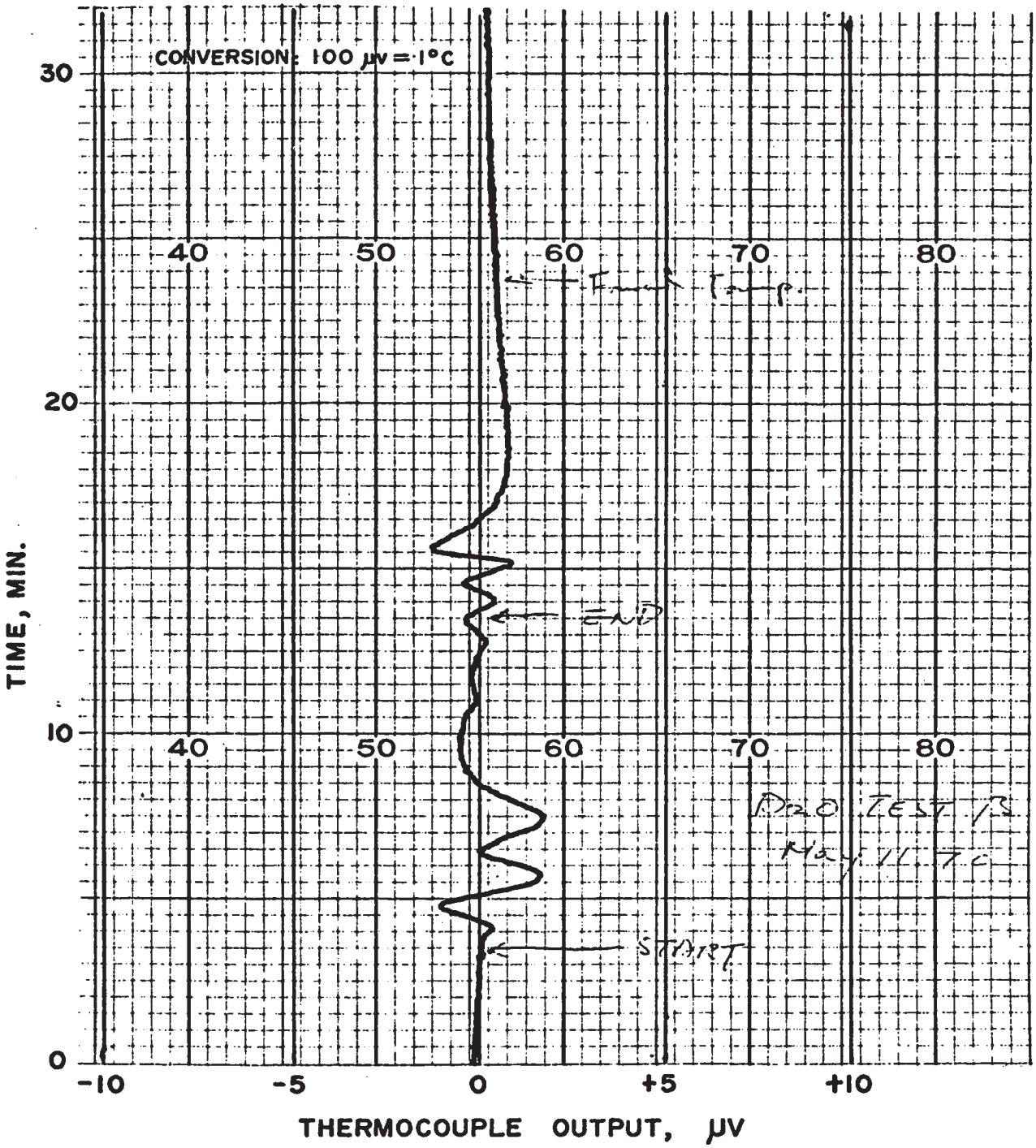

FIGURE 28 TEMPERATURE VARIATIONS OF THE CALORIMETER DURING A TYPICAL LIQUID WITHDRAWAL TEST

CHAPTER 4

INSTRUMENTATION

Highly precise instruments were employed in this research to measure the absolute temperature, the energy input into the calorimeter, the mass of water sample and the temperature difference between the calorimeter, adiabatic shield and outer guard. Figure 29 is a schematic diagram of the instrumentation circuit.

4-1. Temperature Measurement

The temperature of the water sample was determined by a laboratory standard platinum resistance capsule. This capsule thermometer was carefully calibrated against a long stemmed 25 ohm international primary standard platinum resistance thermometer, which in turn was calibrated by the National Research Council of Canada at the triple point of water, steam point and the sulphur point. Details and results of the calibration tests performed on the capsule standard thermometer are given in a later section of this thesis.

An isolating potential comparator in conjunction with a thermostated four terminal resistor was used to measure the resistance of the thermometer. This method of temperature measurement was developed by Dr. Dauphinee (28) of the National Research Council of Canada. A schematic diagram illustrating the principle of operation of the

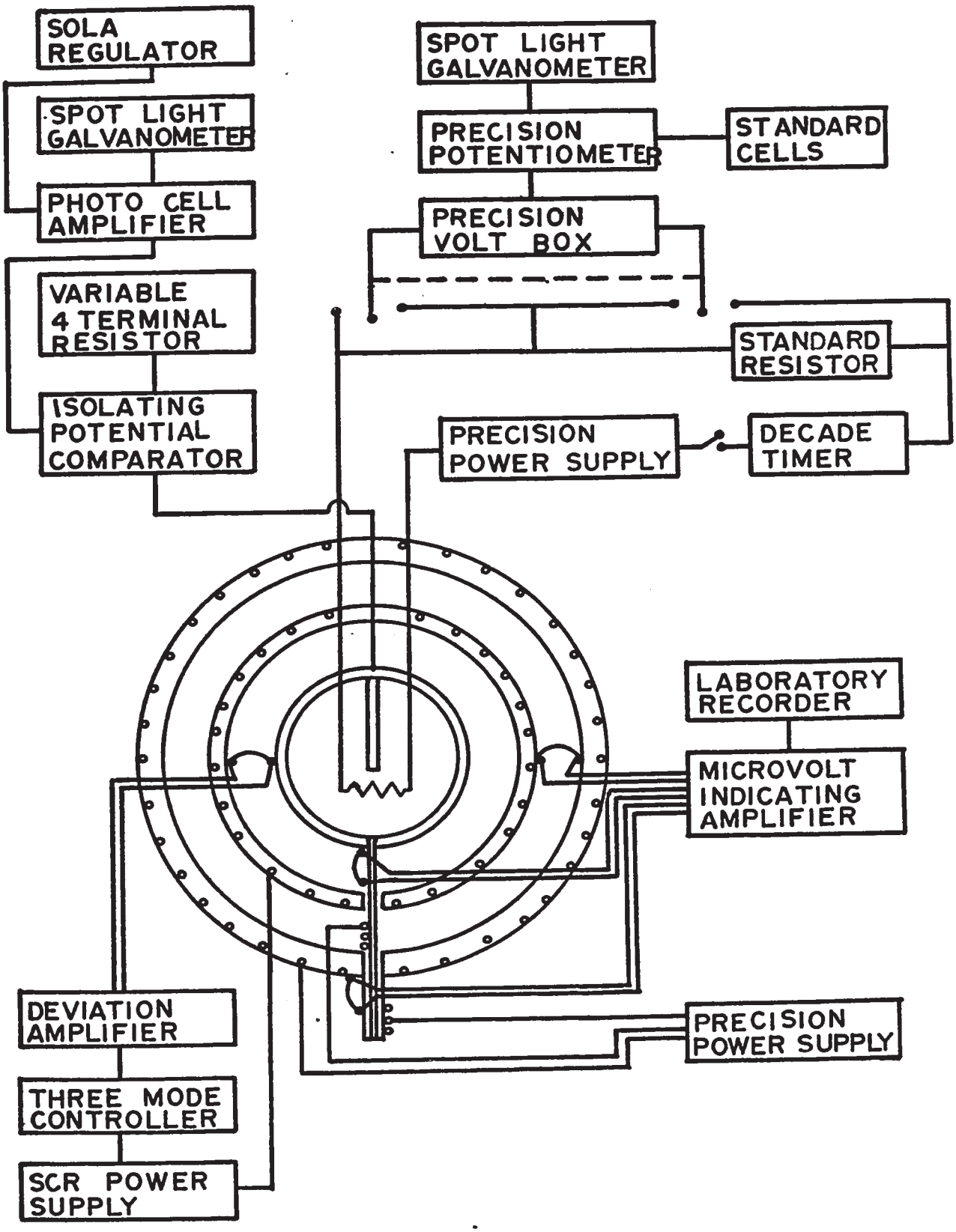

FIGURE 29 INSTRUMENTATION CIRCUIT

comparator method of temperature measurement is shown in Figure 30.

The resistance of the capsule thermometer was measured accurately to within ± 0.001% using an isolating potential comparator (Type 9800), with a thermally insulated four terminal resistor (Type 9801). A direct comparison is made of the voltage drop across the resistance thermometer and the known value of the resistor dialed into the variable four terminal resistor. A low thermal switch, or chopper, switches a capacitor alternately from the potential leads of one resistor to the potential leads of the other. Any difference between the two potential drops results in small pulses of charging current through the capacitor, and these pulses deflect a galvanometer which is connected in series with one of the potential leads.

If the variable four terminal resistor is adjusted to make the potential appearing at its potential terminals equal to the potential across the resistance thermometer, as established by a galvanometer balance, then the two resistors must be equal and the resistance of the thermometer can be read directly from the dial reading of the variable four terminal resistor. The lowest resistance increment of 100 microhm (0.000100 ohms) corresponds to a temperature change of approximately $0.001^{\circ}C$ for 25 ohm resistance thermometer.

4-2. Temperature Difference Measurement

Differential copper-constantan thermocouples were used to detect the temperature difference between the calorimeter, adiabatic shield and the outer guard as well as to survey the surface temperature variations on the calorimeter, adiabatic shield and the outer guard. The reason for using copper-constantan differential thermocouples in this research

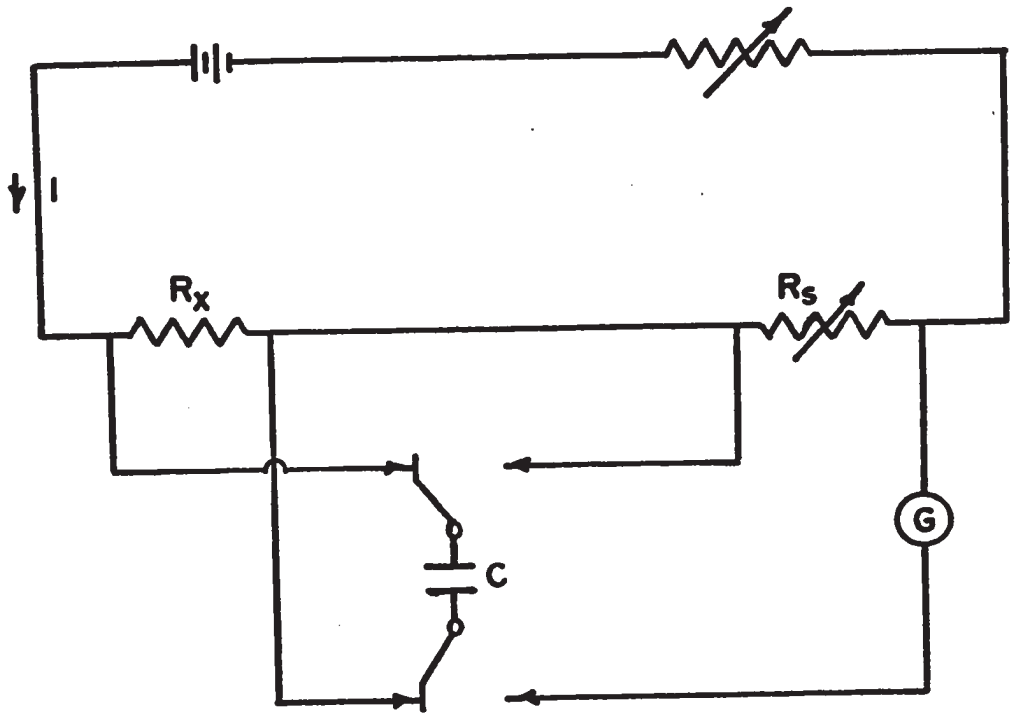

R_s = FOUR TERMINAL VARIABLE RESISTOR

R_X = RESISTOR UNDER TEST I = CURRENT

G = GALVANOMETER C = CAPACITOR

FIGURE 30 THE ISOLATING POTENTIAL COMPARATOR METHOD OF MEASURING RESISTANCES

is that the inhomogeneity emf generated in a pure copper wire (24) is much less than any other kind of wires. Consequently if the copper legs of a differential copper-constantan thermocouple are made to pass from the high temperature region of the calorimeter to the low temperature region of the measuring instrument in the laboratory and the constantan wire is kept in the more or less isothermal environment between the calorimeter and outer guard the error in the thermocouple due to the inhomogeneity emf would be minimized.

A 24 point recorder which required a full scale input signal of 5 millivolts on its most sensitive range and which was connected to a microvolt amplifier was employed to record the voltage outputs from the differential thermocouple. The voltage output from the differential thermocouples was initially amplified by the microvolt amplifier and then fed into the recorder. With this arrangement the most sensitive range on the 10 inches wide recorder chart was 25 microvolts for full scale deflection. This equipment was capable of measuring temperature difference accurate to ± 1 percent. Details of the calibration of this equipment against a microvolt potentiometer may be found in reference (25).

4-3. Energy Measurements

The method of energy measurement was that of the well known potentiometer volt-box technique and it essentially consisted of determining the D.C. current flowing through the calorimeter heater and determining the potential drop developed across the calorimeter heater. The circuits for the energy measurement are shown in Figure 29. Since the D.C. current flowing through the calorimeter heater is the same as

that flowing through the standard resistor, it can be obtained from a determination of the voltage drop across the standard resistor. The voltage across the heater and standard resistor was measured by means of the volt-box and potentiometer whereas the potential drop developed across the standard resistor was measured by virtue of the potentiometer.

The power supplied to the calorimeter can be evaluated by means of the following equation,

$$P = \frac{V_H V_S}{R_S} \qquad \ldots\ldots\ldots\ldots\ldots\ldots\ldots\ldots \quad (22)$$

where P is the power supplied to the calorimeter

$V_H = V_{H+S} - V_S$ = voltage drop across the calorimeter heater

V_{H+S} = voltage drop across the calorimeter heater and the standard resistor

V_S is the voltage drop across the standard resistor

R_S is the resistance of the standard resistor which in this research had a nominal value of one ohm.

The time during which power was being supplied to the calorimeter heater was measured by means of a precision 0.1 second interval timer operated on a 60 cycle frequency standard. The timer having an accuracy of one part in 10000 was designed and constructed by the Electronics Shop of the Faculty of Engineering Science, The University of Western Ontario.

The potentiometer was certified accurate to 0.005% and was standardized against one of the six cadmium saturated type standard cells which received an absolute calibration from the National Bureau of Standards accurate to ± 0.0005 percent. The volt-box had a reported

accuracy of ± 0.005 percent. The standard four terminal one-ohm resistor was calibrated by the National Research Council of Canada and was certified to ± 0.005 percent accuracy.

The total percent error of the energy measurements may be computed from the following relationship,

$$\% E = \% V_H + \% V_S + \% R_S + \% T$$
$$= 0.01\% + 0.005\% + 0.005\% + 0.01\%$$
$$= \pm 0.03\%$$

More specifically the accuracy of calorimeter energy measurement is estimated to be of the order of ± 0.03%.

During a constant mass experiment the resistance of the calorimeter heater increases slightly with temperature. Thus the total power supplied to the calorimeter decreases slightly with time. In view of this the D.C. power to the calorimeter heater was measured at every 500 seconds interval. A graph of the variation of the input power with time is shown in Figure 31. It is evident from this curve that the total variation of power is of the order of 0.5% and that the overall precision of power measurement is well within 0.01%.

The experimental data of the energy measurements were analysed by three different methods (i.e. arithmetic mean method, graphical method and least squares method). In the arithmetic mean method the "average voltage" and "average current" were obtained from the individual measurements of voltage and current over the length of the test. In the graphical method a straight line was drawn through the individual points whereas in the least squares method a straight line was fitted through the individual points. Table 4 gives a typical set of the analytical results. It can be seen that the maximum deviation between

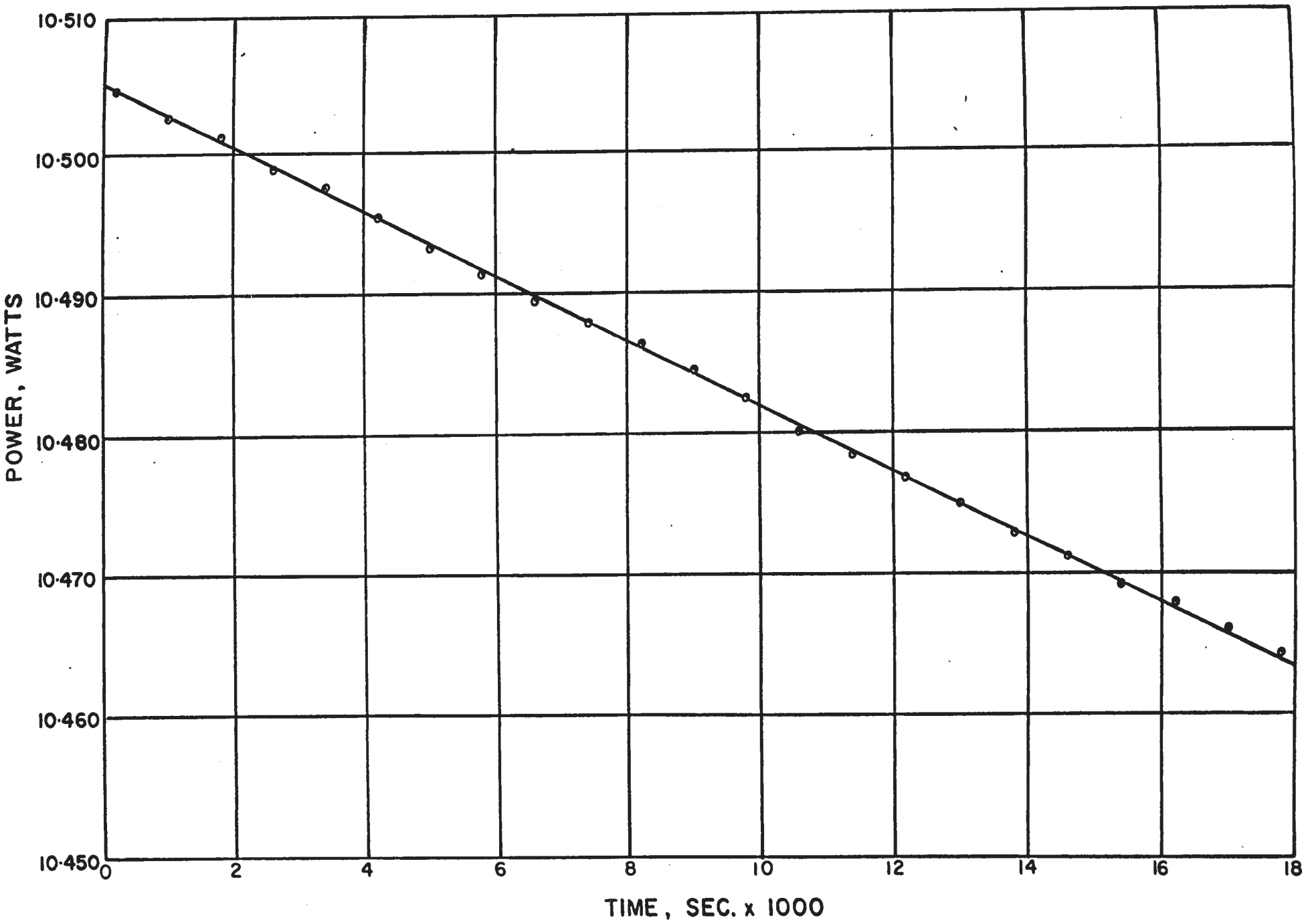

FIGURE 31 VARIATION OF THE INPUT POWER WITH TIME

each method is no more than 0.003%. In view of the fact that this small deviation is ten times smaller than the estimated accuracy of measurement the arithmetic mean method was employed to evaluate the input power to the calorimeter in this thesis.

TABLE 4

ANALYTICAL VALUES OF THE POWER MEASUREMENTS OF A CONSTANT MASS EXPERIMENT ON LIGHT WATER (RUN #4)

Data Reduction Method	Total Energy Added (I.J.)
Arithmetic Mean Method	248769.5
Graphic Method	248777.9
Least Squares Method	248775.4

4-4. Mass Measurement

The masses of the light and heavy water samples used in this research were determined by the method of substitution as described in Chapter 6. All weighing of the water samples and the containers were measured by means of precise Mettler analytical balance.

This balance had a maximum capacity of 1000 grams and an accuracy of approximately 0.0001 grams. Since the masses of the samples involved in this research were no less than 200 grams for the constant mass experiments and 20 grams for the liquid withdrawal tests, the maximum errors which resulted through the use of this analytical balance were no more than ± 0.0001% and ± 0.001% for the constant mass experiments and the liquid withdrawal tests respectively.

4-5. Temperature Control

In order to maintain the temperature of the adiabatic shield as closely as possible to the temperature of the calorimeter during test conditions, a commercial automatic control system was employed in this apparatus. The temperature differences between the calorimeter, adiabatic shield and outer guard were detected by two copper-constantan differential thermocouples each having four junctions. The emf error signal due to temperature inequality between the calorimeter and the adiabatic shield from the control thermocouple was firstly amplified by a deviation amplifier and then fed into a three mode controller which had proportional, reset and rate control. This controller in turn drove a SCR power supply to give proper current to the heaters of the adiabatic shield. With this equipment, it was possible to control and maintain the temperature difference between the calorimeter and the adiabatic shield in the vicinity of the differential thermocouple junctions constant to within ± 0.002°C. A typical temperature difference between the calorimeter and the adiabatic shield obtained by means of the four junction differential thermocouple is shown in Figure 32.

Manual operations were used to maintain the temperature of the outer guard at a level very close to that of the adiabatic shield. The signal from the control thermocouple was amplified by a microvolt amplifier and recorded by a potentiometer recorder. The operator would either increase or decrease the current flowing in the heaters of the outer guard, depending on the algebraic sign of the signals. By means of this type of simple control the temperature difference signal between the adiabatic shield and the outer guard was well within ± 0.01°C.

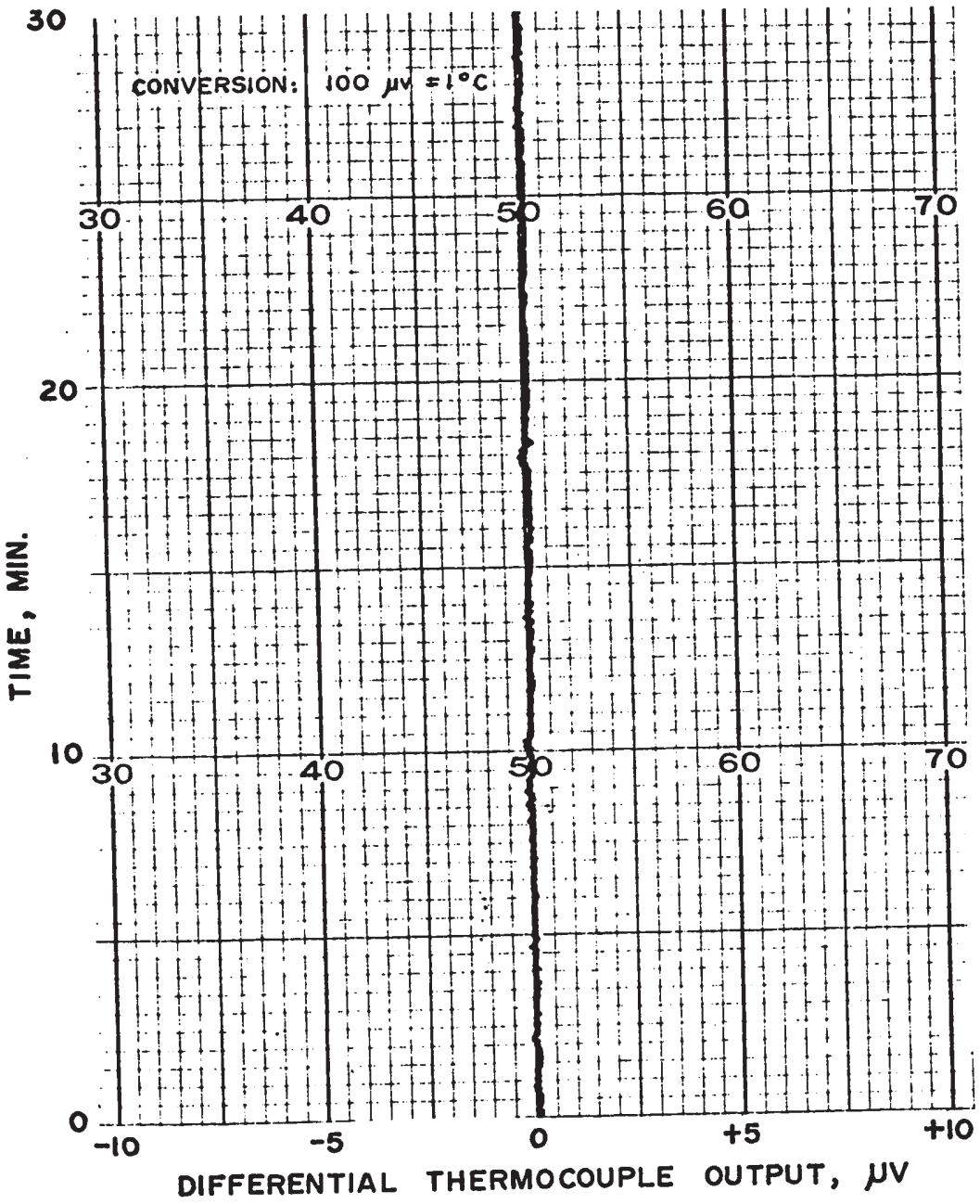

FIGURE 32 TEMPERATURE DIFFERENCES BETWEEN CALORIMETER AND ADIABATIC SHIELD

CHAPTER 5

CALIBRATION OF INSTRUMENTATION

5-1. Absolute Temperature Standards

A long stemmed 25 ohm laboratory platinum resistance thermometer served as the absolute standard of temperature in the Thermodynamics laboratory of the Faculty of Engineering Science of The University of Western Ontario. This highly stable laboratory platinum resistance thermometer was calibrated against the International Practical Temperature Scale by the Division of Pure Physics of the National Research Council of Canada at the ice point, steam point and sulphur point. The constants in the internationally recognized resistance-temperature relationship $R/R_o = 1 + AT + BT^2$ for the laboratory standard were certified by the National Research Council of Canada (29) to be as follows:

R_o = ice point resistance = 25.5400 ohms

$A = 3.98478 \times 10^{-3}$

$B = -5.8568 \times 10^{-7}$

T = temperature in ^oC.

In addition the ratio of the resistance of thermometer at steam point (100^oC) and at ice point (0^oC) was found to be 1.3926.

According to the specifications of the International Committee on Weights and Measures (30) if the ratio of the steam point resistance

and the ice point resistance of a resistance thermometer is 1.3920 or greater (i.e. $R_{100}/R_0 \geq 1.3920$) and the B constant is in the range from -5.8670×10^{-7} to -5.8470×10^{-7} (i.e. $B = 5.8570 \pm 0.0100 \times 10^{-7}$) the thermometer may be classified as an "International Standard" which is capable of faithfully reproducing the "International Practical Temperature Scale". On the basis of the certified values for R_{100}/R_0 and B given by National Research Council of Canada (29) it may be concluded that the U.W.O. laboratory standard thermometer is a recognized "International Standard".

The U.W.O. international standard thermometer was checked frequently with a triple point of water apparatus. According to the manufacturers' specifications the triple point cell reproduces the triple point of water to within $\pm 0.0005^{\circ}C$. The results of a few of these routine checks at the triple point is given in Table 5. Based on all of the test results on the triple point, it may be concluded that the resistance temperature calibration of the U.W.O. international standard resistance thermometer has not shifted from its original calibration by more than four parts in one million (i.e. 4 parts in 10^6). This small shift in temperature ($0.001^{\circ}C$) is entirely acceptable in this research program.

5-2. Calibration of the Laboratory Standard Platinum Resistance Thermometer Capsule

The capsule thermometer was 1.75 inches in length and 0.219 inches in diameter, made from fully annealed, high purity platinum wire and mounted essentially strain free in a platinum case. A view of the primary laboratory standard thermometer of U.W.O. and the capsule

TABLE 5

TRIPLE POINT RESISTANCE OF THE

STANDARD RESISTANCE THERMOMETER

Date	Triple Point Resistance* Ohms	Corresponding Ice Point Resistance Ohms	NRC Ice Point Resistance Ohms
May 20, 1966	25.5410	25.5400	25.5400
June 13, 1966	25.54105	25.54005	25.5400
June 8, 1967	25.5411	25.5401	25.5400
Sept. 12, 1967	25.5411	25.5401	25.5400
Sept. 25, 1968	25.5411	25.5401	25.5400
May 4, 1969	25.5411	25.5401	25.5400

*The triple point resistance inferred from the NRC calibration is 25.5410 ohms.

thermometer is given in Figure 33.

The capsule thermometer which was to be inserted into the thermowell of the calorimeter had an initial triple point resistance value of 25.5653 ohms. It was calibrated by comparison against the previously mentioned U.W.O. international standard platinum resistance thermometer in an isothermal comparator furnace. Details of which are given in Appendix D.

Thirty two calibration points were obtained mainly at 100, 200, 250 and 400°C and are summarized in Table 1D of Appendix D. The constants A and B in the equation $R/R_o = 1 + AT + BT^2$ were calculated from these calibration data and found to be 3.98447×10^{-3} and -5.8568×10^{-7} respectively. The ice point resistance R_o was inferred from the triple point resistance to be 25.5643 ohms. The ratio of the steam point resistance and the ice point resistance of the capsule thermometer was also found to be 1.3925.

Since the ratio of the steam point resistance and the ice point resistance and the B constant of this capsule thermometer satisfy the specifications of the International Committee on Weights and Measures, this thermometer may be classified as an "International Standard Thermometer".

5-3. Absolute Voltage Standard

A group of six cadmium saturated standard cells mounted in a temperature controlled oven served as the absolute voltage reference for the Faculty of Engineering Science of The University of Western Ontario. These cells were initially calibrated accurate to 0.0005% by the National Bureau of Standards before being transported carefully to

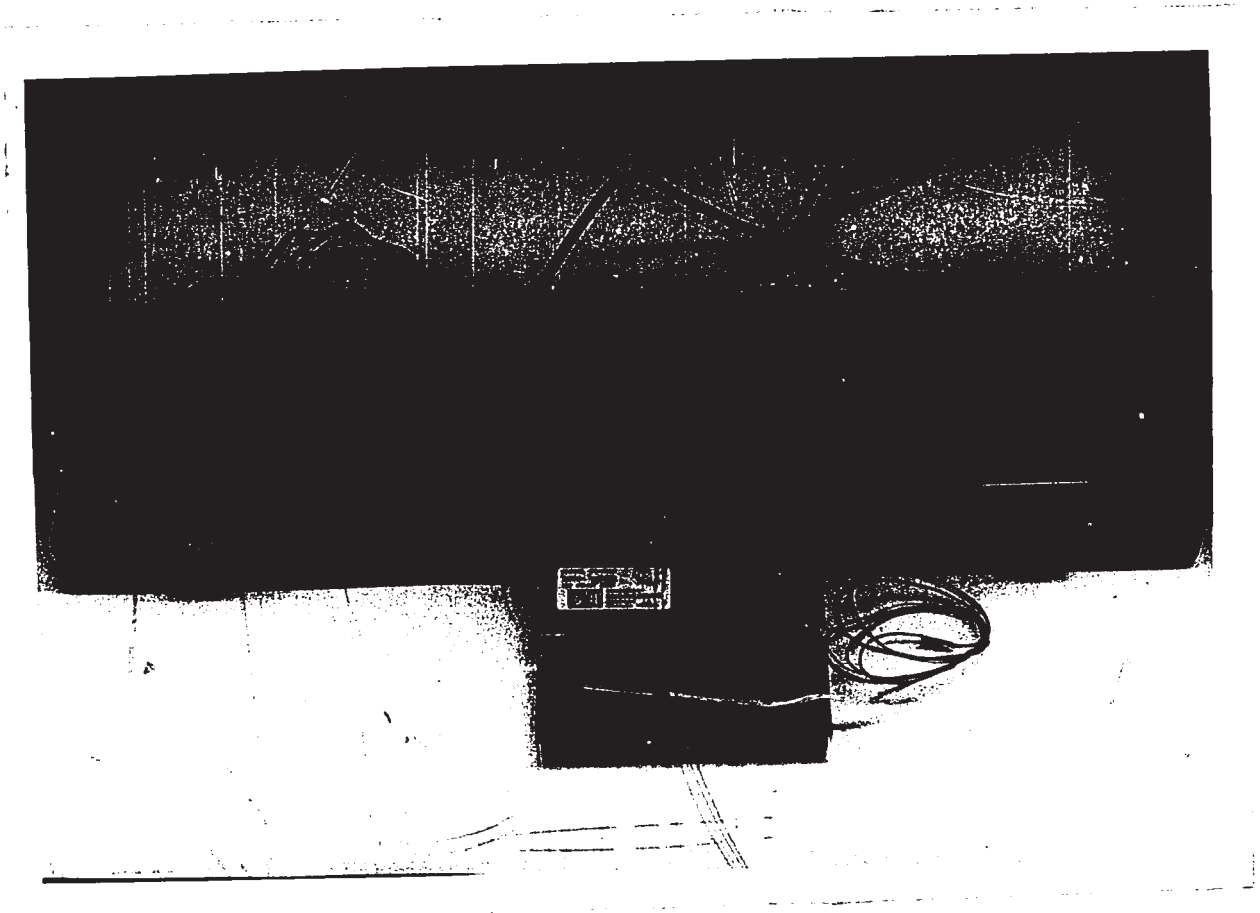

FIGURE 33 VIEW OF PRIMARY LABORATORY STANDARD THERMOMETER AND CAPSULE STANDARD THERMOMETER

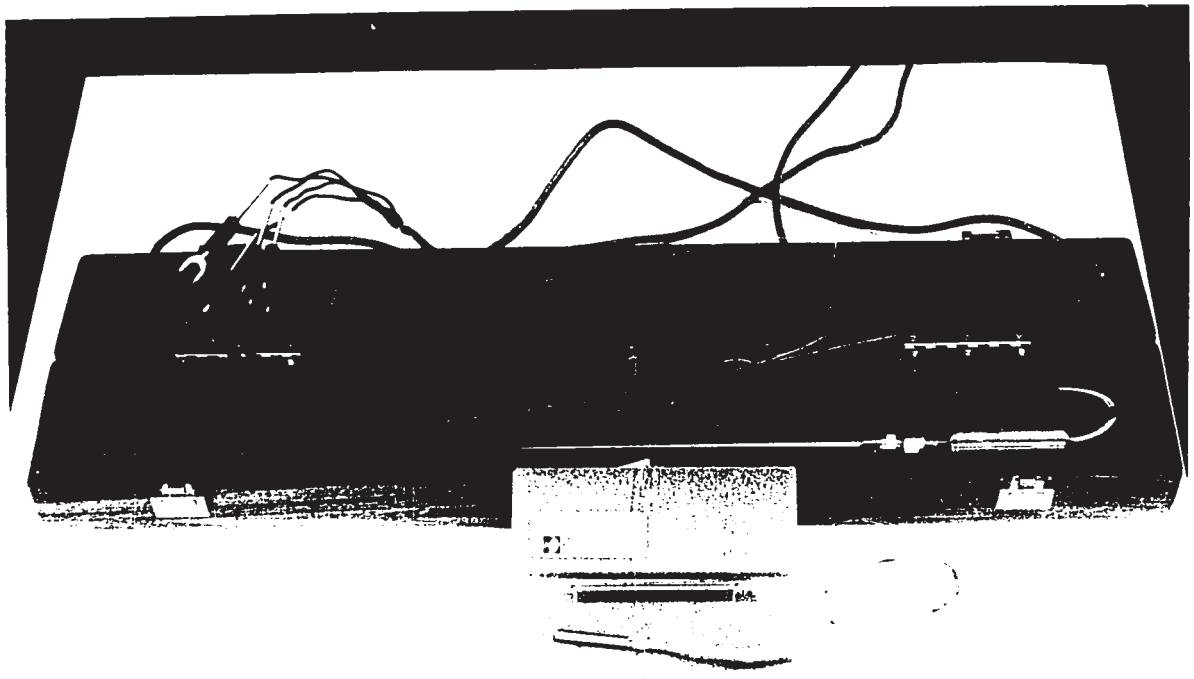

FIGURE 33 VIEW OF PRIMARY LABORATORY STANDARD THERMOMETER AND CAPSULE STANDARD THERMOMETER

the Applied Thermodynamics laboratory of the Faculty of Engineering Science in January 1966. From that date until the most recent calibration test on these cells, the temperature of the cells never varied by more than ± 0.03°C.

The standard cells were intercompared frequently to check their stability with time. The technique of the intercomparisons consisted of connecting two cells in series opposition and measuring the difference in voltage between the two cells with a sensitive microvolt potentiometer in conjunction with a photoelectric galvanometer. All connections were made with 20 gauge pure copper wire in PVC insulation to avoid the spurious emfs in the circuit. A schematic diagram of the test set-up used for this purpose is given in Figure 34. A few of the intercomparison test results are shown in Table 6. It can be seen that none of the cells showed any significant deviation from the initial calibration values. The emf of No. 5 cell, however, seemed to have fallen by approximately 4 microvolts in the past four years. It is evident that the six standard cells are stable to three parts in one million.

5-4. Calibration of the Variable Four Terminal Resistor

The variable four terminal resistor consisted of seven dials, each dial had the following resolution:

Dial 1	10 steps of 10000 ohms
Dial 2	10 steps of 1000 ohms
Dial 3	10 steps of 100 ohms
Dial 4	10 steps of 10 ohms
Dial 5	10 steps of 1 ohm

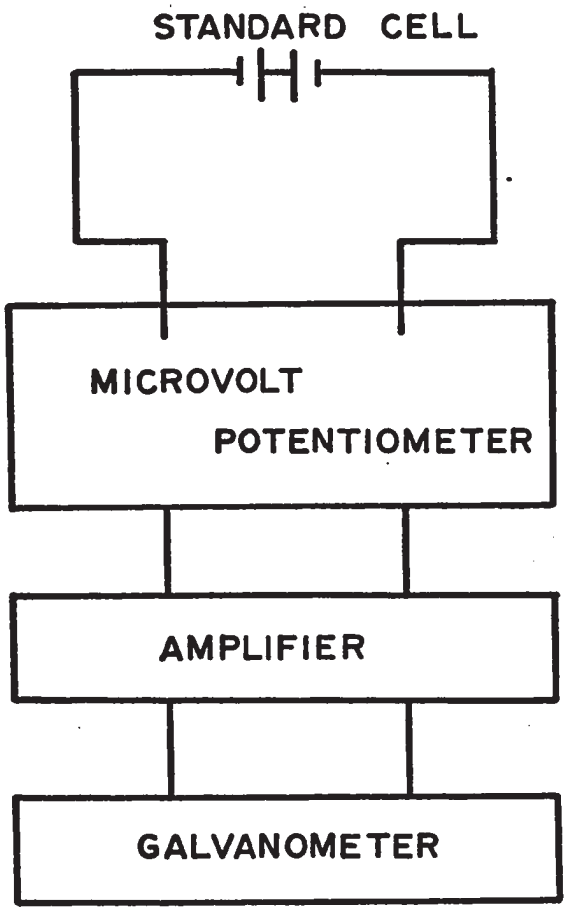

FIGURE 34 SET-UP FOR CALIBRATION OF STANDARD CELLS

TABLE 6 THE STABILITY OF SATURATED STANDARD CELLS

Tester		NBS	U.W.O.	U.W.O.	U.W.O.	U.W.O.	U.W.O.	U.W.O.	U.W.O.
Date		25-8-65	29-9-67	5-10-67	13-10-67	21-10-67	13-5-68	31-3-69	16-7-69
Cell Temperature ^{o}C		29.83	29.78	29.74	29.75	29.76	29.75	29.78	29.79
Cell Position	Absolute Value (Volts)	Difference Between Cells and Cell #6 (μv)							
1	1.018144	-22	-22.2	-21.7	-22.0	-21.9	-23.0	-22.2	-22.4
2	1.018170	+4	+3.5	+3.0	+3.5	+3.5	+3.3	+4.3	+3.9
3	1.018167	+1	+0.7	+0.7	+1.0	+1.0	+1.0	+1.9	+2.3
4	1.018163	-3	-3.0	-3.0	-3.2	-3.5	-3.3	-5.0	-4.6
5	1.018164	-2	-4.6	-4.5	-4.6	-4.3	-5.0	-5.3	-5.6
6.	1.018166	0	0	0	0	0	0	0	0

Note: 1) The positive sign indicates that the absolute value of the cell being compared is higher than the reference cell. The negative sign is reverse.

2) Cell #6 was used as a reference cell.

Dial 6 10 steps of 0.1 ohms

Dial 7 100 steps of 0.001 ohms

In addition Dials 3 to 7 could be used independently for six figure resolution of low resistance values. If dials 1 and 2 were set to zero, dials 3 to 7 could be shunted by means of a single plug switch to give a total resistance of 111.110, 11.1110 or 1.11110 ohms with six figure resolution as follows:

111.110 ohms total in steps of 0.0001 ohms

11.1110 ohms total in steps of 0.00001 ohms

1.11110 ohms total in steps of 0.000001 ohms.

The variable four terminal resistor was calibrated by the manufacturer against a set of standard resistors supplied by the National Research Council of Canada. The total resistance of the lower five dials which was employed in the temperature measurements in this research was adjusted accurate to one part per one million (i.e. one part per 10^6), the precision of these five dials was limited only by the linearity of the dials. It was, therefore, necessary to know the linearity of the dials and a linearity check was conducted in the Applied Thermodynamics laboratory of the Faculty of Engineering Science. Details of which are given in Appendix E.

The calibration results are summarized in Tables 1E to 4E of Appendix E. On the basis of these calibration data, it may be concluded that the percentage error of the lower five dials on the variable four terminal resistor is well within the manufacturer's specification of ± 0.001% of reading.

5-5. Calibration of the Potentiometer

There were two Cambridge Vernier Potentiometers employed in this research program. Both potentiometers were initially calibrated by the manufacturer in accordance with British National Standard and certified to be accurate to 0.005%. The older one, V.P.1, was calibrated in 1965, the other, V.P.2, in 1969. For V.P.2, the uncertainty on the voltage across any measuring section of the potentiometer to the voltage across section 10 of the dial marked x 0.1 volt was no more than ± 5 parts in one million. The uncertainty in corresponding ratio of the standard cell section to section 10 of the dial marked x 0.1 volt was estimated within ± 10 parts in one million. During the progress of this research program V.P.1 was used as a working potentiometer whereas V.P.2 was kept as a laboratory standard. In order to ascertain their relative stability, both potentiometers were intercompared in the Applied Thermodynamics laboratory. Details of this intercomparison are given in Appendix F.

Tables 1F to 3F of Appendix F give the intercomparison test results conducted on the two potentiometers. It may be concluded that the two potentiometers are evidently stable to about 4 parts in one million.

5-6. Calibration of the Standard Shunt

The standard shunt used in this research was one of the multiple standard resistors which was intended for the potentiometric measurement of direct currents. This compact unit consisted of seven four terminal standard resistors with one set of current and potential terminals and two plugs for the selection of the required resistance

value. This whole unit was initially calibrated by the National Research Council of Canada. For one-ohm standard resistor it was certified to within ± 0.005% accuracy. In order to confirm this certification calibration test was conducted on this one-ohm standard resistor in this laboratory.

The method of checking the standard shunt was the potentiometric comparative method in which the standard shunt was compared directly with a primary standard resistor using an isolating potential comparator. The primary standard resistor was the Thomas type one-ohm standard resistor. The primary standard resistor was calibrated by the National Bureau of Standards, the resistor was certified to have a resistance of 1.0000002 ohms accurate to 0.0001 percent at the temperature of 25.0°C. The temperature coefficients of this standard resistor were reported as follows:

$$\text{Alpha } (\alpha) = + 0.000003$$

$$\text{Beta } (\beta) = - 0.0000005$$

Thus the absolute value at any temperature within the 20 to 30°C interval (31) may be calculated by the following equation:

$$R_t = R_{25}\ 1 + \alpha\ (t - 25) + \beta\ (t - 25)^2 \qquad \ldots\ldots\ldots\ldots\ldots\ldots\ (23)$$

where R_t is the resistance at temperature t°C

R_{25} is the resistance at 25°C.

Since the comparison test was conducted at 21°C, the absolute value of the primary standard resistor had a calculated value of 0.999980 ohms. The difference of resistance between the primary standard resistor and the shunt was found to be 26×10^{-6} ohms. The absolute value of the standard shunt was determined in terms of the

reference standard resistor to be 1.000006 ohms. In view of this it may be concluded that this standard shunt is accurate to within 10 parts in one million (i.e. 10 parts in 10^6) or 0.001 percent.

5-7. Calibration of the Volt Box

The volt box employed in this research program was certified by the manufacturer to be accurate to within ± 0.005%. In addition a self-check was conducted in this laboratory to confirm the manufacturer's statement related to the accuracy of the volt box. The method of checking the volt box was fully described by the writer of this thesis in reference (32). Table 7 gives a typical set of calibration test results conducted on the volt box. It may be concluded that the percentage error in the normal ratio factor given for the volt box is well within ± 0.005%. These tests verify the manufacturer's statement related to the accuracy of the volt box.

TABLE 7

VOLT BOX CALIBRATION TESTS

Binding Post From	Binding Post To	Vx (Volt)	Vs (Volt)	$Rx=100.003\frac{Vx}{Vs}$ (ohm)	Normal Resistance (ohm)	Normal Ratio	Actual Ratio	Error %
C	1.5	0.010040	0.0006693	1500.119	1500			
3	C	0.019929	0.0006643	3000.090	3000	2	1.999901	-0.0049
7.5	3	0.029678	0.0006595	4500.210	4500	5	4.999803	-0.0039
15	7.5	0.048744	0.0006499	7500.455	7500	10	9.999710	-0.0029
30	15	0.094081	0.0006272	15000.609	15000	20	19.999322	-0.0033
75	30	0.24773	0.0005505	45002.258	45000	50	49.998448	-0.0031
150	75	0.36784	0.0004904	75010.406	75000	100	100.001418	+0.0014
300	150	0.57815	0.0003854	150017.473	150000	200	200.005133	+0.0026
750	300	0.93418	0.0002076	450003.866	450000	500	499.983912	-0.0032
1500	750	1.06519	0.0001420	750156.304	750000	1000	1000.048440	+0.0048

CHAPTER 6

EXPERIMENTAL PROCEDURES

6-1. Light Water and Heavy Water Samples

The light water employed was ordinary distilled water taken from a communal supply. It was further purified and degassed by two successive distillations in a special corning all-glass water distillation unit. The electrical conductivity of the triple distilled and degassed light water sample just prior to it being charged into the calorimeter was 10^{-6} mho per cm.

The heavy water samples used in this research were supplied by the Atomic Energy of Canada Limited in 1968. The heavy water was stored in a Polyethelene bottle and possessed a purity of 99.78%. This material was degassed by boiling under vacuum before being charged into the calorimeter.

6-2. Constant Mass Experiments

The heavy water or light water sample was first transferred to a glass container. After the initial weighing, the glass container with its charge of water was connected to the filling tube as shown in Figure 35. The calorimeter and the filling tube were then evacuated to a pressure of less than 0.005 mm Hg. Under this pressure the calorimeter was considered sufficiently gas-free. The

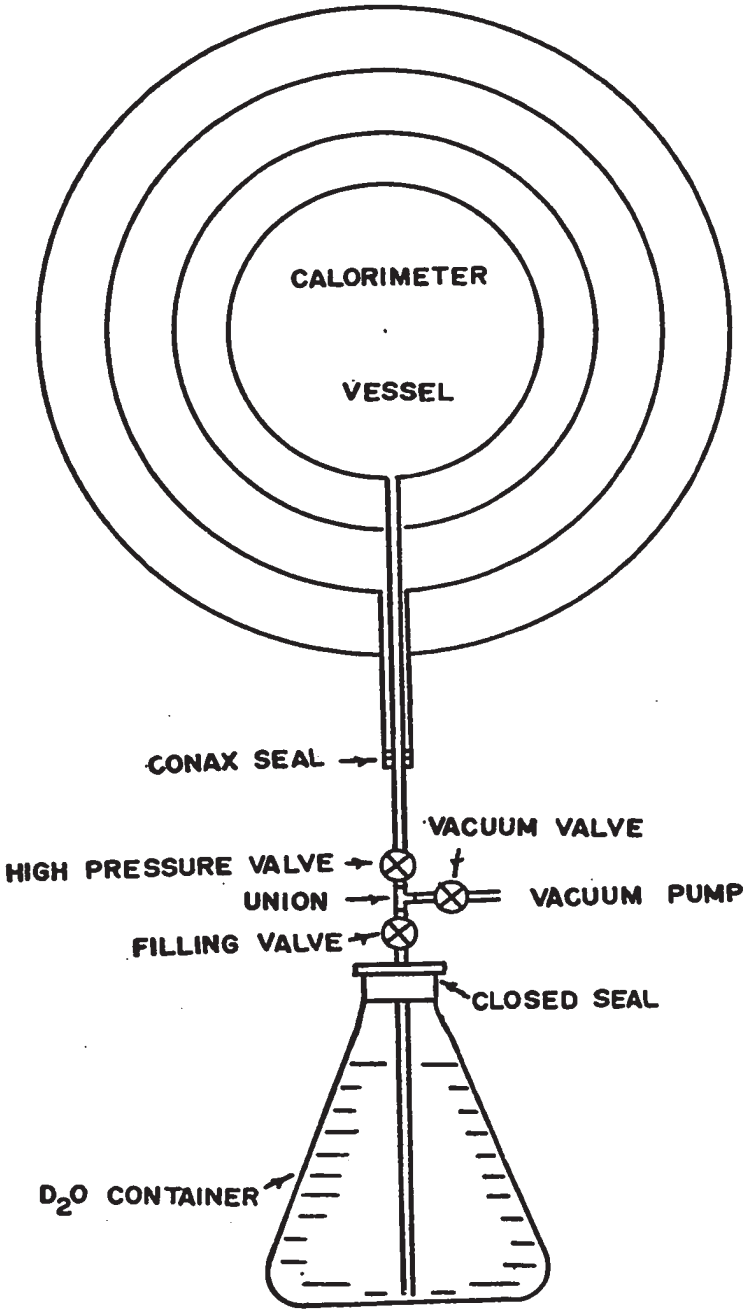

FIGURE 35 SET-UP FOR CHARGING THE CALORIMETER WITH HEAVY WATER

vacuum valve was then closed and the filling valve opened. The water sample in the glass container was forced into the calorimeter by its own vapour pressure using a hot plate to heat the glass container. Upon the completion of charging the calorimeter, the high pressure valve was closed and the glass container and the union were detached and weighed to the nearest 0.0001 gram on an analytical balance. The net charge introduced into the calorimeter system was obtained by subtracting the final weight from the initial weight*. In order to ensure the experiments were conducted in two phase region, the heavy water samples were added to the calorimeter no more than 760 grams for high filling constant mass experiments or no less than 80 grams for low filling constant mass experiments. This was based on the calculation of the known volume of the calorimeter and the specific volumes of saturated heavy water liquid and vapour (33). At 300°C there would be still a small amount of vapour or liquid in equilibrium with its liquid or vapour respectively.

Before starting a series of constant mass experiments, the apparatus was brought to a desired initial temperature and allowed to reach equilibrium. Just prior to starting an experiment, the temperature of the water sample was measured very carefully, and then a constant electrical power was supplied to the calorimeter heater or heaters. During the heating period, the temperature of the adiabatic shield and the temperature of the outer guard were maintained essentially at the same level as the calorimeter by automatically and

---

*The bouyancy corrections were eliminated by this procedure.

manually adjusting the electrical energy to the adiabatic shield and outer guard heaters respectively. In addition, adjustments were made to the electrical power going into the calorimeter support tube and vacuum tube heaters. These later adjustments insured that the heat flows by conduction along the tubes from or to the calorimeter were eliminated.

The input power to the calorimeter was recorded every 500 seconds whereas the temperature difference between the calorimeter and the adiabatic shield, and between the adiabatic shield and the outer guard were recorded by a recorder every 20 seconds.

After a predetermined amount of time, the electric energy to the calorimeter was turned off. The temperature of the calorimeter was recorded until the apparatus reached a final equilibrium state. The total energy added to the fluid related to its temperature change was then calculated.

6-3. Liquid Withdrawal Test

In preparation for a series of liquid withdrawal tests, the calorimeter was charged a measured quantity of water sample and the apparatus was then brought to a chosen temperature and allowed to reach equilibrium.

Before starting the test, a liquid receiver was attached to the liquid withdrawal line. The energy required for the experiment was estimated so that the flow rate would be approximately a chosen value. The initial equilibrium temperature of the calorimeter was measured firstly and the input power was turned on. The operator opened the control valve as quickly as possible and adjusted the flow rate until

the calorimeter was maintained at an isothermal condition. Readings of the differential thermocouples and the power to the calorimeter heater were recorded as before. At a chosen instant, the input power was turned off. The control valve was manually adjusted several times in order to bring the calorimeter and its contents back to the initial equilibrium temperature. The final temperature was then observed. The water withdrawn was collected and weighed. The total energy added and the mass withdrawn were calculated.

CHAPTER 7

HEAT EXCHANGE BETWEEN THE CALORIMETER AND ADIABATIC SHIELD

The net heat exchange between the calorimeter and adiabatic shield is dependent on, (i) the heat transfer coefficient between the calorimeter and adiabatic shield, (ii) temperature variations along the surface of the calorimeter and adiabatic shield, (iii) the overall temperature difference between the calorimeter and adiabatic shield.

In order to ascertain the magnitude of the heat transfer coefficient between the calorimeter and adiabatic shield, two series of heat transfer experiments were conducted at approximately 100 and 300^{o}C during the early part of the research program. These tests were made by offsetting the adiabatic shield by approximately 1^{o}C on the control thermocouple and adding just enough energy into the calorimeter to maintain the temperature difference. Under steady state the energy added to the calorimeter was just equal to the energy being transferred from the calorimeter to the adiabatic shield. By measuring the input power and the temperature difference between the calorimeter and adiabatic shield the heat transfer coefficient was found.

Table 8 summarizes the experimental results of these two tests. It should be mentioned that during heat transfer coefficient determinations the calorimeter contained approximately 650 grams of light

TABLE 8

HEAT TRANSFER COEFFICIENT DETERMINATION

Run No.	Temp. ($^{o}_{C}$)	Input Power (Watts)	Temp. Difference Between the Calorimeter and Adiabatic Shield (^{o}C)	Mass Contained In the Calorimeter (g)	Heat Transfer Coefficient Watts/$^{o}_{C}$ - Overall Surface Area of the Cal.
1	300.17	0.22	0.83	660.6374	0.264
2	100.09	0.10	0.64	636.5632	0.156

water sample. The temperature variations along the surface of the calorimeter at steady state were found to be no more than 0.1°C which is in contrast to a temperature variation of 0.25°C during a typical constant mass experiment. Consequently the heat transfer coefficients obtained in this study are somewhat different from the actual values of the constant mass experiments.

The radiant exchange between the calorimeter and the adiabatic shield may be estimated by the following equation (34)

$$q_{1\to 2} = \frac{\sigma A_1 (T_1^4 - T_2^4)}{\frac{1}{\varepsilon_1} + \frac{A_1}{A_2}(\frac{1}{\varepsilon_2} - 1)} \qquad \ldots\ldots\ldots\ldots\ldots\ldots \quad (24)$$

in which subscripts 1 and 2 refer to the outside surface of the calorimeter and the inside surface of the adiabatic shield respectively. The magnitude of the net heat exchange essentially depends on the emissivity factor of the surface of the calorimeter and the adiabatic shield. On the basis of the heat transfer coefficients it was found that the emissivity of the calorimeter was approximately 0.35 which was considered a relatively low value for the material of Inconel 600.

In view of the fact that the average temperature difference between the calorimeter and adiabatic shield was maintained to within 0.05°C the heat leak was estimated to be approximately 0.1 percent of the total energy added during a constant mass experiment. It should be emphasized that this figure is only an estimate based on the information obtained from the heat transfer study described in this Chapter. The actual heat leak that occurs during a constant mass experiment will be somewhat larger due to the larger temperature variation on the calorimeter shell. The best method to eliminate the heat

leak error is by employing the experimental procedure as described in Chapter 2.

CHAPTER 8

EVALUATION OF THE PERFORMANCE OF THE APPARATUS

The reliability of the calorimeter apparatus and its associated instrumentation was evaluated from the calibration measurements using light water. Details of the constant mass experiments and the liquid withdrawal tests are described separately below.

8-1. Constant Mass Experiments on Light Water

Four series of the calibration measurements were made on light water from 50 to 300^{0}C. The first two series of experiments were conducted on the calorimeter with high filling mass whereas the second two series of experiments were conducted on the calorimeter with low filling mass. The masses of the light water samples were charged into the calorimeter amounting to 636.5632 and 256.3798 grams for the high filling and low filling experiments respectively. Upon the successive completion of the investigations, the samples were collected and weighed a second time. The final mass values in these two types of experiments were found to be 636.4814 and 256.2836 grams. The differences between the initial and final mass values in the high filling and low filling experiments were evidently less than 0.1 grams. This may be attributed to extremely small amounts of liquid and vapour which remained entrapped in the lines of the calorimeter. The initial

mass values, therefore, were used to evaluate the α quantities.

The test results of the constant mass experiments on light water are assembled in Table 9. It was described previously in Chapter 2 that the general energy equation for a constant mass experiment might be derived as follows:

$$Q = M \left(h_f - T v_f \frac{dp}{dT}\right)_1^2 + V \left(T \frac{dp}{dT} - P\right)_1^2 + c_{p_c} \Delta T + q_E \quad \ldots\ldots\ldots\ldots\ldots\ldots (2)$$

Since the last three terms on the right hand side are independent of the mass of the sample, equation (2) can be rewritten in the following form

$$Q = M \Delta \alpha + Z \quad \ldots\ldots\ldots\ldots\ldots\ldots (25)$$

The values of Q and M of each group experiments for a single temperature interval were fitted to the above equation by means of a least squares technique. This reduction yielded mean values for α and Z. Using the mean value of Z, the individual values of α for each experiment were computed and compared with the mean value of α for each group as shown in Table 9.

The comparison of α quantities for saturated light water between Osborne et al and this work are given in Figure 36. It can be seen that the experimental data obtained in this research are entirely within the realm of Osborne's observed values. The reproducibility of the α quantity measurements of this work is within ± 0.07 percent whereas the overall scatter of Osborne's results is approximately ±0.25 percent. In view of this it may be concluded that the α results obtained with the present apparatus are at least comparable and perhaps even superior to those obtained by Osborne.

TABLE 9

CONSTANT MASS EXPERIMENTS ON LIGHT WATER

Test No.	Mass (g)	Initial Temp.(°C)	Final Temp.(°C)	Total Energy Added (Int.J.)	Energy Added For 50°C Interval	Δ α (Int.J./g)	Deviation From Mean Value (%)
1	636.5632	100.040	150.038	218796.3	218805.1	208.37	-0.01
2	636.5632	99.890	150.010	219334.9	218827.1	208.41	+0.01
3	256.3798	99.748	150.853	142674.1	139589.0	208.39	0.00
	For temperature interval from 100 to 150°C Z_m = 86161.5 Int.J. α_m = 208.39 Int.J./g						
4	636.5632	150.192	200.141	225582.5	225812.8	208.12	+0.01
5	636.5632	149.846	200.036	226648.3	225790.2	208.09	-0.01
6	256.3798	150.293	200.122	146312.6	146696.8	208.16	+0.03
7	256.3798	150.283	200.196	146413.4	146668.6	208.05	-0.03
	For temperature interval from 150 to 200°C Z_m = 93328.2 Int.J. α_m = 208.11 Int.J./g						
8	636.5632	200.188	250.128	235270.8	235553.3	207.36	-0.01
9	636.5632	200.111	250.973	239643.6	235582.1	207.40	+0.01
10	256.3798	200.143	249.999	156285.9	156737.3	207.43	+0.03
11	256.3798	200.160	250.124	156600.4	156713.1	207.33	-0.03
	For temperature interval from 200 to 250°C Z_m = 103557.1 Int.J. α_m = 207.38 Int.J./g						

TABLE 9 (Continued)

Test No.	Mass (g)	Initial Temp.(°C)	Final Temp.(°C)	Total Energy Added (Int.J.)	Energy Added For 50°C Interval	Δ α (Int.J./g)	Deviation From Mean Value (%)
12	636.5632	250.396	300.138	247540.3	248827.2	206.19	±0.02
13	636.5632	250.041	300.147	249293.5	248766.0	206.09	-0.02
14	256.3798	249.969	299.992	170470.0	170391.6	206.00	-0.07
15	256.3798	249.997	300.057	170665.3	170460.7	206.27	+0.07

For temperature interval from 250 to 300°C Z_m = 117576.3 Int.J. α_m = 206.14 Int.J./g

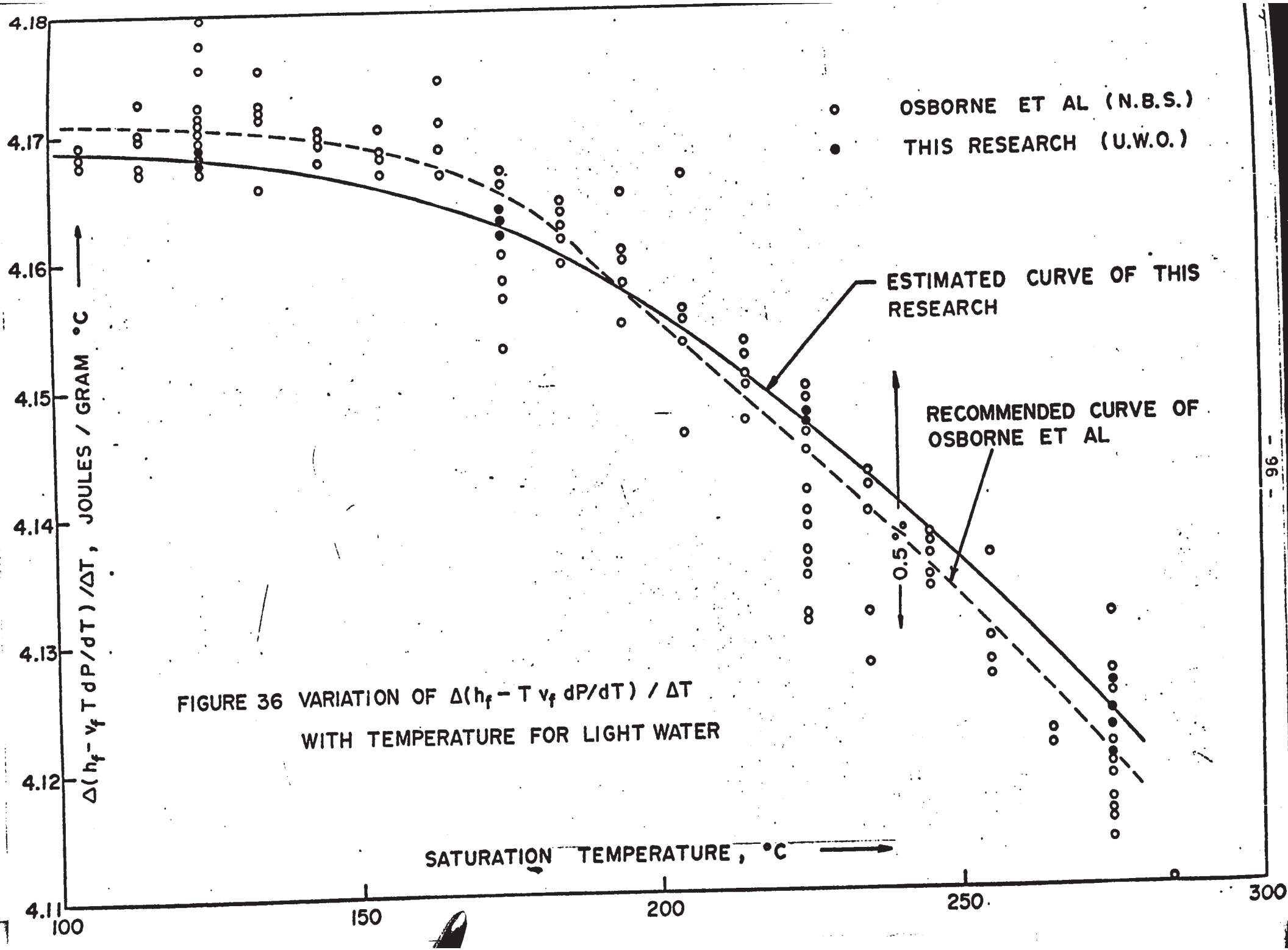

FIGURE 36 VARIATION OF $\Delta(h_f - T v_f dP/dT) / \Delta T$ WITH TEMPERATURE FOR LIGHT WATER

It should be stressed that the only direct calorimetric measurement of α conducted on saturated light water prior to research of this thesis were those of Osborne et al of the National Bureau Standard. The results of Osborne et al have been utilized by the different compilers of the various national steam tables (35, 36, 37, 38, 39).

8-2. Liquid Withdrawal Tests on Light Water

As mentioned previously the liquid withdrawal test yields a measured quantity of β which is relatively small for saturated liquid light water or heavy water at low temperature and difficult to measure with precision. In view of this fact that Osborne et al only used their experimental results of liquid withdrawal tests on saturated light water in the temperature range from 330 to 374°C and evaluated the β values below the temperature of 330°C directly from P-V-T data proposed by Smith and Keyes (40).

The liquid withdrawal tests were carried out on light water only in the temperature range from 100 to 150°C. The test results are summarized in Table 10. Since the final temperature of the experiment was slightly different from the initial temperature, a correction was necessary to apply to the energy term to bring the calorimeter and its contents back to the initial temperature. The corrections (ΔQ) shown in Table 10 were calculated by using the following equation:

$$\Delta Q = \left(\frac{dZ}{dt} + M\frac{d\alpha}{dt}\right) \Delta t \qquad \text{..... (26)}$$

where $\Delta t = T_{initial} - T_{final}$

The values of dZ/dt and dα/dt were determined in the constant mass experiments. It should be pointed out that the energy corrections in the liquid withdrawal tests were on the average about 10% of the total

TABLE 10

LIQUID WITHDRAWAL TESTS ON LIGHT WATER

Test No.	Initial Temp.(°C)	Final Temp.(°C)	Initial Mass (g)	Approximate Flow Rate (g/min.)	Mass of Liquid Withdrawn (g)	Total Energy Added (Int.J.)	Energy Corrections (Int.J.)	β at Even Temp. (Int.J./g)
1	99.991	99.988	634.1689	16.5	74.7195	93.88	+12.17	1.42
2	100.015	100.017	559.4494	12.6	53.6755	87.00	- 7.66	1.48
3	99.990	99.985	505.7739	8.3	129.3260	170.60	+16.46	1.45
4	125.131	125.124	376.4479	7.3	54.3760	153.17	+21.44	3.21
5	125.051	125.046	321.0719	7.3	54.9161	153.23	+14.17	3.05
6	124.973	124.968	266.1558	7.2	54.6375	153.14	+13.03	3.04
7	149.931	149.940	211.5183	4.6	36.8308	245.40	-22.06	6.07
8	149.895	149.873	174.6875	5.9	57.4650	295.49	+48.66	5.99
9	149.761	149.689	117.2225	7.6	75.7393	300.17	+136.53	5.78

energy added. These corrections may be reduced by withdrawing larger amounts of liquid and by extending the duration of a withdrawal test.

The most important factor affecting the accuracy of this type of experiment was the maintenance of isothermal conditions within the calorimeter. Since the resistance thermometer which had a slow response was used as a temperature indicator of the calorimeter, it was very difficult for the operator to maintain the calorimeter at isothermal conditions. If the temperature of the calorimeter departed from its original temperature by only 0.001°C an error of the order of 2% could be introduced to the β value at a temperature of 100°C.* This error may be reduced by using a fast response multijunction differential thermocouple in the temperature control system and also by withdrawing larger amounts of fluid from the calorimeter.

Figure 37 shows the temperature variations of the calorimeter with time during a typical liquid withdrawal test. It is seen that the temperature differences between the calorimeter and adiabatic shield were maintained within ± 0.02°C during test. The temperature variations along the surfaces of the calorimeter, adiabatic shield and the outer guard during liquid withdrawal were almost the same with the steady state.

The comparisons between the observed values of this work and the calculated values from P-V-T data of Smith and Keyes are given in Table 11. It can be seen that the maximum error is no more than + 3 percent occurring at 100°C and the error decreases as the temperature increases.

---

*This assumes that the mass of liquid left in the calorimeter was approximately 100 grams whereas the mass of liquid withdrawn was approximately 75 grams.

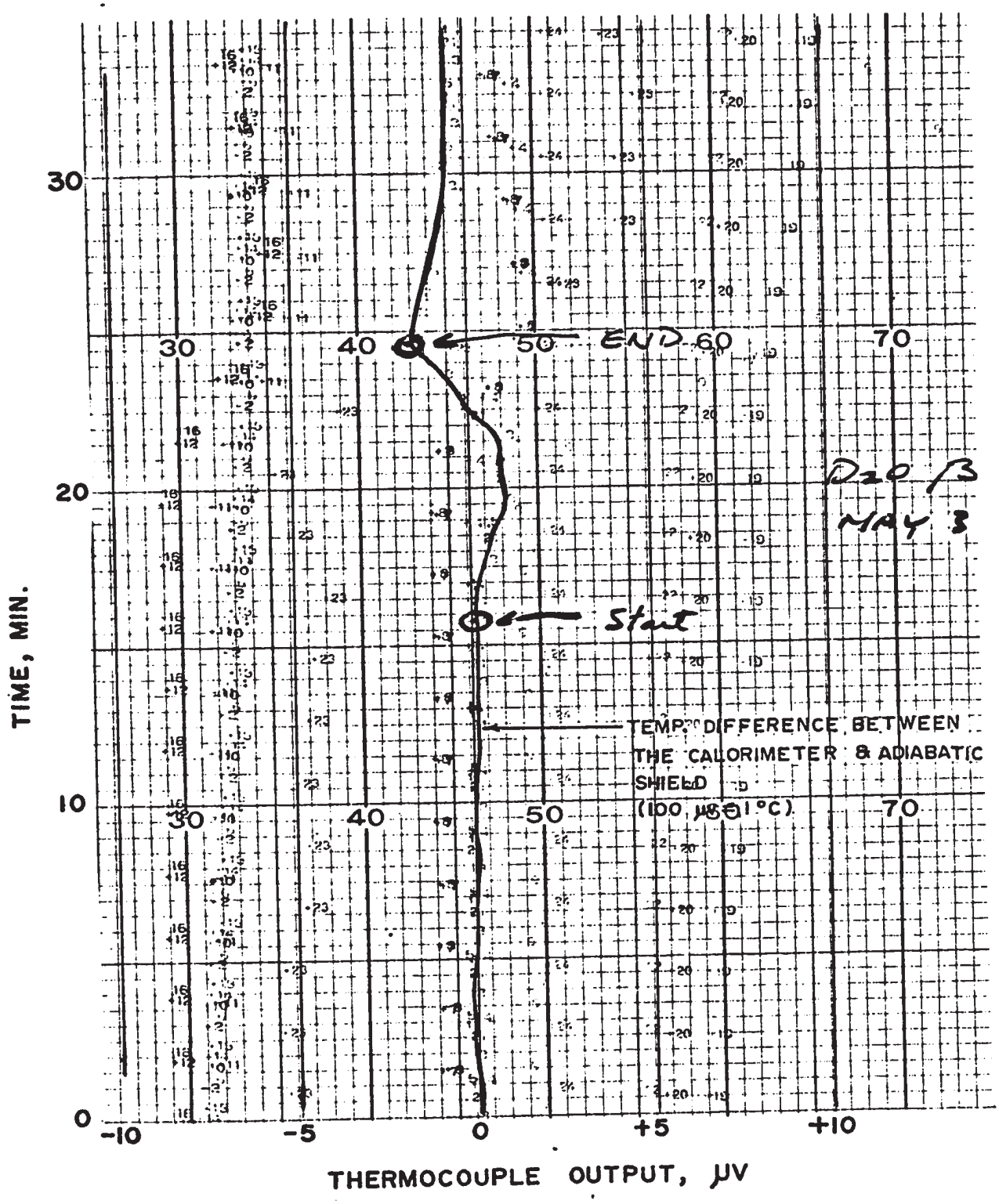

FIGURE 37 TEMPERATURE VARIATIONS OF THE CALORIMETER WITH TIME

TABLE 11

COMPARISONS BETWEEN THE OBSERVED VALUES OF THIS WORK AND THE CALCULATED VALUES OF SMITH AND KEYES

Temperature (°C)	β Values (Int.J./g)		Deviation $\frac{\beta_o - \beta_{S.K.}}{\beta_{S.K.}}$ (%)
	This Work	Smith & Keyes	
100	1.45	1.41	+2.8
125	3.10	3.03	+2.3
150	5.95	5.89	+1.0

8-3. Derivation of the Heat Capacity of the Empty Calorimeter from the Constant Mass Experiments

The heat capacity of the empty calorimeter may be derived from the results of the constant mass experiments. It was described previously that a constant value of Z for a single temperature interval was obtained in computing the mean value of α. The heat capacity of the empty calorimeter system can be evaluated by the following relationship:

$$c_{p_c} \Delta T + q_E = Z - V \left(T \frac{dp}{dT} - P\right)_1^2 \qquad \text{..... (26)}$$

The second term on the right hand side in the above equation was calculated by means of values accurate to 0.03 percent in reference 20. Table 12 summarizes the heat capacity of the empty calorimeter derived from the results of the constant mass experiments on light water.

TABLE 12

HEAT CAPACITY OF THE EMPTY CALORIMETER

INFERRED FROM CONSTANT MASS EXPERIMENTS

Temperature Interval (°C)		Heat Capacity of the Empty Calorimeter* (Int.J.)
From	To	$c_{p_c}\ \Delta T$
100	150	82383.5
150	200	84166.4
200	250	85754.7
250	300	87096.6

*No attempt was made to evaluate the heat leak q_E and consequently the heat capacity values of this table deviate from the "true heat capacity values" by an amount equal to the heat leak.

CHAPTER 9

EXPERIMENTAL RESULTS ON HEAVY WATER

9-1. Constant Mass Experiments on Heavy Water

Subsequent to the above mentioned calibration measurements on light water, 664.3845 grams heavy water were charged into the calorimeter and four series of (thirty measurements) high filling tests were conducted from 50 to 300°C. The first two series measurements were carried out in 25°C temperature intervals whereas the others were carried out in 50°C temperature intervals. The results of the first two series experiments are summarized in Table 13 and 14 and the others are given in Table 1G and 2G of Appendix G. The comparisons of these experimental data are shown in Figure 38. It can be seen from Tables 12 and 13 that the consistency of the first two series measurements is within ± 0.05 percent. Figure 38 however indicates that the last series measurements shifted from first two series measurements by approximately 0.7 percent. This is because a small leakage of heavy water occurred in the calorimeter*. The final mass value was found to be 655.0214 grams and indicated that approximately 9.4 grams of heavy water sample was lost during these tests. The results shown in Table 1G and 2G which are

*Supplementary tests indicated that the leakage occurred in the top zone heater of the calorimeter and only showed up at elevated temperatures and pressures.

TABLE 13

HIGH FILLING CONSTANT MASS EXPERIMENTS

ON HEAVY WATER (FIRST SERIES)

Test No.	Initial Temp.(°C)	Final Temp.(°C)	Total Energy Added (Int.J.)	Energy Added For 25°C Interval (Int.J.)
1	50.154	74.933	107985.2	108948.2
2	74.930	99.983	109622.1	109390.2
3	100.149	124.978	109357.1	110110.3
4	124.960	150.023	111403.4	111123.3
5	149.927	175.068	113170.1	112535.3
6	175.048	200.043	114259.5	114282.3
7	200.007	225.044	116768.3	116595.8
8	225.018	249.981	119089.6	119266.1
9	249.947	275.115	123391.2	122567.5
10	275.088	299.998	126102.4	126558.0

TABLE 14

HIGH FILLING CONSTANT MASS EXPERIMENTS

ON HEAVY WATER (SECOND SERIES)

Test No.	Initial Temp.(°C)	Final Temp.(°C)	Total Energy Added (Int.J.)	Energy Added For 25°C Interval (Int.J.)
11	50.130	74.990	108299.6	108909.4
12	75.010	100.012	109336.4	109327.7
13	100.072	125.078	110068.8	110042.4
14	125.074	150.052	111028.1	111125.8
15	150.933	175.125	108945.1	112583.8
16	175.114	200.107	114293.3	114325.3
17	200.091	225.054	116456.6	116629.2
18	225.037	250.038	119271.8	119267.0
19	250.016	275.101	122962.3	122545.6
20	275.085	299.989	126017.4	126503.0

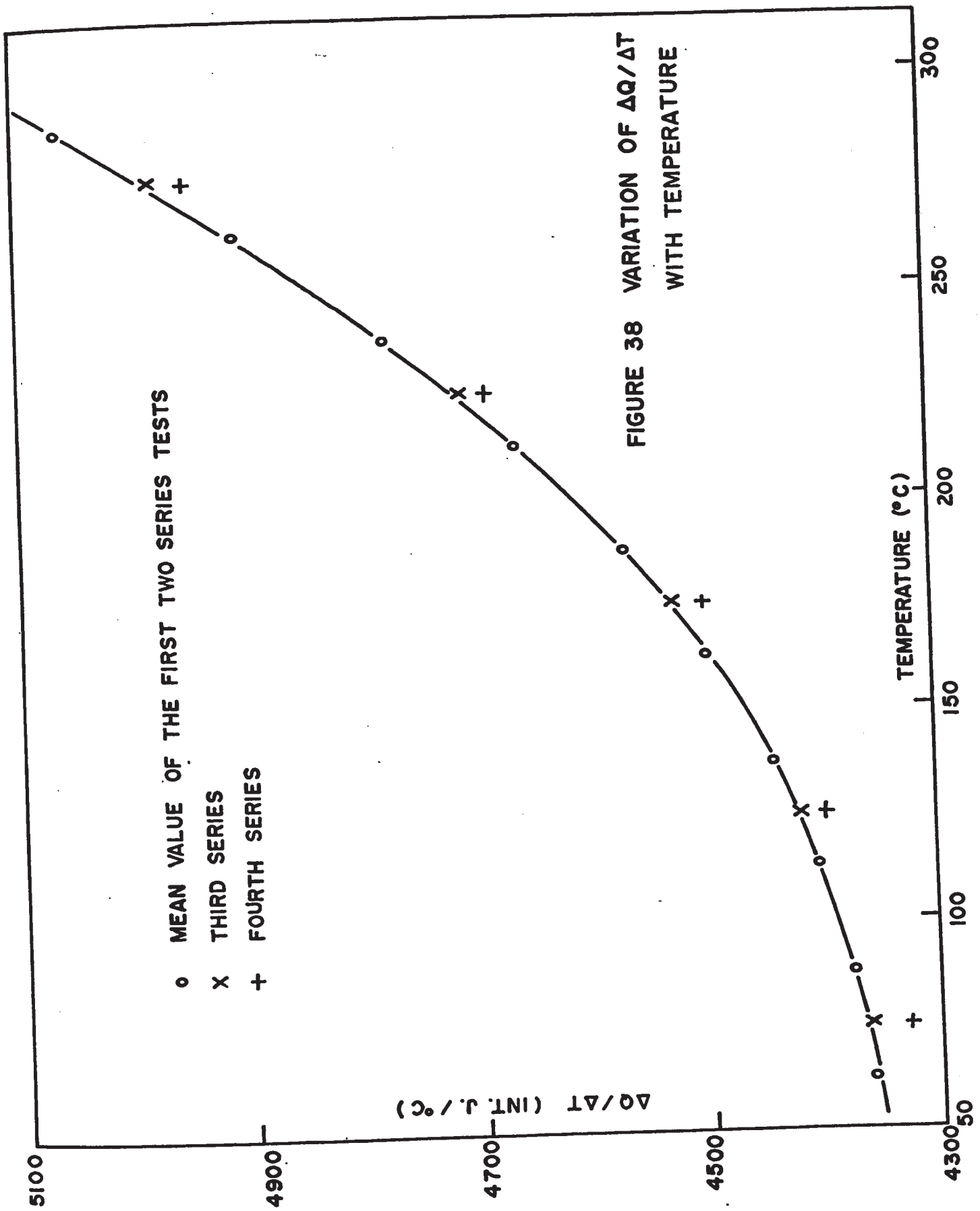
FIGURE 38 VARIATION OF ΔQ/ΔT WITH TEMPERATURE
o MEAN VALUE OF THE FIRST TWO SERIES TESTS
X THIRD SERIES
+ FOURTH SERIES
ΔQ/ΔT (INT. J./°C)
TEMPERATURE (°C)
5100
4900
4700
4500
4300
50
100
150
200
250
300

uncorrected for the effect of the small leak of 9.4 grams were therefore rejected.

Three series of low filling constant mass experiments on heavy water were conducted below 200°C. Upon the completion of each series measurements, the samples were collected and weighed a second time and no significant differences were found between the initial and final mass values (refer to Table 3G of Appendix G). The experimental results of these three series tests are tabulated in Tables 15 to 17.

The α quantities for heavy water in the temperature range from 50 to 200°C were evaluated by using least squares method as described previously to combine the high filling and low filling experiment results and are given in Table 18. The α value for heavy water in the temperature range from 100 to 300°C may also be derived from the results of the high filling constant mass experiments and the previously mentioned values for the heat capacity of the empty calorimeter by using the following equation:

$$\Delta \alpha = \frac{Q_H - Z_{calc.}}{M_H} \qquad \text{..... (27)}$$

where $Z_{calc.} = V \left(T \frac{dp}{dT} - P\right)_1^2 + c_{P_c} \Delta T + q_E$

The term $V \left(T \frac{dp}{dT} - P\right)_1^2$ is approximately 1.7% and 12.2% of the total energy added (Q_h) at temperatures of 100 and 300°C respectively and was evaluated by means of the data accurate to 0.3% in reference (41). The error in α quantities for heavy water in the above mentioned temperature range caused by such an error in this term was less than 0.05 percent.

TABLE 15

LOW FILLING CONSTANT MASS EXPERIMENTS

ON HEAVY WATER (FIRST SERIES)

Test No.	Initial Temp.(°C)	Final Temp.(°C)	Total Energy Added (Int.J.)	Energy Added For 25°C Interval (Int.J.)
31	50.153	75.036	61280.9	61569.0
32	75.031	100.051	62440.8	62391.0
33	100.051	125.052	63463.3	63460.7

Mass contained in first series of low filling tests = 207.4610 grams

TABLE 16

LOW FILLING CONSTANT MASS EXPERIMENTS

ON HEAVY WATER (SECOND SERIES)

Test No.	Initial Temp.(°C)	Final Temp.(°C)	Total Energy Added (Int.J.)	Energy Added For 25°C Interval (Int.J.)
34	49.830	75.834	64497.6	62007.3
35	75.825	100.023	60813.6	62829.1
36	100.012	125.039	63933.0	63864.0
37	124.911	149.990	65435.1	65228.9
38	149.990	174.962	66868.7	66943.6
39	174.956	199.810	68673.9	69077.3

Mass contained in second series of low filling tests = 211.6122 grams

TABLE 17

LOW FILLING CONSTANT MASS EXPERIMENTS

ON HEAVY WATER (THIRD SERIES)

Test No.	Initial Temp.(°C)	Final Temp.(°C)	Total Energy Added (Int.J.)	Energy Added For 50 and 25°C Interval (Int.J.)
40	50.023	99.975	125215.4	125335.7
41	99.970	150.011	129656.1	129549.7
42	149.914	174.830	66938.3	67163.9
43	124.851	149.937	65674.2	65449.0

Mass contained in third series of low filling tests = 213.9551 grams

TABLE 18

α VALUES FOR HEAVY WATER

Test No.	Mass (g)	Energy Added For Even Temperature Interval (Int.J.)	Δα (Int.J./g)	Deviation $\frac{\Delta\alpha - \Delta\alpha_m}{\Delta\alpha_m}$ %
1	664.3845	108948.2	103.67	+0.03
11	664.3845	108909.4	103.61	-0.03
31	207.4610	61569.0	103.62	-0.02
34	211.6122	62007.3	103.66	+0.02
	For temperature interval from 50 to 75°C		α_m = 103.64 Int.J./g Z_m = 40071.7 Int.J.	
2	664.3845	109390.2	102.83	+0.05
12	664.3845	109327.7	102.73	-0.05
32	207.4610	62391.0	102.75	-0.03
35	211.6122	62829.1	102.81	+0.03
	For temperature interval from 75 to 100°C		α_m = 102.78 Int.J./g Z_m = 41074.1 Int.J.	
3	664.3845	110110.3	102.09	+0.05
13	664.3845	110042.4	101.99	-0.05
33	207.4610	63460.7	102.09	+0.05
36	211.6122	63864.0	101.99	-0.05
	For temperature interval from 100 to 125°C		α_m = 102.04 Int.J./g Z_m = 42280.8 Int.J	
4	664.3845	111123.3	101.38	0.00
14	664.3845	111125.8	101.39	0.00
37	211.6122	65228.9	101.43	+0.04
43	213.9551	65449.0	101.34	-0.04
	For temperature interval from 125 to 150°C		α_m = 101.38 Int.J/g Z_m = 43765.9 Int.J.	

TABLE 18 (Continued)

Test No.	Mass (g)	Energy Added For Even Temperature Interval (Int.J.)	$\Delta\alpha$ (Int.J./g)	Deviation $\frac{\Delta\alpha - \Delta\alpha_m}{\Delta\alpha_m}$ %
5	664.3845	112535.3	100.73	-0.04
15	664.3845	112583.8	100.80	+0.04
38	211.6122	66943.6	100.80	+0.04
42	213.9551	67163.9	100.73	-0.04
	For temperature interval from 150 to 175°C			α_m = 100.77 Int.J./g Z_m = 45612.6 Int.J.
6	664.3845	114282.3	99.86	-0.03
16	664.3845	114325.3	99.92	+0.03
39	211.6122	69077.3	99.89	0.00
	For temperature interval from 175 to 200°C			α_m = 99.89 Int.J./g Z_m = 47939.9 Int.J.
1,2,11 & 12	664.3845	218287.7*	206.36	-
40	213.9551	125335.7	206.36	-
	For temperature interval from 50 to 100°C			α_m = 206.36 Int.J./g Z_m = 81183.4 Int.J.
3,4,13 & 14	664.3845	221200.9*	203.48	-
41	213.9551	129549.7	203.47	-
	For temperature interval from 100 to 150°C			α_m = 203.47 Int.J./g Z_m = 86015.3 Int.J.

*Mean Value

Table 19 summarizes the α quantities for heavy water derived from the results of the high filling mass experiments utilizing equation 27. Comparing the α values from 100 to 200°C in Table 18 to the corresponding values in Table 19 it is seen that the differences of the α values obtained by two different methods as described previously are approximately 0.05 percent. On the basis of the results summarized in Tables 18 and 19, it may be estimated that the α quantities for heavy water obtained in this research are accurate to within ± 0.1%.

9-2. Liquid Withdrawal Tests on Heavy Water

The liquid withdrawal tests were carried out on heavy water in this research in the temperature range from 100 to 300°C. Table 20 summarizes the results of the experiments. The comparisons between the observed values of this work and calculated values from the existing P-V-T data of heavy water in reference (33) and (40) are given in Table 21. The maximum deviation between the results of this work and those calculated from P-V-T data is approximately 3% at the temperature of 100°C. It is noteworthy that the deviation between the observed values and the calculated values above 200°C is no more than 1% which is entirely within the error of the existing P-V-T data of heavy water.

In view of the fact that the liquid withdrawal tests were made in a short period of time, the error due to heavy water leakage in the calorimeter would be very small, even though the tests were conducted at elevated temperatures and pressures. For example, it is estimated that in a 24 hour period and a mass of 0.6 grams of heavy water is lost. The leakage of heavy water that does occur during various runs lasting 5 minutes or so is evidently insignificant.

TABLE 19

α VALUES FOR HEAVY WATER

Temperature Range (^{o}C) From	To	Mass (g)	Energy Added For High Filling Test (Int.J.)	$Z_{calc.}$ (Int.J.)	$\Delta\alpha$ (Int.J./g)
100	150	663.7252	221200.9 (Mean Value of Test #3, 4, 13 & 14)	86179.6	203.43
150	200	663.7252	226863.4 (Mean Value of Test #5, 6, 15 & 16)	93592.4	200.79
200	250	663.7252	235879.1 (Mean Value of Test #7, 8, 17 & 18)	103760.1	199.06
250	300	663.7252	249087.1 (Mean Value of Test #9, 10, 19 & 20)	118211.6	197.18

TABLE 20

LIQUID WITHDRAWAL TESTS ON HEAVY WATER

Test No.	Initial Temp.(°C)	Final Temp(°C)	Initial Mass (g)	Approximate Flow Rate (g/min.)	Mass of Liquid Withdrawn (g)	Total Energy Added (Int.J.)	Energy Corrections (Int.J.)	β at Even Temp. (Int.J./g)
1	100.071	100.077	579.1816	3.7	27.9585	59.42	-23.55	1.28
3	100.051	100.044	544.6421	8.8	76.2262	67.57	+27.48	1.25
4	125.291	125.281	468.4159	6.5	64.8705	140.92	+33.63	2.69
5	125.249	125.252	403.5454	4.7	47.1694	141.00	- 9.49	2.78
6	149.869	149.874	356.376	4.4	44.1877	249.41	-15.25	5.30
7	149.833	149.856	312.1883	3.3	33.3640	248.65	-67.05	5.45
8	175.142	175.169	278.8243	3.8	38.7567	454.05	-76.54	9.73
9	175.120	175.142	240.0676	4.1	41.1410	453.96	-58.73	9.60
11	200.041	200.070	198.9266	4.2	42.3527	762.449	-68.63	16.38
12	224.937	224.976	558.7503	4.2	40.7135	1238.61	-161.27	26.47
13	224.946	224.973	518.0368	4.5	43.1160	1237.47	-107.02	26.22
14	250.137	250.146	474.9208	4.7	47.2768	1942.41	-35.13	40.42

TABLE 20 (Continued)

Test No.	Initial Temp.(°C)	Final Temp.(°C)	Initial Mass (g)	Approximate Flow Rate (g/min.)	Mass of Liquid Withdrawn (g)	Total Energy Added (Int.J.)	Energy Corrections (Int.J.)	β at Even Temp. (Int.J./g)
15	250.106	250.143	427.6440	4.5	44.7421	1942.20	-137.86	40.31
16	274.954	275.002	382.9019	4.5	44.7948	2927.30	-177.42	61.40
17	274.970	275.019	338.1071	4.4	44.3417	2899.80	-172.56	61.51
18	300.019	300.031	293.7654	4.6	45.9512	4200.11	- 42.07	90.48
19	300.011	300.053	247.8142	4.5	136.1388	12475.49	-125.50	90.71

TABLE 21

COMPARISONS BETWEEN THE OBSERVED VALUES OF THIS WORK AND THE CALCULATED VALUES FROM P-V-T DATA

Temp. (°C)	β Values (Int.J./g) Measured Values of this Research	β Values (Int.J./g) Values Computed from a Knowledge of P, dp/dT & v	Deviation $\frac{\beta_o - \beta_c}{\beta_o}$ %
100	1.27	1.23	+3.1
125	2.74	2.68	+2.2
150	5.38	5.28	+1.9
175	9.67	9.57	+1.0
200	16.38	16.20	+1.1
225	26.35	26.11	+0.9
250	40.32	40.05	+0.7
275	61.46	61.04	+0.7
300	90.60	90.52	+0.1

9-3. Derivation of the Enthalpy Change of Saturated Liquid Heavy Water from Calorimetric Data

The enthalpy difference of a liquid substance as it changes from an initial equilibrium saturation state to a final equilibrium saturation state may be derived from α and β quantities according to the following relationship:

$$h_{f_2} - h_{f_1} = (\alpha + \beta)_1^2$$

Table 22 summarizes the enthalpy difference of saturated liquid heavy water in the temperature range from 50 to 300°C. It can be seen that the β values are relatively small in comparison with the α values at low temperature. It is estimated that the error in the enthalpy difference caused by the error in the β measurements is approximately 0.1 percent. It may be concluded that the overall accuracy of the enthalpy difference of saturated liquid heavy water obtained in this work is within ± 0.2 percent.

9-4. Comparisons

For purpose of comparison, the enthalpy values obtained in this work along with the smoothed data proposed by Baker (7) and by Nowak and Chan (42) are given in Table 23. It can be seen that the deviations between the results of this work and those proposed by Baker in the temperature range from 50 to 200°C is approximately 0.7% which is well within the error of measurement estimated by Baker (±1.5%). The measured enthalpy difference values of this work and those obtained previously by Nowak and Chan are in good accord. The maximum deviation between two independent measurements is approximately 0.5 percent which is

TABLE 22

ENTHALPY DIFFERENCE OF SATURATED

LIQUID HEAVY WATER

Temperature Interval (^{o}C) From	To	$\Delta\alpha$ (Int.J./g)	$\Delta\beta$ (Int.J./g)	h_f (Int.J./g)
50	75	103.64	0.33*	103.97
75	100	102.78	0.73*	103.51
100	125	102.05	1.47	103.52
125	150	101.39	2.64	104.03
150	175	100.77	4.29	105.06
175	200	99.89	6.71	106.60
200	250	199.06	23.94	223.00
250	300	197.18	50.28	247.46

*Values were calculated from P-V-T data

TABLE 23

COMPARISONS OF THE ENTHALPY VALUE OF HEAVY WATER

BETWEEN OBSERVATIONS OF THIS WORK AND OTHERS

Temperature Interval (^{o}F)		Enthalpy Difference (BTU/lb)		
From	To	This Work	Baker	Nowak & Chan
122	167	44.71	44.91	44.5
167	212	44.51	44.74	44.4
212	257	44.51	44.74	44.5
257	302	44.73	44.87	44.9
302	347	45.18	45.22	45.3
347	392	45.84	46.14	
392	482	95.89	98.18	
482	572	106.41	110.31	

within the estimated error of previous measurement.

The deviation between the enthalpy difference value obtained in this research in the temperature range from 250 to 300°C and the corresponding value proposed by Baker is 3.7%. This confirms the preliminary measurements of Nowak (16) on the enthalpy difference of saturated liquid heavy water for temperature interval from 248.88 (480°F) to 293.33°C (560°F) indicated in Baker's value for the same temperature interval to be in error by 4 or 5 percent.

It should be pointed out that the enthalpy values above 200°C proposed by Baker were based on the extrapolation of the fragmentary latent heat values available to him at the time. In view of the disagreement between the results of this work and the results of Baker, it may be concluded that the enthalpy values above 200°C proposed by Baker for saturated liquid heavy water are in error and the values at temperatures of around 300°C depart from the true values by approximately 4%. Moreover, either the latent heat values employed by Baker or his extrapolation of such data would appear to be in error.

The specific heat values of the saturated liquid light water and heavy water of this thesis were estimated by using the following relationship:

$$c_{p_f} = \frac{\Delta h_f}{\Delta T} \qquad \text{..... (28)}$$

The results of this work along with the experimental data of Brown et al (4), Cockett et al (5), Eucken et al (6), Rivkin et al (12, 13), Baker (7) and Nowak & Chan (28) are given in Figure 39. The maximum deviation between the results of this work and the above mentioned authors is around 2%. This is entirely within the limits of error

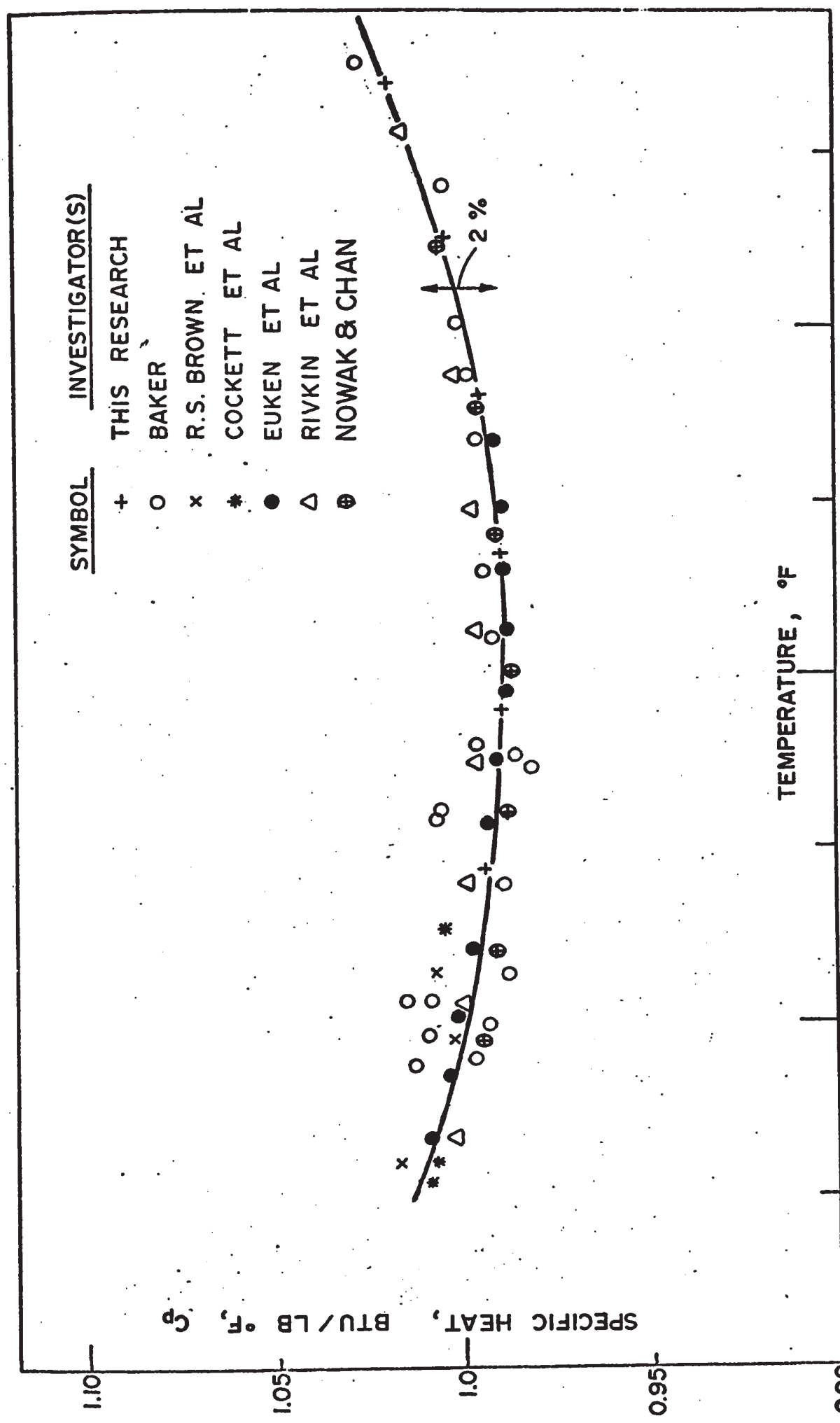

FIGURE 39 SPECIFIC HEAT AT CONSTANT PRESSURE FOR SATURATED HEAVY WATER LIQUID

estimated in references 4, 6, 7, 12, 13 and 18.

A comparison of the specific heat between light water and heavy water is given in Figure 40. It is of interest to point out that the specific heat of heavy water is approximately 1% higher than light water at 50°F and 5% lower at 550°F.

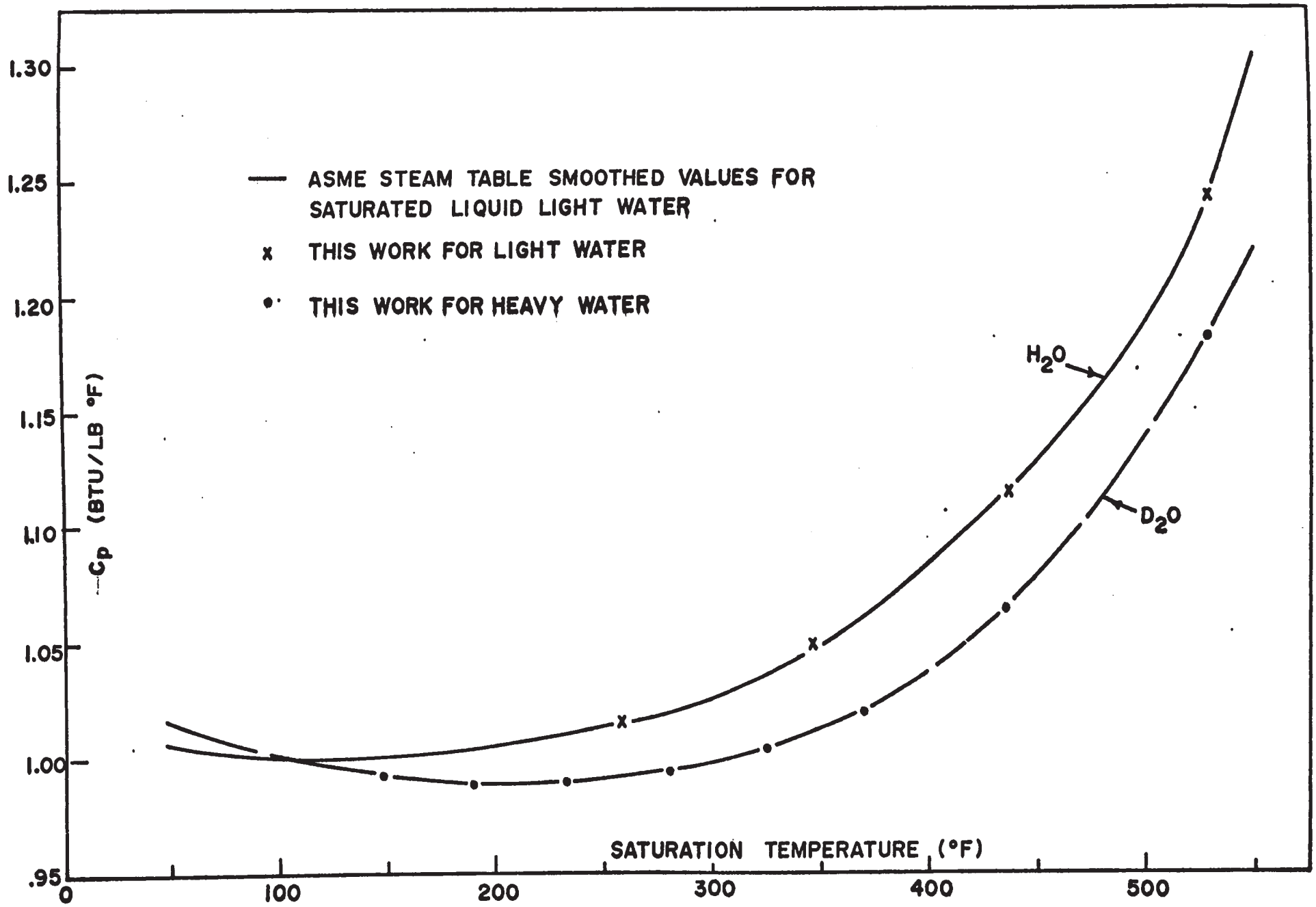

FIGURE 40 THE SPECIFIC HEAT, C_p, OF SATURATED LIQUID LIGHT WATER & HEAVY WATER

CHAPTER 10

CONCLUSIONS AND RECOMMENDATIONS

10-1. Conclusions

1. A calorimeter apparatus was designed, constructed and developed for studying the thermodynamic properties of heavy water. Based on the constant mass experiments of this thesis the performance of the apparatus was superior to that of Osborne's apparatus (21) which was employed to investigate the thermophysical properties of light water and yielded the various saturation data utilized by compilers of the various national steam tables (35, 36, 37, 38, 39).
2. It is estimated the α measurements conducted on saturated liquid heavy water in this thesis are accurate to ± 0.1% whereas the β measurements are accurate to + 3% below 200°C and 1% above 200°C.
3. The overall accuracy of the enthalpy difference values of saturated heavy water liquid obtained in the work is estimated to be within ± 0.2%. This accuracy can further be improved by refining the β measurement.
4. The enthalpy values for saturated liquid heavy water above 200°C confirmed early research which showed that the

extrapolated values proposed by Baker are in error. The existing latent heat values for heavy water are in question.

5. The specific heat of saturated liquid heavy water obtained in this research below 200°C is in reasonable accord with the earlier measurements of Brown, Cockett, Euken, Rivkin, Baker and Nowak & Chan with the maximum deviation being approximately 2%.

10-2. Recommendations

1. It is recommended to repair the leak in the calorimeter by sealing the top heater and extend the present enthalpy difference measurement up to the critical point.
2. Since the existing latent heat values for heavy water are in question, it is recommended to investigate the enthalpy of vaporization of heavy water from room temperature to the critical point using the present apparatus.
3. The β values obtained in this work may be improved by modifying the temperature indicating system of the calorimeter and also by withdrawing a larger amount of liquid from the calorimeter. It is recommended that a differential thermocouple having eight junctions be used in the temperature control, so that the temperature change of the calorimeter of the order of 0.001°C can be easily detected with the present equipment and that a liquid sample of 150 grams be withdrawn during a single β test.
4. Since the change of pressure with respect to temperature at saturation conditions is an important factor in correlating

the thermodynamic properties of heavy water, it is recommended that saturation pressure measurements be conducted on heavy water using the present apparatus.

5. In view of its performance, the present apparatus can be recommended to investigate the thermodynamic properties of other important engineering coolants.

APPENDIX A

DERIVATION OF EXPERIMENTAL EQUATIONS

1. Constant Mass Experiment

According to the First Law of Thermodynamics, the following energy balance may be written for the constant volume heat addition processes shown diagrammatically in Figure 2:

$$Q + m_{f_1} u_{f_1} + m_{g_1} u_{g_1} = m_{f_2} u_{f_2} + m_{g_2} u_{g_2} + c_{p_c} \Delta T + q_E + q_s \quad \ldots\ldots\ldots\ldots\ldots\ldots \text{(1A)}$$

By utilizing the definition of enthalpy, i.e. $h_f = u_f + P\, v_f$ and $h_g = u_g + P\, v_g$ Equation (1A) may be simplified as follows:

$$Q + m_{f_1} h_{f_1} + m_{g_1} h_{g_1} - P_1 (m_{f_1} v_{f_1} + m_{g_1} v_{g_1}) = m_{g_2} h_{g_2} + m_{f_2} h_{f_2}$$

$$- P_2 (m_{g_2} v_{g_2} + m_{f_2} v_{f_2}) + c_{p_c} \Delta T + q_E + q_s$$

$$\ldots\ldots\ldots\ldots\ldots\ldots \text{(2A)}$$

The interval volume of the calorimeter may be expressed in terms of the masses of saturated liquid and vapour and the specific volume of saturated liquid and vapour as follows:

$$V = m_{f_1} v_{f_1} + m_{g_1} v_{g_1} = m_{g_2} v_{g_2} + m_{f_2} v_{f_2}$$

Substituting for the total inner volume in equation (2A) and rearrangement of the terms results in the following:

$$Q + (P_2 - P_1)\, V + m_{f_1} h_{f_1} + m_{g_1} h_{g_1} = m_{g_2} h_{g_2} + m_{f_2} h_{f_2} + c_{p_c}\, \Delta T + q_E + q_s$$

..... (3A)

Equation (3A) may be rewritten and rearranged as follows by noting that $h_g = h_f + h_{fg}$

$$Q + (P_2 - P_1)\, V + (m_{f_1} + m_{g_1})\, h_{f_1} + m_{g_1} h_{fg_1} = (m_{g_2} + m_{f_2})\, h_{f_2}$$

$$+ m_{g_2} h_{fg_2} + c_{p_c}\, \Delta T + q_E + q_s$$

..... (4A)

By employing the Clausius Clapeyron equation $h_{fg} = (v_g - v_f)\, T \frac{dp}{dT}$, the constant volume expression $V = m_f v_f + m_g v_g$ and the constant mass expression $M = m_f + m_g$ equation (4A) may be rewritten and rearranged as follows:

$$Q = M \left(h_f - T\, v_f \frac{dp}{dT}\right)_1^2 + V \left(T \frac{dp}{dT} - P\right)_1^2 + c_{p_c}\, \Delta T + q_E + q_s$$

..... (5A)

If Q_H and Q_L denote the measured quantities of total energy added in the high and low filling experiments having masses of sample M_H and M_L respectively, then the equation (5A) may be written as the following two forms:

$$Q_H = M_H \left(h_f - T\, v_f \frac{dp}{dT}\right)_1^2 + V \left(T \frac{dp}{dT} - P\right)_1^2 + c_{p_c}\, \Delta T + q_{E_H} + q_s$$

..... (6A)

$$Q_L = M_L \left(h_f - T\, v_f \frac{dp}{dT}\right)_1^2 + V \left(T \frac{dp}{dT} - P\right)_1^2 + c_{p_c}\, \Delta T + q_{E_L} + q_s$$

..... (7A)

Subtracting equation (7A) from equation (6A) and rearranging the terms

yields the following expression.*

$$\frac{Q_H - Q_L}{M_H - M_L} = (h_f - T v_f \frac{dp}{dT})^2_1 \qquad \ldots\ldots\ldots\ldots\ldots\ldots (8A)$$

2. Vapour Withdrawal Test

The heat balance for the isothermal vapour withdrawal process shown diagrammatically in Figure 4 may be written as follows:

$$Q_g + m_{f_1} u_{f_1} + m_{g_1} u_{g_1} = \Delta M\, h_{g_2} + m_{f_2} u_{f_2} + m_{g_2} u_{g_2}$$

$\ldots\ldots\ldots\ldots\ldots\ldots (9A)$

By utilizing the definition of enthalpy, i.e. $h_f = u_f + P\, v_f$ and $h_g = u_g + P\, v_g$ and assuming the temperature of the calorimeter to be invariant, i.e. $h_f = h_{f_1} = h_{f_2}$ and $h_g = h_{g_1} = h_{g_2}$ equation (9A) may be written in the following form:

$$Q_g + h_f (m_{f_1} - m_{f_2}) + h_g (m_{g_1} - m_{g_2}) - P (m_{f_1} v_{f_1} + m_{g_1} v_{g_1}) = \Delta M\, h_g$$

$$- P (m_{f_2} v_{f_2} + m_{g_2} v_{g_2})$$

$\ldots\ldots\ldots\ldots\ldots\ldots (10A)$

The internal volume of the calorimeter may be expressed in terms of the masses of saturated liquid and vapour and the specific volume of saturated liquid and vapour as follows:

$$V = m_{f_1} v_{f_1} + m_{g_1} v_{g_1} = m_{f_2} v_{f_2} + m_{g_2} v_{g_2}$$

Substituting for the total inner volume in equation (10A) and simplification of the terms results in the following:

$$Q_g + h_f (m_{f_1} - m_{f_2}) + h_g (m_{g_1} - m_{g_2}) = \Delta M\, h_g$$

$\ldots\ldots\ldots\ldots\ldots\ldots (11A)$

---

*It is traditional to assume the net heat exchange between the calorimeter and the adiabatic shield remaining the same during two types of experiment, i.e. $q_{E_H} = q_{E_L}$

Equation (11A) may be written and rearranged as follows by noting that $h_f = h_g - h_{fg}$

$$Q_g + h_g \left[(m_{f_1} - m_{f_2}) + (m_{g_1} - m_{g_2}) \right] - h_{fg} (m_{f_1} - m_{f_2}) = \Delta M \, h_g$$

..... (12A)

The total mass withdrawn from the calorimeter may be expressed in terms of the mass differences of saturated liquid and vapour from an initial equilibrium saturation state to a final equilibrium saturation state, i.e. $\Delta M = M_1 - M_2 = (m_{f_1} - m_{f_2}) + (m_{g_1} - m_{g_2})$ Substituting for the total mass withdrawn in equation (12A) and rearrangement of the terms results in the following:

$$Q_g = h_{fg} (m_{f_1} - m_{f_2})$$ ..... (13A)

By employing the Clausius Clapeyron equation $h_{fg} = (v_g - v_f) T \frac{dp}{dT}$, the mass difference expression $m_{f_1} - m_{f_2} = (M_1 - M_2) - (m_{g_1} - m_{g_2})$ and the constant volume expression $V = m_f v_f + m_g v_g$ equation (13A) may be rewritten and rearranged as follows:

$$\frac{Q_g}{M_1 - M_2} = T \, v_g \frac{dp}{dT}$$ ..... (14A)

3. Liquid Withdrawal Test

The heat balance for the isothermal liquid withdrawal process shown diagrammatically in Figure 5 may be written as follows:

$$Q_f + m_{f_1} u_{f_1} + m_{g_1} u_{g_1} = \Delta M \, h_{f_2} + m_{f_2} u_{f_2} + m_{g_2} u_{g_2}$$

..... (15A)

By utilizing the definition of enthalpy, i.e. $h_f = u_f + P \, v_f$ and $h_g = u_g + P \, v_g$ and assuming the temperature of the calorimeter to be

invariant during test, i.e. $h_f = h_{f_1} = h_{f_2}$ and $h_g = h_{g_1} = h_{g_2}$ equation (15A) may be written in the following form:

$$Q_f + h_f (m_{f_1} - m_{f_2}) + h_g (m_{g_1} - m_{g_2}) - P (m_{f_1} v_{f_1} + m_{g_1} v_{g_1}) = \Delta M\, h_f - P (m_{f_2} v_{f_2} + m_{g_2} v_{g_2})$$

..... (16A)

The internal volume of the calorimeter may be expressed in terms of the masses of saturated liquid and vapour and the specific volume of saturated liquid and vapour as follows:

$$V = m_{f_1} v_{f_1} + m_{g_1} v_{g_1} = m_{f_2} v_{f_2} + m_{g_2} v_{g_2}$$

Substituting for the total inner volume in equation (16A) and simplification of the terms results in the following:

$$Q_f + h_f (m_{f_1} - m_{f_2}) + h_g (m_{g_1} - m_{g_2}) = \Delta M\, h_f$$

..... (17A)

Equation (11) may be rewritten and rearranged as follows by noting that $h_g = h_f + h_{fg}$

$$Q_f + h_f \left[(m_{f_1} - m_{f_2}) + (m_{g_1} - m_{g_2})\right] + h_{fg} (m_{g_1} - m_{g_2}) = \Delta M\, h_f$$

..... (18A)

The total mass withdrawn from the calorimeter may be expressed in terms of the mass differences of saturated liquid and vapour from an initial equilibrium saturation state to a final equilibrium saturation state, i.e. $\Delta M = M_1 - M_2 = (m_{f_1} - m_{f_2}) + (m_{g_1} - m_{g_2})$
Substituting for the total mass withdrawn in equation (18A) and rearrangement of the terms results in the following:

$$Q_f = - h_{fg} (m_{g_1} - m_{g_2})$$ ..... (19A)

By employing the Clausius Clapeyron equation $h_{fg} = (v_g - v_f)\, T \frac{dp}{dT}$, the mass difference expression $m_{g_1} - m_{g_2} = (M_1 - M_2) - (m_{f_1} - m_{f_2})$ and the constant volume expression $V = m_f v_f + m_g v_g$ equation (19A) may be rewritten and rearranged as follows:

$$\frac{Q_f}{M_1 - M_2} = T\, v_f \frac{dp}{dT} \qquad \text{..... (20A)}$$

If the measured quantities of the constant mass experiment, vapour withdrawal test and liquid withdrawal test are denoted by α, γ and β respectively, then equation (8A), (14A) and (20A) may be rewritten as follows:

$$\Delta\alpha = \Delta h_f - \Delta T\, v_f \frac{dp}{dT} \qquad \text{..... (21A)}$$

$$\gamma = T\, v_g \frac{dp}{dT} \qquad \text{..... (22A)}$$

$$\beta = T\, v_f \frac{dp}{dT} \qquad \text{..... (23A)}$$

By simple algebraic combination of the above equations, it may be reduced to the following group of equations:

$$\Delta h_f = \Delta\alpha + \Delta\beta \qquad \text{..... (24A)}$$

$$\Delta h_g = \Delta\alpha + \Delta\gamma \qquad \text{..... (25A)}$$

$$h_{fg} = \gamma - \beta \qquad \text{..... (26A)}$$

By utilizing the thermodynamics relationship the entropy may be written in the following form:

$$ds = \frac{dh}{T} - \frac{v}{T} dp \qquad \text{..... (27A)}$$

Equation (27A) may be reduced as follows by noting that $\frac{dh}{T} \equiv d(\frac{h}{T}) + \frac{h}{T^2} dT$

$$ds = d\left(\frac{h}{T}\right) + \frac{h}{T^2} dT - \frac{v}{T} dp \qquad \text{..... (28A)}$$

Applying equation (28A) to the saturated liquid and using equation (21A), the above equation may be written as follows:

$$d\,s_f = d\left(\frac{h_f}{T}\right) + \frac{\alpha}{T^2}^{*}\,dT \qquad \ldots\ldots\ldots\ldots\ldots\ldots \text{(29A)}$$

Integration of equation (29A) gives the entropy of the saturated liquid as

$$s_f = \frac{h_f}{T} + \int \frac{\alpha}{T^2}\,dT + c \qquad \ldots\ldots\ldots\ldots\ldots\ldots \text{(30A)}$$

Where c is a constant of integration depending on the arbitrary zeros chosen for the various quantities in the equation (30A). In a similar manner the entropy of the saturated vapour may be derived as follows:

$$s_g = \frac{h_g}{T} + \int \frac{\alpha}{T^2}\,dT + c \qquad \ldots\ldots\ldots\ldots\ldots\ldots \text{(31A)}$$

The specific heat of the saturated liquid may be derived from equation (29A) by noting that $\delta Q = T\,ds$

$$\delta Q = T\,d\left(\frac{h_f}{T}\right) + \frac{\alpha}{T}\,dT$$

whence

$$c_{p_f} = \frac{\delta Q}{dT} = T\,\frac{d}{dT}\left(\frac{h_f}{T}\right) + \frac{\alpha}{T} \qquad \ldots\ldots\ldots\ldots\ldots\ldots \text{(32A)}$$

and similarly for the saturated vapour

$$c_{p_g} = T\,\frac{d}{dT}\left(\frac{h_g}{T}\right) + \frac{\alpha}{T} \qquad \ldots\ldots\ldots\ldots\ldots\ldots \text{(33A)}$$

---

*The α value can be calculated by the empirical equation which is derived from the constant mass experiment results.

APPENDIX B

DESIGN CALCULATIONS OF THE CALORIMETER SHELL

The upper limit of the operating temperature and pressure for the calorimeter are 705°F and 3200 psi respectively.

If the design stress of the material is known, the thickness of the calorimeter shell may be calculated by using the following equation,

$$t = \frac{P\ R\ F}{2\sigma}^{*} \qquad \ldots\ldots\ldots\ldots\ldots\ (1B)$$

where t is the thickness of the calorimeter shell,

P is the internal pressure of the calorimeter,

R is the internal radius of the calorimeter,

σ is the design stress,

F is the safety factor.

For Inconel 600 the design stress under the above given working condition is approximately 29500 psi (43). If the internal diameter of the calorimeter and the safety factor are set to be equal to 2.5 inches and 1.8 respectively, thus

$$t = 0.246 \simeq 0.25 \text{ inches.}$$

---

*This formula is valid for a sphere in which the ratio of the wall thickness to the inside diameter is less than 0.1.

APPENDIX C

DETAILED DRAWINGS OF THE SILVER HEAT DIFFUSION SYSTEM

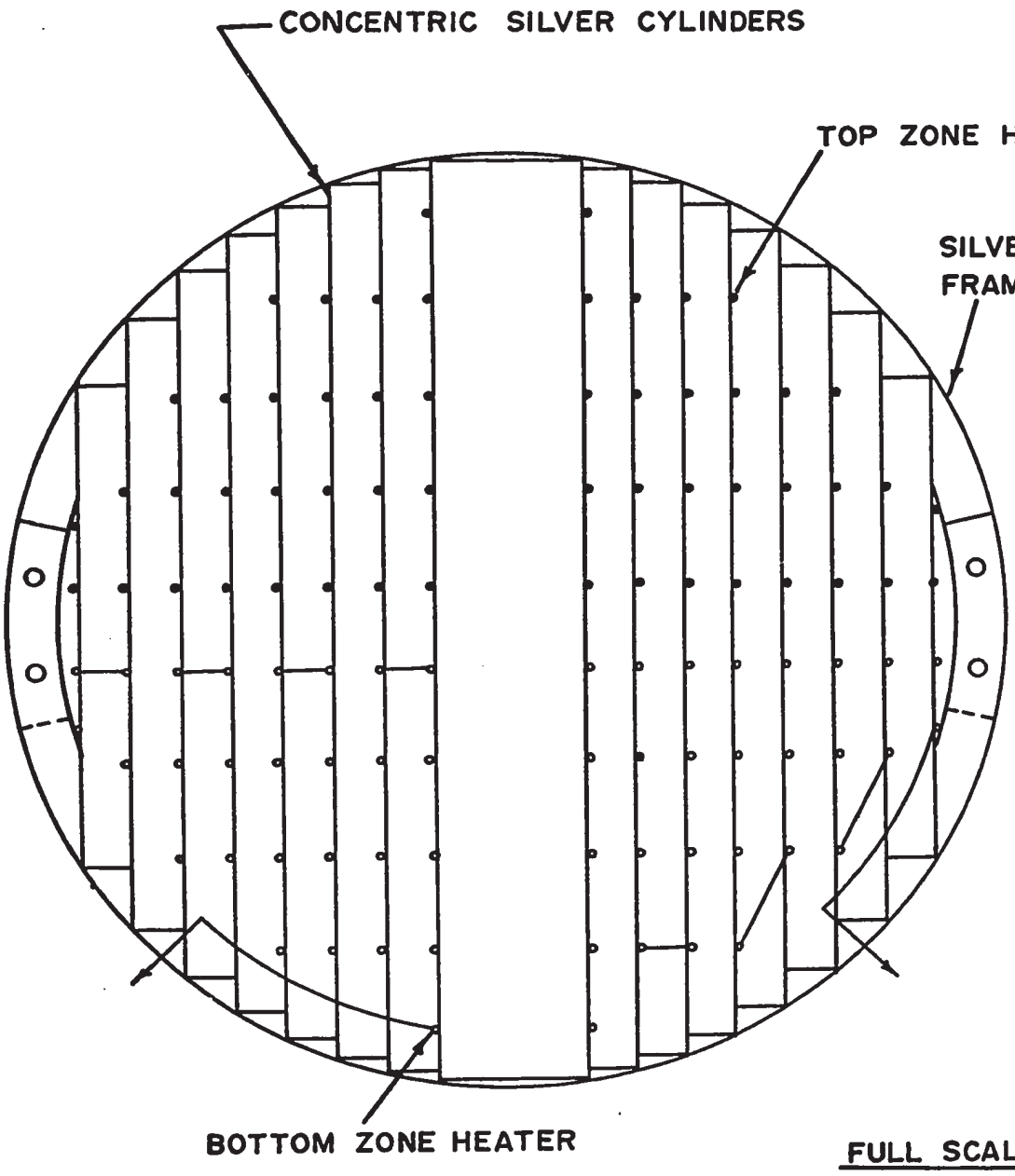

FIGURE IC ASSEMBLY DRAWING OF SILVER HEAT DIFFUSION SYSTEM

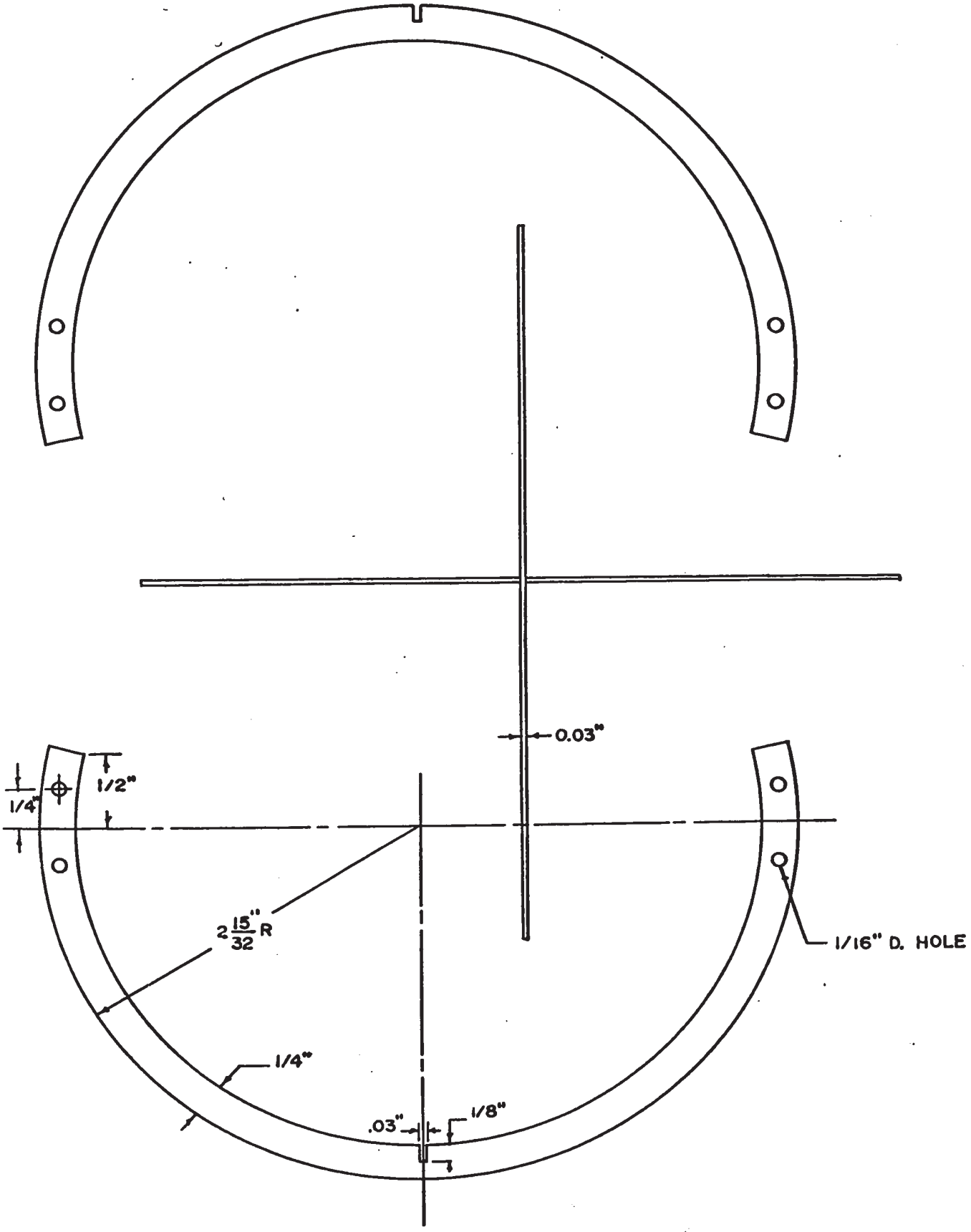

FIGURE 2C SILVER SUPPORT FRAME (LOWER PART) FOR HEAT DIFFUSION SYSTEM

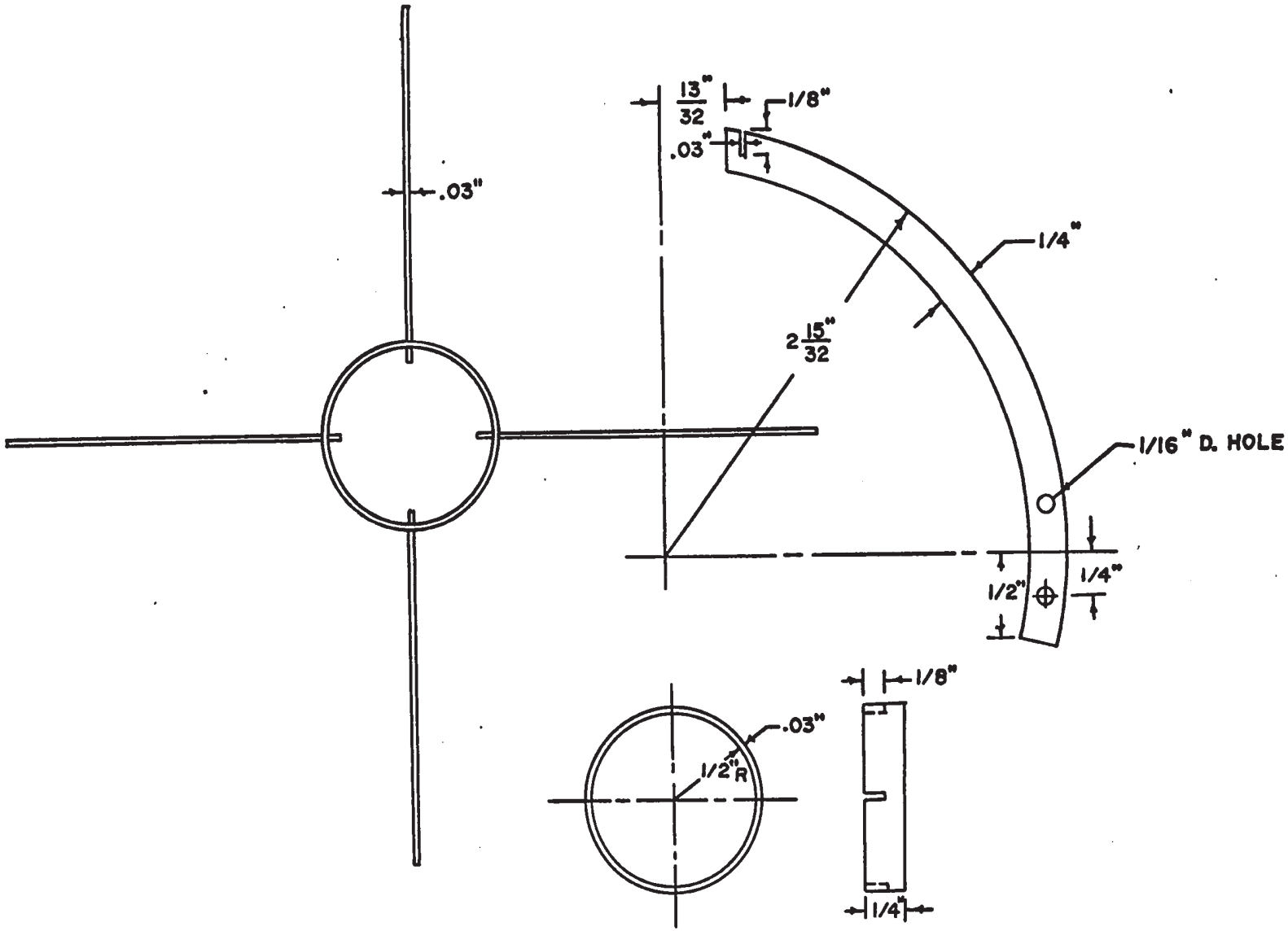

FIGURE 3C SILVER SUPPORT FRAME (UPPER PART) FOR HEAT DIFFUSION SYSTEM

APPENDIX D

CALIBRATION OF THE CAPSULE THERMOMETER

The capsule thermometer was calibrated by comparison against the U.W.O. international standard platinum resistance thermometer at temperatures in the immediate vicinity of 100, 200, 250 and 400°C. The comparisons were made in an isothermal comparator furnace.

The comparator furnace essentially consisted of an aluminum block 6 inches in diameter and 15 inches long. Two 1/4 in. and 3/8 in. diameter holes were drilled in the block to a depth of 10 inches. Their centers were on a circle of half inches in diameter. The block carried three separate heaters (a main heater and two guard heaters). The main heater was embedded in grooves which were machined uniformly into the surface of the aluminum block and the other two guard heaters were wound over the end sections of the main heater. The purpose of these guard heaters is to provide additional energy to compensate the heat loss from both ends of the aluminum block and to eliminate the temperature variation along the length of the comparator. The aluminum block was contained in a stainless steel Dewar flask. The annular space between the aluminum block and the Dewar flask was filled with diatomaceous earth powder. A schematic diagram of part of the experimental set-up employed is given in Figure 1D. By careful

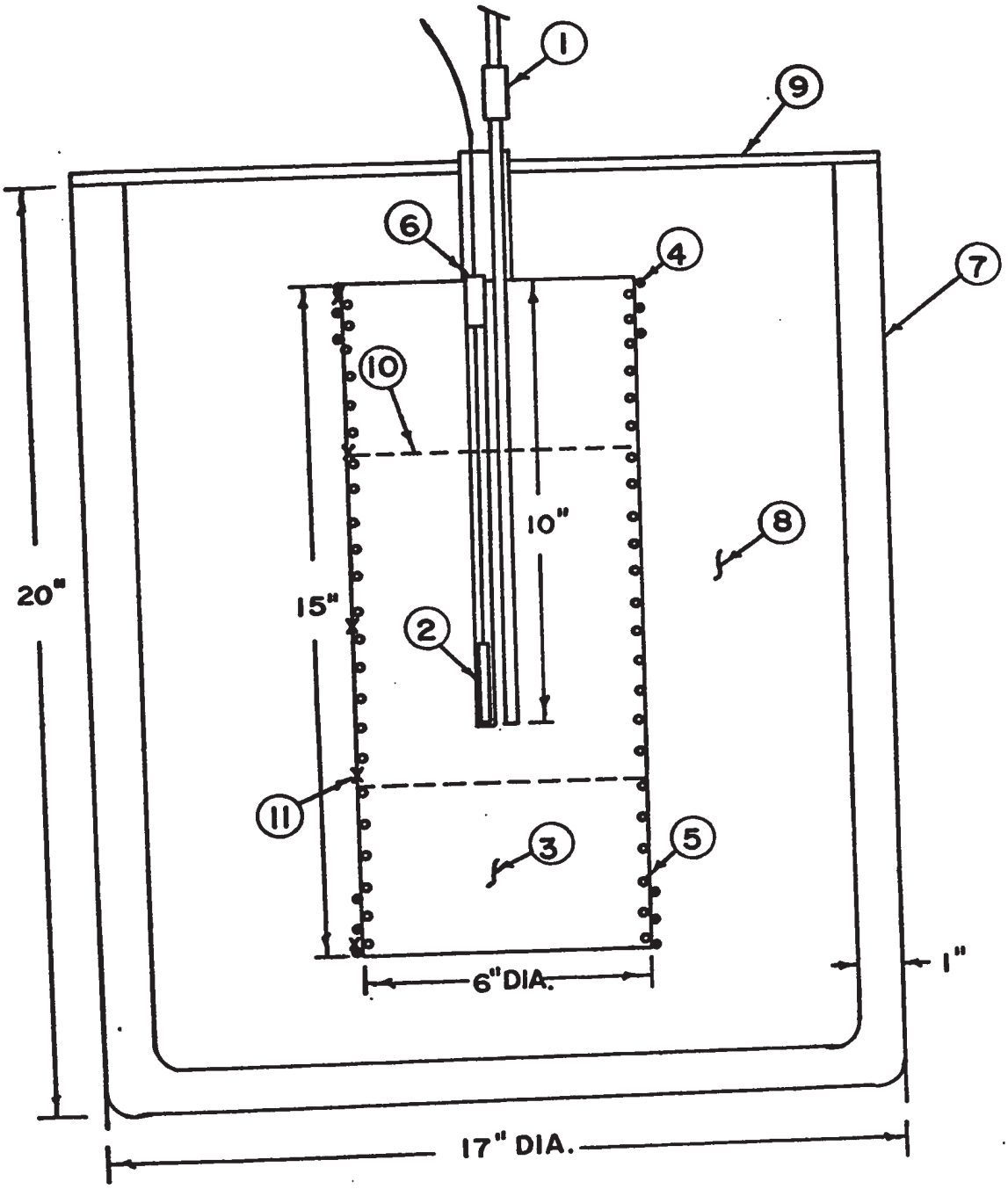

1. STANDARD THERMOMETER 2. CAPSULE THERMOMETER UNDER TEST
3. ALUMINUM BLOCK 4. GUARD HEATERS 5. MAIN HEATERS 6. PLUG
7. STAINLESS STEEL DEWAR FLASK 8. DIATOMACEOUS POWER 9. COVER
10. CALIBRATION ZONE 11. DIFFERENTIAL THERMOCOUPLE JUNCTIONS

FIGURE ID EXPERIMENTAL SET-UP FOR THE CALIBRATION OF THE CAPSULE THERMOMETER

adjusting the D.C. current flowing through the aluminum block heaters it was possible to maintain the temperature variations over the entire surface of the block within $0.03^{\circ}C$. The temperature variations along the length of the calibration zone of the comparator were no more than $0.005^{\circ}C$. The temperature control (manual) of the comparator furnace was such that the temperature change of the entire aluminum block was less than $0.01^{\circ}C$ per hour. A graph illustrating the temperature change of the aluminum block with time is shown in Figure 2D.

There are thirty-two calibration points obtained mainly at four different temperatures. The calibration data are summarized in Table 1D. Column one is the temperature at which the capsule thermometer was calibrated. Column two is the resistances of the capsule thermometer at its corresponding calibration temperatures. These results were fitted to the resistance-temperature relationship $R/R_o = 1 + AT + BT^2$ by least squares technique. The ice point resistance R_o was inferred from the triple point resistance to be 25.5643 ohms. The constants A and B were determined to be 3.98447×10^{-3} and -5.8568×10^{-7} respectively. The ratio of the steam point resistance and the ice point resistance of the capsule thermometer was also found to be 1.3925. The smooth values of the resistance at different calibration temperatures are given in Column 3 of Table 1D. Finally the percentage deviations of the observed values from the smooth values are shown in Column 4. On the basis of all of the calibration results it may be concluded that the maximum calibration error is no more than 10 parts in one million (i.e. 10 parts in 10^6).

Since the ratio of the steam point resistance and the ice point

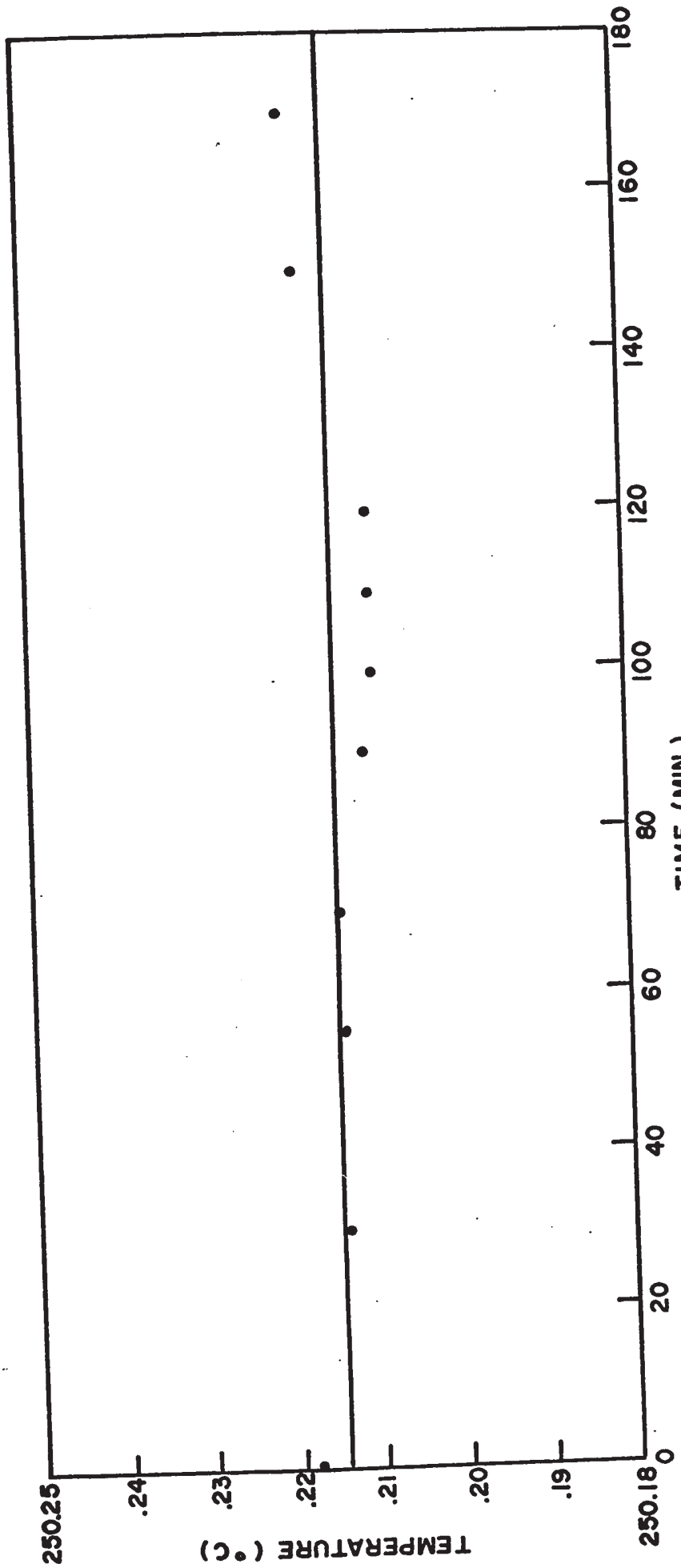

FIGURE 2D TEMPERATURE CHANGE OF THE ALUMINUM BLOCK WITH TIME

TABLE 1D

CALIBRATION OF THE STANDARD CAPSULE THERMOMETER

Temperature °C	Observed Resistance ohms	Calculated Resistance ohms	Deviation %
99.8139	35.58235	35.58220	0.0004
99.8154	35.58250	35.58235	0.0004
99.9959	35.60025	35.60019	0.0001
99.9977	35.60050	35.60037	0.0003
99.9955	35.60030	35.60015	0.0004
99.9948	35.60020	35.60009	0.0003
99.9946	35.60015	35.60007	0.0002
99.9960	35.60030	35.60020	0.0002
199.7845	45.31725	45.31679	0.0010
199.7829	45.31705	45.31664	0.0009
199.7826	45.31700	45.31661	0.0008
199.7828	45.31705	45.31663	0.0009
199.7834	45.31710	45.31669	0.0008
250.2161	50.11450	50.11398	0.0010
250.2145	50.11430	50.11383	0.0009
250.2143	50.11410	50.11381	0.0005
250.2104	50.11385	50.11344	0.0008
250.2098	50.11380	50.11338	0.0008
250.2184	50.11450	50.11418	0.0006
250.1935	50.11225	50.11184	0.0008
250.1917	50.11205	50.11167	0.0007
250.1901	50.11185	50.11152	0.0006

TABLE 1D (Continued)

Temperature °C	Observed Resistance ohms	Calculated Resistance ohms	Deviation %
250.1934	50.11215	50.11183	0.0006
250.1952	50.11235	50.11201	0.0006
399.0718	63.82910	63.82936	-0.0004
399.0703	63.82890	63.82923	-0.0005
399.0693	63.82885	63.82913	-0.0004
399.0673	63.82865	63.82896	-0.0004
399.0656	63.82850	63.82880	-0.0004
399.0643	63.82835	63.82868	-0.0005
399.0637	63.82840	63.82862	-0.0003
399.0632	63.82825	63.82859	-0.0005
399.0623	63.82820	63.82851	-0.0004

resistance and the B constant of this capsule thermometer satisfy the specifications of the international committee on Weights and Measures, this thermometer may be classified as an "International Standard Thermometer".

APPENDIX E

THE LINEARITY DETERMINATION OF THE VARIABLE FOUR TERMINAL RESISTOR

The linearity of the measuring dials 3 to 7 of the variable four terminal resistor was determined by intercomparison of each dial using the isolating potential comparator. This comparator method for comparing resistors was also developed by Dauphinee. A schematic diagram illustrating the principle of operation of this method is shown in Figure 1E. It can be seen that the galvanometer deflection due to inequality of the two resistors being compared can be reduced to zero by algebraically adding a voltage from the Lindeck potentiometer to equalize the potential drops across the two resistors. This added voltage is then used to determine the ohmic difference between the two resistors.

The procedure of the intercomparisons of dials 3 to 7 of the variable four terminal resistor was as follows:

1. Connect a decade resistance box to the measured terminals on the isolating potential comparator and also connect a short length of bare resistance wire in series with the decade box to give better resolutions. The purpose of the resistance box and the resistance slide-wire is to provide a temporarily

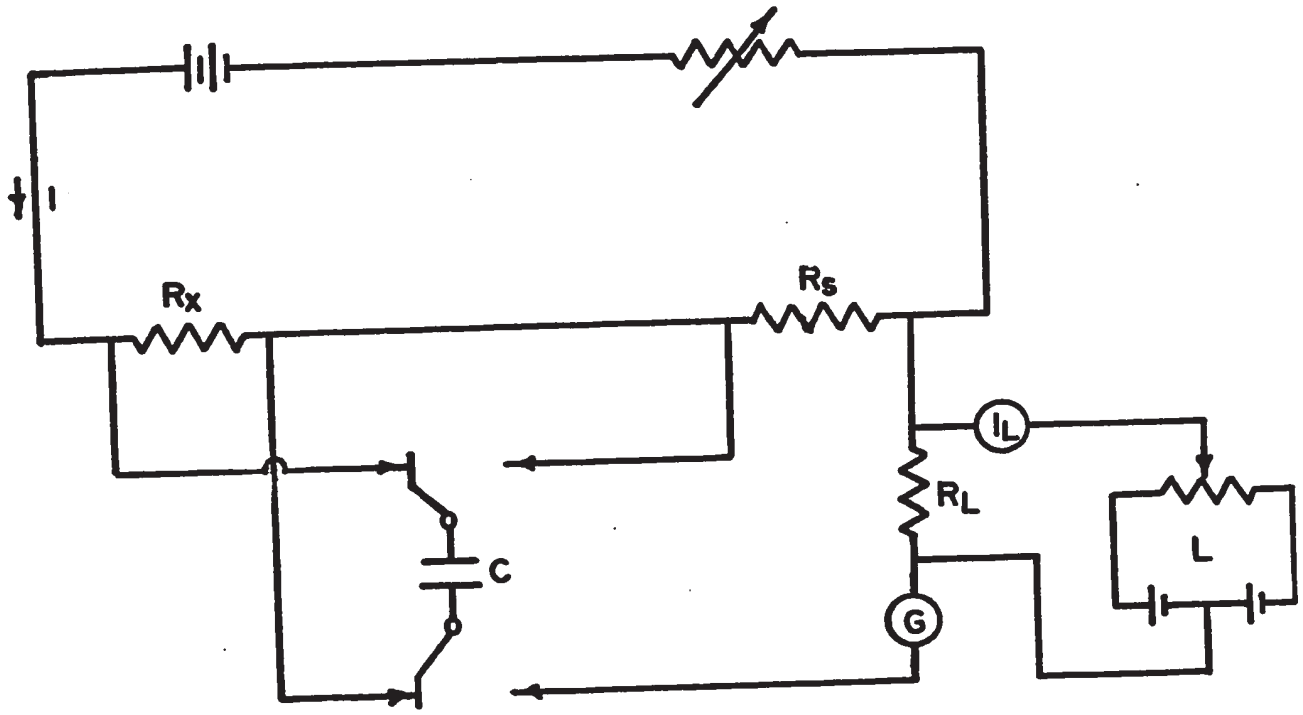

R_s = STANDARD RESISTOR R_x = RESISTOR UNDER TEST

I = CURRENT C = CAPACITOR

G = GALVANOMETER L = LINDECK POTENTIOMETER

R_L = LINDECK POTENTIOMETER RESISTOR

I_L = LINDECK POTENTIOMETER CURRENT

FIGURE IE THE ISOLATING POTENTIAL COMPARATOR METHOD OF COMPARING RESISTANCES OF TWO FIXED RESISORS

stable resistance value to match exactly each step of the dial.

2. Starting with 100 ohms on the decade resistance box and one step of dial 3 obtain a balance by adjustment of the decade box and slidewire. When a balance has been obtained turn the galvanometer sensitivity switch to off and then set dial 3 to zero and dial 4 to 10. Add Lindeck voltage to reduce any galvanometer deflection resulting from this interchange to zero. Observe the equivalent resistance added or subtracted.
3. Repeat the same procedure for step 2 of dial 3 initially balancing this dial setting against 200 ohms in the decade box and slidewire with zero Lindeck potentiometer voltage, and then rebalancing dial 3 step 1 and dial 4 step 10 against the undisturbed decade box and a compensating Lindeck potentiometer reading. Observe the resistance difference between the second resistor of dial 3 and the total of dial 4.
4. Repeat the above procedure to compare each step of dial 3 against the total of dial 4.

A typical set of linearity determinations of dial 3 is given in Table 1E. The procedure for obtaining the linearity for dials 4 to 6 was the same as for dial 3. The test results are shown in Tables 2E to 4E. It can be seen that the resistance error of any dial below the 4th was insignificant.

The overall linearity of the five measuring dials of the variable four terminal resistor is a combination of the individual linearity of

TABLE 1E

VARIABLE FOUR TERMINAL RESISTOR DIAL 3

LINEARITY DETERMINATION

Coil No.	Difference from total of next lower dial ΔR_x ($\times 10^{-4}$ ohms)	Difference between each individual difference and the average difference $\Delta R_x - \overline{\Delta R}$ ($\times 10^{-4}$ ohms)	Deviation from linearity (Algebraic sum of Col. 3) ohms ($\times 10^{-4}$)	PPM of Reading
1	+6	+1	+1	+1
2	-4	-9	-8	-4
3	+4	-1	-9	-3
4	-4	-9	-18	-4.5
5	+18	+13	-5	-1
6	+10	+5	0	0
7	+10	+5	+5	0.7
8	+1	-4	+1	0.1
9	+10	+5	+6	0.7
10	-1	-6	0	0

Average difference

$\overline{\Delta R}$ (ohms)$_{-4}$

-5.0×10^{-4}

TABLE 2E

VARIABLE FOUR TERMINAL RESISTOR DIAL 4

LINEARITY DETERMINATION

Coil No.	Difference from total of next lower dial ΔR_x ($\times 10^{-4}$ ohms)	Difference between each individual difference and the average difference $\Delta R_x - \overline{\Delta R}$ ($\times 10^{-4}$ ohms)	Deviation from linearity (Algebraic sum of Col. 3) ohms ($\times 10^{-4}$)	PPM of Reading
1	-6	-2.1	-2.1	-2.1
2	-5	-1.1	-3.2	-1.6
3	-5	-1.1	-4.3	-1.4
4	-5	-1.1	-5.4	-1.3
5	-3	+0.9	-4.5	-0.9
6	-10	-6.1	-10.6	-1.8
7	+1	+4.9	-5.7	-0.8
8	+1	+4.9	-0.8	-0.1
9	-10	-6.1	-6.9	-0.7
10	+3	+6.9	0	0

Average difference

$\overline{\Delta R}$ (ohms)

-3.9×10^{-4}

TABLE 3E

VARIABLE FOUR TERMINAL RESISTOR DIAL 5

LINEARITY DETERMINATION

Coil No.	Difference from total of next lower dial ΔR_x ($\times 10^{-4}$ ohms)	Difference between each individual difference and the average difference $\Delta R_x - \overline{\Delta R}$ ($\times 10^{-4}$ ohms)	Deviation from linearity (Algebraic sum of Col. 3) ohms $_{-4}$ ($\times 10^{-4}$)	PPM of Reading
1	+2	-0.6	-0.6	-0.6
2	+3	+0.4	-0.2	-0.1
3	+3	+0.4	+0.2	+0.1
4	+2	-0.6	-0.4	-0.1
5	+2	-0.6	-1.0	-0.2
6	+2	-0.6	-1.6	-0.3
7	+4	+1.4	-0.2	0.0
8	0	-2.6	-2.8	-0.4
9	+5	+2.4	-0.4	0.0
10	+3	+0.4	0.0	0.0

Average difference

$\overline{\Delta R}$ (ohms) $_{-4}$
$+2.6 \times 10^{-4}$

TABLE 4E

VARIABLE FOUR TERMINAL RESISTOR DIAL 6
LINEARITY DETERMINATION

Coil No.	Difference from total of next lower dial ΔR_x ($\times 10^{-4}$ ohms)	Difference between each individual difference and the average difference $\Delta R_x - \overline{\Delta R}$ ($\times 10^{-4}$ ohms)	Deviation from linearity (Algebraic sum of Col. 3) ohms ($\times 10^{-4}$)	PPM of Reading
1	-1	-0.1	-0.1	-0.1
2	0	+0.9	+0.8	+0.4
3	0	+0.9	+1.7	+0.5
4	-4	-3.1	-1.4	-0.3
5	0	+0.9	-0.5	-0.1
6	0	+0.9	+0.5	+0.1
7	0	+0.9	+1.3	+0.2
8	-2	-1.1	+0.2	0.0
9	-1	-0.1	+0.1	0.0
10	-1	-0.1	0.0	0.0

Average difference
$\overline{\Delta R}$ (ohms)
-0.9×10^{-4}

each dial. On the basis of the linearity determinations summarized in Tables 1E to 4E, it may be concluded that the percentage error of the lower five dials on the variable four terminal resistor is well within the manufacturer's specification of ± 0.001% of reading.

APPENDIX F

INTERCOMPARISON OF THE TWO POTENTIOMETERS

Figure 1F shows the simplified testing circuits for comparison of the two potentiometers. It can be seen that the measuring terminals of the potentiometers were connected to oppose. The galvanometer terminals of V.P.1 were linked together while the galvanometer terminals of V.P.2 were connected to an extremely sensitive galvanometer. The battery circuits could be simultaneously reversed by means of a low resistance gold-plated copper thermoelectric free switch providing compensation for parastic emfs in the galvanometer. All external connections were made with 20 gauge pure copper wire in PVC insulation to avoid the thermal emfs generating at the contacts. The batteries were connected to the circuit for several days to obtain current stability before any intercomparisons were made.

The procedure of the intercomparison of the two potentiometers was that the dials marked x 0.1 volt of the two potentiometers were set at 10. The battery current rheostats were adjusted until no current flowed in the galvanometer circuit, indicating that the potential differences across the measuring terminals of both potentiometers were exactly the same. The sensitivity of the photocell amplifier galvanometer was set so that the smallest adjustment of the dials gave at least 100 mm deflections. Then the dials of the potentiometers were

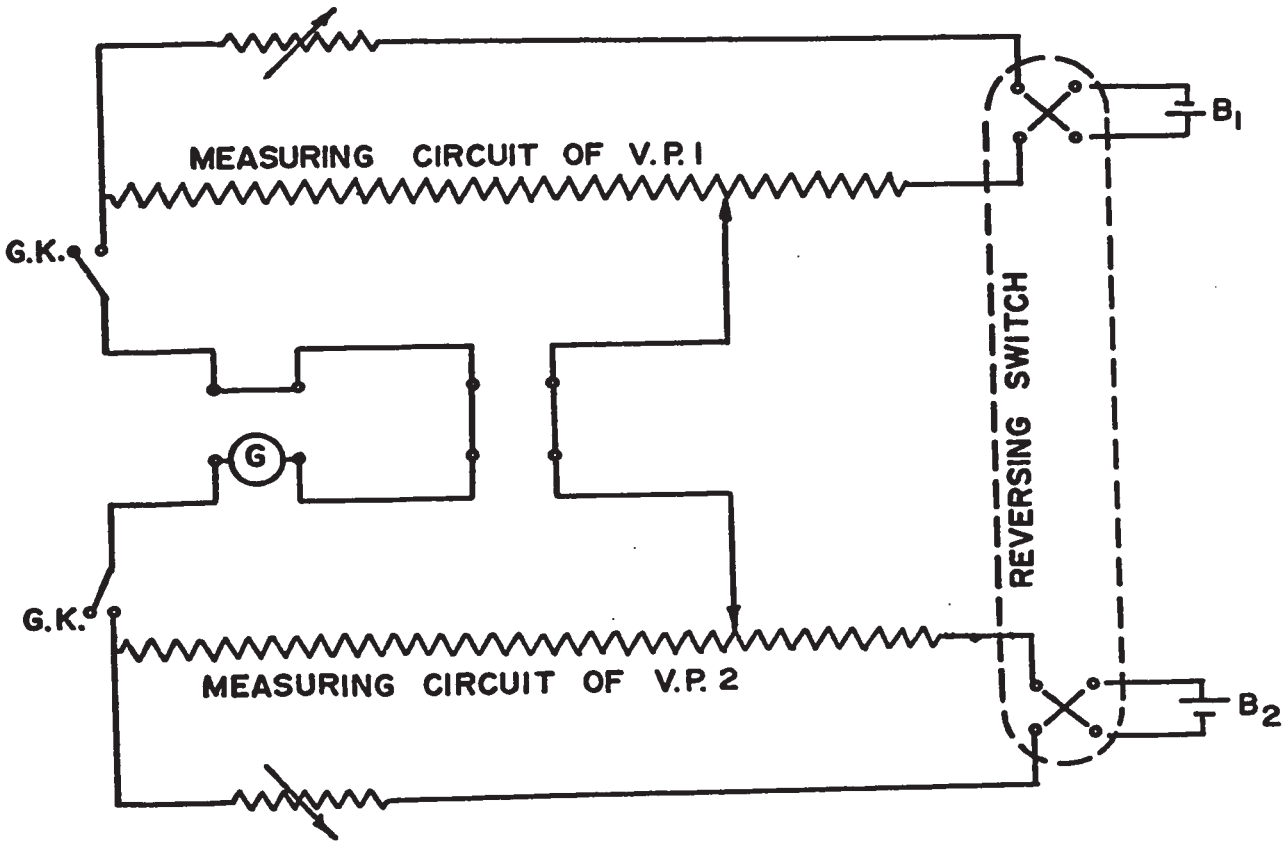

G = GALVANOMETER
G.K = GALVANOMETER KEY
B = BATTERY
V.P.1 = VERNIER POTENTIOMETER NO. 1
V.P.2 = VERNIER POTENTIOMETER NO.2

FIGURE 1F THE SIMPLIFIED CIRCUITS FOR COMPARISION POTENTIOMETERS

set at any other potential difference to be compared and the ratio of the voltages across the same settings of the dials of the two potentiometers was obtained by observing the galvanometer deflections. A few of the intercomparison tests are shown in Table 1F.

Similar comparisons were made on the standard cell circuits of the two potentiometers. The test results are given in Table 2F and 3F. On the basis of the intercomparisons carried out on the two potentiometers it may be concluded that the two potentiometers are evidently stable to about 4 parts in one million.

TABLE 1F

THE STABILITY OF POTENTIOMETER MEASURING CIRCUITS

Main Dials

Date	30-7-69	27-8-69	26-9-69
Pot. Temp.	21.0°C	21.2°C	21.2°C
Section	Potential Difference Between V.P.1 & V.P.2, μv		
1	-3.8	-4.0	-4.0
2	-5.0	-5.6	-5.3
3	-5.9	-5.9	-5.8
4	-2.9	-3.5	-3.6
5	-3.5	-3.5	-3.4
6	-2.8	-2.7	-2.9
7	-1.2	-2.2	-2.0
8	-1.7	-1.5	-1.9
9	-0.3	-0.4	-0.4
10	0.0	0.0	0.0
11	-0.4	-0.3	-0.4
12	+0.4	+0.1	0.0
13	-0.9	-1.0	-1.0
14	-1.6	-1.9	-1.9
15	-4.7	-4.8	-4.8
16	-5.7	-5.7	-5.7
17	-7.5	-7.6	-7.5
18	-8.7	-9.0	-9.0

Note: The positive sign indicates that the potential of V.P.1 is greater than V.P.2. The negative sign is reverse.

TABLE 1F (Continued)

	x 0.001 Dials			x 0.00001 Dials		
Date	1-8-69	27-8-69	26-9-69	1-8-69	27-8-69	26-9-69
Pot. Temp. (^{o}C)	21.0	21.2	21.2	21.0	21.2	21.2
Section	Potential Difference Between V.P.1 & V.P. 2, μv					
10	+0.6	+0.7	+0.7	0.0	0.0	0.0
20	+0.4	+0.4	+0.5	0.0	0.0	0.0
30	+0.5	+0.5	+0.5	0.0	0.0	0.0
40	+0.1	+0.3	+0.2	0.0	0.0	0.0
50	0.0	0.0	0.0	0.0	0.0	0.0
60	0.0	+0.1	+0.1	0.0	0.0	0.0
70	+0.4	+0.4	+0.4	0.0	0.0	0.0
80	+0.9	+0.9	+1.0	0.0	0.0	0.0
90	+0.1	+0.4	+0.4	0.0	0.0	0.0
100	+0.4	+0.5	+0.5	0.0	0.0	0.0

TABLE 2F

THE STABILITY OF POTENTIOMETER STANDARD CELL CIRCUITS

Range x 1.0

Date	1-8-69	27-8-69	26-9-69
Pot. Temp.(^{o}C)	21.0	21.2	21.2
Section	Potential Difference between V.P.1 & V.P.2, μv		
1.01800	-1.6	-2.0	-2.0
1.01810	-2.7	-2.9	-2.7
1.01820	-4.6	-5.0	-5.1
1.01830	-2.2	-3.2	-3.3
1.01840	-3.1	-3.1	-3.1
1.01850	-3.5	-3.5	-3.5
1.01860	-5.2	-5.4	-5.3
1.01870	-5.3	-5.6	-5.1
1.01880	-6.7	-6.7	-6.8
1.01890	-6.0	-8.0	-8.0
1.01900	-4.9	-5.1	-5.2

Note: The positive sign indicates that the potential of V.P.1 is greater than V.P.2. The negative sign is reverse.

TABLE 3F

THE STABILITY OF POTENTIOMETER STANDARD CELL CIRCUITS

	Range x 0.1		
Date	1-8-69	27-8-69	26-9-69
Pot. Temp.(^{o}C)	21.0	21.2	21.2
Section	Potential Difference Between V.P.1 & V.P. 2, μv/10		
1.01800	-2.1	-3.3	-2.2
1.01810	-1.4	-1.8	-1.6
1.01820	-1.4	-2.0	-2.2
1.01830	-2.8	-3.1	-1.9
1.01840	-3.2	-3.6	-3.8
1.01850	-3.3	-5.1	-5.0
1.01860	-2.8	-5.2	-4.7
1.01870	-3.9	-3.6	-4.0
1.01880	-5.2	-9.0	-8.7
1.01890	-5.3	-6.0	-7.0
1.01900	-5.4	-5.9	-5.1

Note: The positive sign indicates that the potential of V.P.1 is greater than V.P.2. The negative sign is reverse.

APPENDIX G

SOME OF THE α EXPERIMENTAL DATA ON HEAVY WATER

TABLE 1G

HIGH FILLING CONSTANT MASS EXPERIMENTS ON HEAVY WATER (THIRD SERIES)

Test No.	Initial Temp. (°C)	Final Temp. (°C)	Total Energy Added (Int.J.)	Energy Added For 50°C Interval (Int.J.)
21	49.905	99.996	218472.5	218075.5
22	99.956	149.887	220657.1	220961.8
23	149.955	199.805	225929.7	226609.5
24	199.930	249.929	235544.2	235548.9
25	249.892	299.931	248923.2	248729.1

TABLE 2G

HIGH FILLING CONSTANT MASS EXPERIMENTS ON HEAVY WATER (FOURTH SERIES)

Test No.	Initial Temp. (°C)	Final Temp. (°C)	Total Energy Added (Int.J.)	Energy Added For 50°C Interval (Int.J.)
26	50.133	100.213	216751.6	216405.3
27	100.020	150.063	219437.6	219248.9
28	150.854	199.933	220866.7	225011.3
29	199.964	249.947	234305.7	234385.4
30	249.850	299.945	247680.7	247210.9

TABLE 3G

THE INITIAL AND FINAL MASS VALUES OF THE LOW FILLING CONSTANT MASS EXPERIMENTS ON HEAVY WATER

Test Series No.	Mass (Grams) Initial*	Final
1	207.4610	207.3712
2	211.6122	211.4037
3	213.9551	213.6468

*Since it is conceivable that a small fraction of a gram of liquid could remain entrapped in the calorimeter hydraulic lines it was concluded that the previously mentioned leak only showed up at temperatures in excess of 200 ^{0}C.

APPENDIX H

HEAT CAPACITY OF THE EMPTY CALORIMETER

In order to compare the difference between the measured heat capacity of the empty calorimeter and the value inferred from the constant mass experiments, one series of the tare measurement under vacuum conditions was conducted recently from 50 to 300°C. The test results are summarized in Table 1H. It should be mentioned that the temperature variations over the surface of the calorimeter in the tare measurements as shown in Figure 1H were found to be almost four times larger than that in the constant mass experiments, consequently the net heat exchange between the calorimeter and the adiabatic shield could not be ignored and a small correction was necessary to apply to the energy term. This correction was estimated from the heat transfer coefficient obtained in the heat transfer study and the actual temperature differences between the calorimeter and adiabatic shield.

The comparisons between the results of the tare measurements and the corresponding values inferred from the constant mass experiments conducted on light and heavy water are shown in Table 2H. It is seen that the measured values deviate from the actual values by 2.6 percent on the high side. The reason for this large disagreement may be attributed to the heat leak.

TABLE 1H

HEAT CAPACITY MEASUREMENTS ON EMPTY CALORIMETER

UNDER VACUUM CONDITIONS

Test No.	Initial Temp. (°C)	Final Temp. (°C)	Total Energy Added (Int.J.)	Heat Leak (Int. J.)	Energy Added for 50°C Interval (Int.J.)
1	52.570	99.832	76423.8	-330.1	80502.0
2	99.979	150.433	83986.3	-462.9	82771.8
3	149.973	200.405	86482.4	-757.2	84990.9
4	200.345	250.132	87700.4	-881.8	87190.0
5	249.714	300.007	90875.6	-1019.9	89332.2

TABLE 2H

COMPARISONS BETWEEN THE OBSERVED VALUES AND THE

ACTUAL VALUES OF THE HEAT CAPACITY OF THE EMPTY CALORIMETER

Temperature Interval (°C)		Measured Value Obtained Under Vacuum Conditions (Int.J.)	Actual Value Inferred From Constant Mass Measurements (Int.J.)	Deviation From Actual Value %
From	To			
50	100	80502.0	80114.5	+0.5
100	150	82771.8	82383.5	+0.5
150	200	84990.9	84166.4	+1.0
200	250	87190.0	85754.7	+1.7
250	300	89332.2	87096.6	+2.6

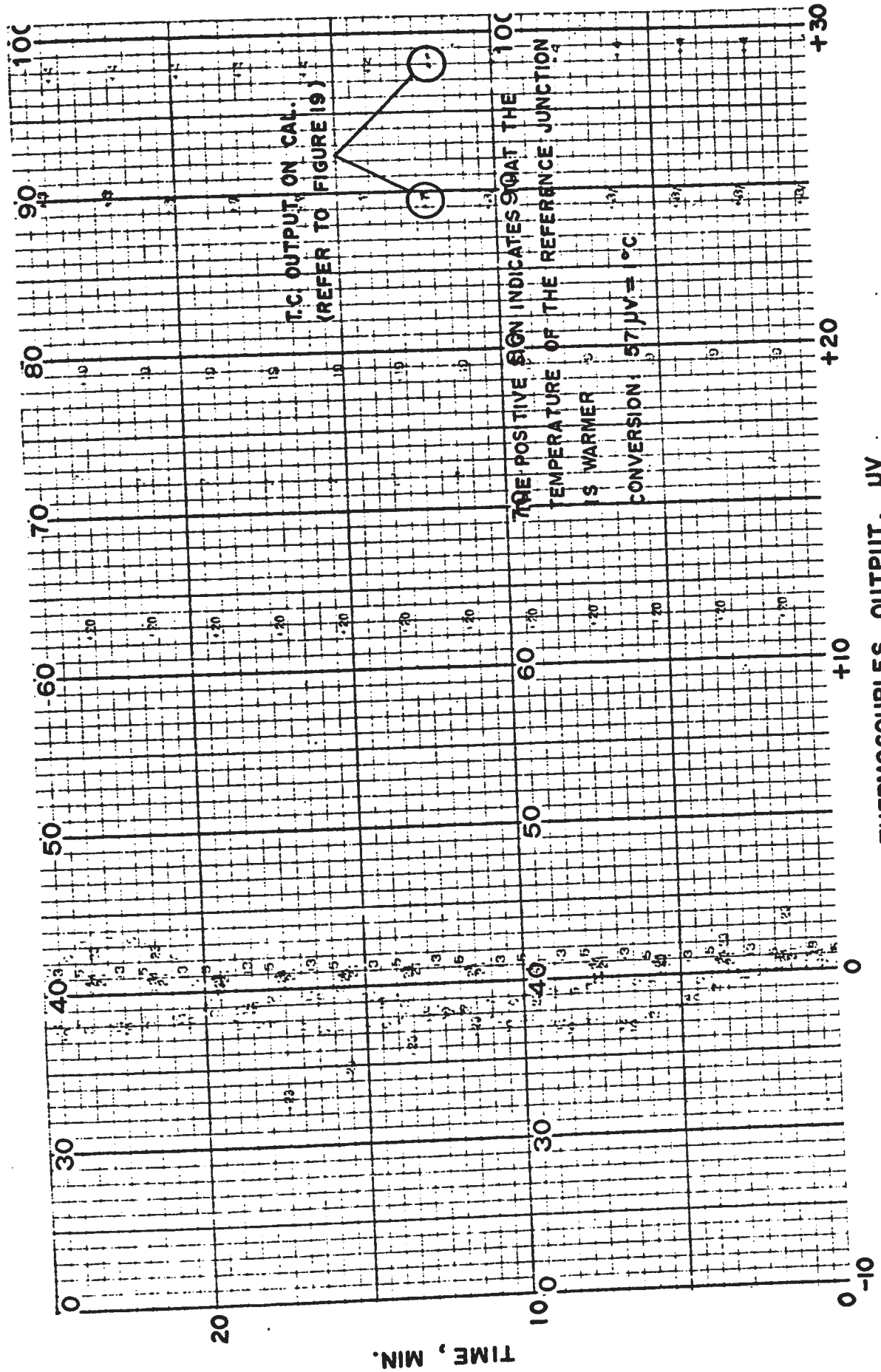

FIGURE 1H TEMPERATURE VARIATIONS ON THE CALORIMETER DURING A TYPICAL RUN OF HEAT CAPACITY OF EMPTY CALORIMETER

It should be pointed out that the heat transfer coefficient was determined under steady state and the temperature variations on the calorimeter were no more than 0.1°C which is in contrast to a temperature variation of approximately 0.8°C during the tare measurements. Consequently the heat transfer coefficient in the tare measurements is definitely different to that value obtained in the heat transfer study.

It was mentioned previously that the heat transfer coefficient was measured during the early part of the research program and it might shift with time. Osborne et al (21) observed this phenomenon in their calorimetric measurements and made more than 300 separate determinations on the heat transfer coefficient at different time and different temperature. In view of the foregoing reasons, it may be concluded that the energy corrections shown in Table 1H would be in error.

APPENDIX I

LIST OF EQUIPMENT

1. Absolute Temperature Measurement

   Isolating Potential Comparator, Model 9800, S/N 25889 Guildline Instrument Company Limited.

   Four Terminal Variable Resistor, Model 9801-T, S/N 26124 Guildline Instrument Company Limited.

   Photo Cell Galvanometer Amplifier, Model 9460, S/N 180641 Guildline Instrument Company Limited.

   Spotlight Galvanometer Model 9461-A, S/N 26605 Guildline Instrument Company Limited.

   Laboratory Standard Resistance Thermometer, S/N 331 Rosemount Engineering Company Limited.

   Water Triple Point Cell, Model 130, S/N 57937, Trans-Sonics Company Limited.

2. Power Measurement

   Multiple Standard Resistors, Model 9200, S/N 25799, Guildline Instrument Company Limited.

   Volt Box, Model 2851, S/N M-3545, Honeywell Control Company Limited.

Vernier Potentiometer, S/N C-391692, Cambridge Instrument Company Limited.

Spotlight Galvanometer, Model 2430-A, S/N 1693079, Leeds and Northrup Company Limited.

Bank of Standard Cells in a Temperature Controlled Oven, Model 2778, S/N P-1940, Honeywell Control Limited.

Precision Quartz Crystal Timer, U.W.O. Shop.

3. Temperature Difference Measurement and Control

Electronic 16 Laboratory Recorder, S/N K 710 951 8001, Honeywell Control Limited.

D C Microvolt Amplifier, Cat 9835-B, Leeds & Northrup Company Limited.

Deviation Amplifier, Model 687293, Honeywell Control Limited.

Silicon Controlled Rectifier (SCR), Model R7170A, Honeywell Control Limited.

Three Mode Temperature Controller, Model M5755231001, Honeywell Control Limited.

4. Power Supply Equipment

D.C. Power Supply, Model Sy-60-6, NJE Corporation.

D.C. Power Supply, Model 865C, Harrison Laboratories Incorporated.

D.C. Power Supply, Model Sy-60-18, NJE Corporation.

D.C. Power Supply, Model Sy-40-2, NJE Corportion.

5. Mass Measurement

Mettler Analytical Balance, 0-1000 gram, Model k-4, Fischer Scientific Company Limited.

6. Miscellaneous

Vacuum Pump, S/N 21052, Consolidated Vacuum Company Limited.

Vacuum Pump, S/N 60038, Consolidated Vacuum Company Limited.

Valustat Valve, Model (1B-2B-1G-2G, 1-E-2E), S/N 21052, Edwards High Vacuum Limited.

BIBLIOGRAPHY

1. Lewis, W. B., "Achievements and Prospects of Heavy Water Reactors", Giornate dell'Energia Nucleare, 1966.

2. Anonymous, Nuclear Engineering International, Vol. 15, Feb., 1970.

3. Lewis, W. B., "Nuclear Power -- The Next Decade of Development", Proceedings of The American Power Conference, 1967.

4. Brown, R. S., Barness, W. H. and Maass, O., "The Measurement of Some Thermal Properties of Deuterium Oxide and Their Interpretation", Canadian Journal of Research, Vol. 13, p.p. 699-701, 1935.

5. Cockett, A. H. and Ferguson, A., "The Specific Heat of Water and of Heavy Water", Philosophic Magazine, Vol. 29, p.p. 185-199, 1940.

6. Euken, V. A. and Eigen, M. E., Elektrochemic und Phys. Chem., Vol. 55, p.p. 343-354, 1951.

7. Baker, B. L., "Heat Capacity and Thermodynamic Properties of Saturated Deuterium Oxide", AECU-4738, 1959.

8. Friedman, A. S. and Haar, L., Journal of Chem. and Phys., Vol. 22, p.p. 2051, 1954.

9. Kirshenbaum, I., "Physical Properties and Analysis of Heavy Water", McGraw-Hill Company, New York, 1951.

10. Elliott, J. N., "Tables of The Thermodynamic Properties of Heavy Water", AECL-1673, 1963.

11. Bishop, A. A. and Nelson, P. A., "Transport and Thermodynamic Properties of Saturated and Compressed Heavy Water", Carolinas-Virginia Nuclear Power Associates. Inc., 1961.

12. Rivkin, S. L. and Egorov, B. N., "Experimental Study of Heavy Water Specific Heat", Atomnaya Energiya, Vol. 7, No. 5, p.p. 462-465, 1959.

13. Rivkin, S. L. and Egorov, B. N., "Specific Heat of Heavy Water at High Temperatures and Pressures", Atomnaya Energiya, Vol. 14, No. 4, p.p. 416-418, 1963.

14. Sheindlin, A. E. and Gorbunova, N. I., "Experimental Study of the Enthalpy of Heavy Water in the Supercritical Range of Parameters of State", Teplotizika Vysokikh Temperature, Vol. 2, No. 3, p.p. 484-487, 1964.

15. Nowak, E. S., "The Enthalpy Change of Saturated Heavy Water", Presented at the Seventh International Conference on Properties of Steam, Tokyo, Japan, Sept., 1968.

16. Nowak, E. S., "A Calorimetric Investigation of the Enthalpy of Heavy Water", Research Report HT-1-69, Faculty of Engineering Science, The University of Western Ontario, 1969.

17. Nowak, E. S. and Chan, J., "A Calorimeter Apparatus to Measure the Enthalpy Difference of Heavy Water", Journal of Heat Transfer, Transactions of the American Society of Mechanical Engineers, Vol. 91, Series C, p.p. 235-240, 1969.

18. Nowak, E. S. and Chan, J., "An Experimental Investigation of the Enthalpy of Saturated Heavy Water Liquid to 350°F", Submitted to Journal of Heat Transfer, Transactions of the American Society of Mechanical Engineers, March, 1970.

19. Osborne, N. S., Stimson, H. F. and Fiock, E. F., "A Calorimetric Determination of Thermal Properties of Saturated Water and Steam From 0 to 270°C", Journal of Research of the National Bureau of Standards, Vol. 5, p.p. 411-480, 1930.

20. Osborne, N. S. and Meyers, C. H., "A Formula and Tables for the Pressure of Saturated Water Vapor in the Range 0 to 374°C", Journal of Research of the National Bureau of Standards, Vol. 13, p.p. 1-20, 1934.

21. Osborne, N. S., Stimson, H. F. and Ginnings, D. C., "Calorimetric Determination of the Thermodynamic Properties of Saturated Water in Both the Liquid and Gaseous States from 100 to 374°C", Journal of Research of the National Bureau of Standards, Vol. 18, p.p. 389-431, 1937.

22. Osborne, N. B., Stimson, H. F. and Ginnings, D. C., "Measurements of Heat Capacity and Heat of Vaporization of Water in the Range 0 to 100°C", Journal of Research of the National Bureau of Standards, Vol. 23, p.p. 197-260, 1939.

23. Williamson, E. D. and Adams, L. H., "Temperature Distribution in Solids during Heating or Cooling", Physics Review, Vol. 14, p.p. 99-144, 1919.

24. Chan, J., "The Design and Construction of An Apparatus to Measure the Enthalpy of Heavy Water", M.E.Sc. Thesis, Faculty of Engineering Science, The University of Western Ontario, Canada, 1968.

25. Kell, G. S. and Whalley, E., "The PVT Properties of Water", Philosophical Transactions of the Royal Society of London, Vol. 258, p.p. 565-617, 1965.

26. Haessler, W., "The Design and Construction of An Isothermal Enclosure", M.E.Sc. Thesis, Faculty of Engineering Science, The University of Western Ontario, Canada, 1969.

27. Moyse, S., "Experimental Investigations of the Enthalpy of Saturated Heavy Water Vapour and Saturated Heavy Water Liquid", U.W.O. Undergraduate Engineering Thesis, 1969.

28. Dauphinee, T. M., "Potentiometric Methods of Resistance Measurement", Temperature - Its Measurement and Control in Science Industry, Vol. 3, Part 1, p.p. 269-283, 1962.

29. Berry, R. J., "Calibration of One Platinum Resistance Thermometer", NRC Report No. APH-1322, 1965.

30. Stimson, H. F., "International Practical Temperature Scale of 1948, Test Revision of 1960", National Bureau of Standards Monograph 37, 1961.

31. Thomas, J. L., "Precision Resistors and Their Measurement", National Bureau of Standards Circular 470, 1948.

32. Chan, J., "The Design and Construction of An Apparatus to Measure the Enthalpy of Heavy Water", M.E.Sc. Thesis, Faculty of Engineering Science, The University of Western Ontario, Canada, p.p. 85-87, 1968.

33. Kirillin, V. A. and Ulivich, S. A., "Experimental Study of Heavy Water Density", Teploenergetika, No. 4, p.p. 67, 1959.

34. Jakob, M. and Hawkins, G. A., Elements of Heat Transfer, p.p. 230, 1962.

35. Keenan, J., Keyes, F., Hill, P. and Moore, J., "Steam Tables", John Wiley & Sons, Inc., New York, 1969.

36. Anonymous, "Thermodynamic and Transport Properties of Steam", The American Society of Mechanical Engineering, New York, 1967.

37. Vukalovitch, M. P., "Thermodynamic Properties of Water and Steam", State Scientific Technical Publication, Moscow, 1955.

38. Anonymous, "1967 Steam Table", The Electrical Research Association, London, 1967.

39. Schmidt, E., "V.D.I. Steam Table", Springer Verlag, Berlin Gottingen and Heidelberg, 1956.

40. Smith, L. B. and Keyes, F. G., "The Volume of Unit Mass of Liquid Water and their Correlation as Function of Pressure and Temperature", Proceedings, American Academy of Arts and Sciences,Vol. 69, p.p. 285-312, 1934.

41. Whalley, E., "The Thermodynamic and Transport Properties of Heavy Water", Proceedings and Communications of the Conference on Thermodynamic and Transport Properties of Fluids, Institution of Mechanical Engineers, London, p.p. 15-26, 1957.

42. Chan, J., Personal Communication, Faculty of Engineering Science, The University of Western Ontario, London, Canada.

43. Anonymous, "Engineering Properties of Inconel 600", Technical Bulletin T-7, The International Nickel Company of Canada.